Distribution Agreement

In presenting this thesis or dissertation as a partial fulfillment of the requirements for an advanced degree from Emory University, I hereby grant to Emory University and its agents the non-exclusive license to archive, make accessible, and display my thesis or dissertation in whole or in part in all forms of media, now or hereafter known, including display on the world wide web. I understand that I may select some access restrictions as part of the online submission of this thesis or dissertation. I retain all ownership rights to the copyright of the thesis or dissertation. I also retain the right to use in future works (such as articles or books) all or part of this thesis or dissertation.

Signature:

_____

Jill Reneé Glausier née Bordelon

D_1 and D_5 dopamine receptor signaling in area 9 of the *Macaca mulatta* dorsolateral prefrontal cortex

By

Jill Reneé Glausier née Bordelon
Doctor of Philosophy

Graduate Division of Biological and Biomedical Sciences
Program in Neuroscience

_____
Emil Christopher Muly, M.D., Ph.D.
Advisor

_____
Yoland Smith, Ph.D.
Committee Member

_____
Donald Rainnie, Ph.D.
Committee Member

_____
Randy Hall, Ph.D.
Committee Member

_____
Lian Li, Ph.D.
Committee Member

Accepted:

_____
Lisa A. Tedesco, Ph.D.
Dean of the Graduate School

_____
Date

D_1 and D_5 dopamine receptor signaling in area 9 of the *Macaca mulatta* dorsolateral prefrontal cortex

By

Jill Reneé Glausier née Bordelon
B.S., Louisiana State University, 2002

Advisor: E. Chris Muly, M.D., Ph.D.

An Abstract of
A dissertation submitted to the Faculty of the Graduate School of Emory University
in partial fulfillment of the requirement for the degree of
Doctor of Philosophy
Graduate Division of Biological and Biomedical Sciences
Program in Neuroscience

2008

Abstract

Schizophrenia is a debilitating disorder that is characterized by impairments in perception, thinking, social functioning and cognition. It is cognitive ability which is the best predictor of employment, social integration and relapse. Working memory (WM) is a core cognitive process that is severely impaired in schizophrenia, and WM depends on intact circuitry and dopaminergic signaling via the D1 family of dopamine receptors (D1R) in the dorsolateral prefrontal cortex (dlPFC). D1R activation and WM performance have an inverted-U relationship, such that too much or too little D1R stimulation results in poor WM performance. It was the goal of my experiments to contribute to understanding what underlies this dose-dependent relationship.

Of the two D1R subtypes, D_1 and D_5, the D_5 receptor has a 10-fold higher affinity for dopamine. The circuitry of the PFC includes excitatory spiny pyramidal cells, and inhibitory interneurons which can be defined by the presence of calcium-binding proteins like parvalbumin (PV) and calretinin (CR). I demonstrate that D_1 and D_5 are co-localized on pyramidal cell spines but not on interneurons. PV interneurons predominately express D_1, while CR interneurons predominately express D_5. The D1R activate a complex signal transduction pathway that includes inhibitor-1 (I-1), DARPP-32, protein phosphatase 1 (PP1) α and PP1γ1. The precise localization of these proteins is critical for D1R signaling. I demonstrate that I-1 and DARPP-32 are infrequently identified in pyramidal cell spines, and that the signaling environments in PV and CR interneurons differ from each other and from pyramidal cell spines. The implications these different signaling environments may have on D1R signaling in the PFC are discussed.

D_1 and D_5 dopamine receptor signaling in area 9 of the *Macaca mulatta* dorsolateral prefrontal cortex

By

Jill Reneé Glausier née Bordelon
B.S., Louisiana State University, 2002

Advisor: E. Chris Muly, M.D., Ph.D.

A dissertation submitted to the Faculty of the Graduate School of Emory University
in partial fulfillment of the requirement for the degree of
Doctor of Philosophy
Graduate Division of Biological and Biomedical Sciences
Program in Neuroscience

2008

Acknowledgements

I would like to thank my advisor, Chris Muly, for being a wonderful mentor and friend. Despite many dumb questions and the inability to perform simple math, he has always treated me as a colleague. I would also like to thank my committee members: Randy Hall, Tig Rainnie, Yoland Smith and Lian Li. Randy allowed me to play in his lab for several months, not getting any data. He and his lab were so nice and helpful to me. Tig has spent many hours trying to teach me how to critically read electrophysiology papers, and has been like a second advisor to me. Yoland has been such a wonderful DGS and Director of the Neuroscience program. Despite being insanely busy, he always thoroughly reviews my manuscripts, and is available any time I needed him. Lian has been instrumental in the design and interpretation of my biochemical data. Other faculty and staff in the program have helped me immeasurably: Ron Calabrese, Tim Cope, Shawn Hochman, Mike Kuhar and Sonia Hayden.

My friends have been an indispensable network of support. Karen Rommelfanger, Liz (Kirk) Webber, Lisa (Imboden) Giles, Heather Ross and Alisa Gutman have spent many nights studying, drinking, freaking out, studying, drinking, watching *Sex and the City*, and gossiping with me. Without my study group which included Karen and Lisa, I never would have passed my first two years in grad school. Moreover, as I'm preparing to get married, each of them has been supportive and attentive bridesmaids.

I also need to acknowledge my Mother. She was the first one in our family to attend college and also get an advanced degree. With two small children, she left all she knew in rural Louisiana and moved to the sprawling metropolis of Hattiesburg, Mississippi. She single-handedly raised two girls into socially and morally responsible adults. As hard as grad school has been, I'm sure it pales in comparison to her experiences. My Mother is the kindest and strongest person I know, and I can only hope that my life and career follow in that legacy.

Finally, I would like to acknowledge my fiancé, Neil. He has nursed me through the horrors of grad school and science, and then reveled with me when I got good reviews or ultrastructure. Neil is well acquainted with most of my flaws and still wants to marry me. He is willing to pick up and move for my career development with nary a complaint. I couldn't ask for a more loyal, trustworthy, fun and loving mate.

Table of Contents

List of Figures

Chapter 1: General Introduction

Chapter 2: Localization of D_1 and D_5 in the neuropil of *Macaca mulatta* prefrontal cortical area 9

Chapter 3: Localization of D_1 and D_5 in parvalbumin and calretinin interneurons in *Macaca mulatta* prefrontal cortical area 9

Chapter 6: Concluding Remarks

Chapter 1

General Introduction

Clinical Features of Schizophrenia

Schizophrenia is a debilitating disorder which affects approximately 1% of the world's population (A. Jablensky, 1995). In the United States alone, over 3 million people are diagnosed with schizophrenia at a cost of $62 million a year (E. Q. Wu et al., 2005). The first in depth study of schizophrenia came from Emil Kraepelin who termed this disorder "dementia praecox" to underscore the progressive nature of the disease and the early onset (E. Kraepelin, 1896). The name "schizophrenia" was coined by Eugen Bleuler in 1911 in his work, "Dementia Praecox or the Group of Schizophrenias." As indicated by the title, schizophrenia is a complex disorder with a variety of symptoms. Today, similar to the description by Dr. Bleuler, the American Psychiatric Association has grouped the clinical symptoms of schizophrenia into three categories: positive, negative and cognitive (A. P. Association, 1994).

Positive symptoms are perhaps the most striking of the three categories and include hallucinations, delusions, thought disorder and movement abnormalities. Hallucinations are sounds, smells and images that the patient is experiencing that nobody else can identify. Auditory hallucinations are the most common, and patients describe "voices" as being threatening, critical, and occasionally positive (E. Bleuler, 1950). Delusions are "false personal beliefs that are not part of the person's culture and do not change, even when other people present proof that the beliefs are not true or logical" (NIMH, 2006). There are four main types of delusions: grandeur, reference, persecution and control. Delusions of grandeur involve the patient believing they are a person of historical importance or famous; for example, a patient may believe they are Jesus Christ or Joan of Arc. Delusions of reference involve the patient attaching a meaning to things

around them; for example, believing that others are communicating with them via the television (S. Bucci et al., 2008). Delusions of persecution involve the patient believing that some entity is plotting against them; for example, believing the government is trying to poison them. Finally, delusions of control involve the patient believing that some outside entity or force is controlling their thoughts or actions; for example, believing that aliens are responsible for their actions. Formal thought disorder is the third type of positive symptom, and it is the unusual thought process and speech that patients diagnosed with schizophrenia can display. For example, questions may be answered vaguely or in an oblique manner, such as answering "Is something weighing heavily on your mind?" with "Yes. Iron is heavy." (E. Bleuler, 1950). Tangential thoughts are another characteristic of thought disorder, and this is illustrated in this except of a letter from a patient to his mother.

"I am writing on paper. The pen which I am using is from a factory called 'Perry & Co.' this factory is in England. I assume this. Behind the name Perry & Co. the city of London is inscribed; but not the city. The city of London is in England. I know this from my school-days. Then, I always liked geography. My last teacher in that subject was Professor August A. He was a man with black eyes. I also like black eyes. There are also blue and gray eyes and other sorts, too. I have heard it said that snakes have green eyes. All people have eyes. There are some, too, who are blind. These blind people are led about by a boy. It must be very terrible not to be able to see. There are people who can't see and, in addition, can't hear. I know some who hear too much. One can hear too much. There are many sick people in Burgholzli; they are called patients. One of them I like a great deal. His name is E. Sch. He taught me that in Burgholzli

there are many kinds, patients, inmates, attendants. Then there are some who are not here at all. They are all peculiar people..."(E. Bleuler, 1950).

Movement abnormalities are the fourth type of positive symptom. Patients may exhibit stereotypies or become catatonic. These categories of positive symptoms are not mutually exclusive; a patient diagnosed with schizophrenia can exhibit more than one type of positive symptom, and the presence of these symptoms alone does not necessitate a diagnosis of schizophrenia.

Negative symptoms include a flattened affect, deriving little pleasure from activities which they would normally enjoy (anhedonia), decreased speech (alogia) and a lack of motivation (avolition). These symptoms are largely unaffected by neuroleptic treatment (reviewed in P. F. Buckley and S. M. Stahl, 2007), but there is emerging evidence suggesting that adjunctive treatment with selective serotonin reuptake inhibitors (SSRIs) may ameliorate some negative symptoms in patients diagnosed with schizophrenia (H. Silver, 2003).

Cognitive dysfunction is the final category of schizophrenia symptoms and includes dysfunctions in attention, executive functions, working memory and learning (reviewed in R. S. Keefe, 2007). For example, patients diagnosed with schizophrenia have difficulty with maintaining information over short periods of time, contextual processing and are more easily distractible (D. M. Barch et al., 1999; J. D. Cohen et al., 1999; J. H. Callicott et al., 2003a; Z. Delawalla et al., 2008). Interestingly, cognitive impairments are present before the first psychotic episode and remain throughout the course of the treatment and disease (B. A. Cornblatt and J. G. Keilp, 1994; M. Byrne et al., 1999; L. Erlenmeyer-Kimling et al., 2000; M. Cannon et al., 2002; W. J. Brewer et

al., 2005). First-degree relatives of schizophrenia patients also exhibit cognitive impairments that are intermediate between the patients and healthy controls (J. H. Callicott et al., 2003b; A. W. MacDonald, 3rd et al., 2003; Z. Delawalla et al., 2008). While positive symptoms may be the most striking, it is cognitive impairments which are the most debilitating. Cognitive ability is the best predictor of social integration, employment, and even relapse in patients diagnosed with schizophrenia (T. Wykes, 1994; M. F. Green, 1996; P. H. Lysaker et al., 1996; S. R. McGurk and H. Y. Meltzer, 2000; M. F. Green et al., 2004). Though neuroleptics are very effective at ameliorating positive symptoms, the data regarding the effect of neuroleptic treatment on cognitive ability has been inconsistent, ranging from small improvements to exacerbation of cognitive impairments (S. R. McGurk et al., 2005; R. S. Keefe et al., 2007). However, what is clear is that the cognitive impairments identified in this patient population are not being currently addressed with pharmacotherapies. The importance of cognitive ability coupled with the lack of treatment indicates cognitive function as a key research topic for schizophrenia.

Working Memory and Schizophrenia

Although deficits in several aspects of cognition have been identified as central to the disorder (reviewed in B. Elvevag and T. E. Goldberg, 2000), working memory (WM) has received particular attention. Working memory (WM) is the ability to maintain and manipulate information over short periods of time in order to guide thought or behavior (A. Baddeley, 1986). Impairments in WM are one of the most widely replicated findings in patients diagnosed with schizophrenia (S. Park and P. S. Holzman, 1992; R. S. Keefe

et al., 1995; C. S. Carter et al., 1998; S. Park et al., 1999; A. Abi-Dargham et al., 2002; J. H. Callicott et al., 2003a). There are several modalities of WM, including spatial, object and auditory (A. Baddeley, 1986). In each of these modalities, the information remembered is also used to guide subsequent behavior. As Patricia Goldman-Rakic noted, the importance of this ability to direct behavior based on "symbolic representations" rather than requiring constant external stimuli "cannot be overemphasized" (P. S. Goldman-Rakic, 1994). WM provides "temporal and spatial continuity between our past experience and present actions" (P. S. Goldman-Rakic, 1994), and it is easy to imagine how disruption of this system could lead to the information processing problems identified in schizophrenia patients (P. S. Goldman-Rakic, 1994; H. Silver et al., 2003). Indeed, in other disorders where there is a paucity of speech and learning ability, WM is also impaired (K. M. Wilson and H. L. Swanson, 2001; T. P. Alloway and L. Archibald, 2008), further suggesting that an intact WM system is required to properly perform other cognitive tasks. Thus, a search into how WM operates has been a central focus of cognitive research, especially in the schizophrenia patient population.

WM ability depends on the proper functioning of the circuitry of the dlPFC and the availability of dopamine in the dlFPC (T. J. Brozoski et al., 1979; T. Sawaguchi et al., 1988). Our lab proposes that in order to understand WM, the interaction of dopamine signaling with the dlPFC circuitry must be understood.

Circuitry of the Dorsolateral Prefrontal Cortex

The major cellular constituents of the PFC are projection pyramidal neurons and local circuit interneurons. Projection neurons are glutamatergic and possess spiny dendrites which receive the vast majority of excitatory input in the PFC (E. G. Gray, 1959; K. M. Harris and S. B. Kater, 1994). Interneurons in PFC are GABAergic with aspiny dendrites and can be divided into sub-populations based on molecular, electrophysiological and morphological properties.

Parvalbumin (PV) is a calcium-binding protein which is expressed in approximately 25% of interneurons in the primate dlPFC (F. Conde et al., 1994). These PV interneurons are morphologically characterized as basket and chandelier cells, and they have fast-spiking electrophysiological properties (S. M. Williams et al., 1992; A. V. Zaitsev et al., 2005). PV basket cells terminate onto the perisomatic region of pyramidal cells, while PV chandelier cells form synaptic "cartridges" onto the initial portion of the pyramidal cell axon. These morphological characteristics result in strong modulation of pyramidal cell output (G. Gonzalez-Burgos et al., 2005a; A. R. Woodruff and P. Sah, 2007). Calretinin (CR) is another calcium-binding protein which is expressed in a non-PV-overlapping population of dlPFC interneurons. Approximately 50% of primate dlPFC interneurons express CR, and they typically exhibit double bouquet morphology. CR-containing double bouquet interneurons synapse primarily onto other interneurons, likely resulting in disinhibition of pyramidal cells (Fig. 1-1) (J. DeFelipe et al., 1985; Y. Kawaguchi, 1995; J. DeFelipe, 1997; Y. Kawaguchi and Y. Kubota, 1997; Y. Kawaguchi and S. Kondo, 2002; X. J. Wang et al., 2004; A. V. Zaitsev et al., 2004). Thus, activation of PV or CR interneurons can have a very different effect on the output of the pyramidal neuron, and their differential activation may contribute to WM processes.

The Cellular Correlate of Working Memory

Although it was known that the dlPFC was critical for WM performance, it was unknown how different components of the dlPFC responded during the different phases of a WM task. The oculomotor delayed-response task (ODR) is a commonly used spatial WM task in monkeys, and it has four distinct phases: fixation, cue, delay and response. During fixation, the monkey maintains focus on a centralized target. A cue is then presented in one of eight peripheral positions. After the cue is presented, the delay period follows. During the delay period the monkey continues to focus on the centralized target. Increasing the delay time can increase the difficulty of the WM task. Finally, after the delay period, the centralized target is removed, and the monkey must make an eye saccade to the remembered cue location. Single unit recordings can be made in the dlPFC while the monkeys is performing this task to identify how pyramidal cells and interneurons respond. Amazingly, there are pyramidal neurons in the dlPFC which increase their activity specifically during the delay period of the WM task in a direction-specific manner (S. Funahashi et al., 1989; G. V. Williams and P. S. Goldman-Rakic, 1995; S. Vijayraghavan et al., 2007). For example, Figure 1-2 shows the activity of one dlPFC pyramidal cell over all four phases of the WM task and for all eight stimulus locations (S. Funahashi et al., 1989). This neuron responds only during the delay period when the monkey is remembering the stimulus at the 270^{o} location. Because these neurons have temporal and spatial "memory fields," they have been termed "delay cells" and are proposed to be the cellular correlate of WM.

Because interneurons are much harder to record from in awake, behaving monkeys, there has been significantly less research performed on interneuron activity

during WM tasks. However, it has been shown that GABAergic neurotransmission is critical for maintaining the memory field of pyramidal cells (S. G. Rao et al., 2000), and it has been proposed that interneuron activity is critical for the temporal and spatial specificity, or tuning, of the pyramidal delay cells (S. G. Rao et al., 1999, 2000; G. Gonzalez-Burgos et al., 2005a). Moreover, tuned delay activity has been identified in putative PV interneurons of the dlPFC that is isodirectional to that of adjacent pyramidal cells, and this type of tuning most likely results in sharper pyramidal cell spatial tuning (S. G. Rao et al., 1999). Thus, GABAergic interneuron activity is critical for maintaining and enhancing the spatial tuning of pyramidal delay cells in the dlPFC.

Dopamine and Working Memory

The other required component for proper WM function is dopamine availability in the dlPFC. The first definitive evidence that dopamine in the dlPFC is important for WM function came in 1979 from the Goldman-Rakic laboratory. In this study, dopamine was specifically depleted in the area around the principal sulcus (areas 9 and 46), and all other neurotransmitter systems remained intact. The WM performance of monkeys who had dlPFC dopamine depletion was almost as poor as monkeys who had the entire dlPFC ablated. Moreover, neither norepinephrine nor serotonin dlPFC depletion impaired WM performance (T. J. Brozoski et al., 1979). Not only did these results demonstrate that dopamine is required in the dlPFC for adequate WM performance, but they suggested that enhancing dlPFC dopamine may improve WM performance. However, this did not prove to be the case. In fact, supranormal levels of dopamine in the PFC also impaired WM (B. L. Murphy et al., 1996; A. F. Arnsten and P. S. Goldman-Rakic, 1998). Thus,

too little dopamine and too much dopamine in the dlPFC impairs WM performance, indicating that WM performance and dlPFC dopamine levels have an "inverted-U" relationship. However, it was still unclear which dopamine receptor(s) was mediating this effect.

Dopamine Receptors and Working Memory

Dopamine can signal via five different receptors, identified as D_1, D_2, D_3, D_4 and D_5. Each subtype is a traditional seven transmembrane metabotropic receptor. The receptors are divided into two families: the D1 family (D1R) which includes D_1 and D_5, and the D2 family (D2R) which includes D_2, D_3 and D_4. D1R are coupled to $G_{\alpha s}$ protein, whereas D2R are coupled to $G_{\alpha i}$ protein (reviewed in C. Missale et al., 1998).

In the PFC, D1R binding is 10-20 times that of D2R binding density, and comparable levels of D_1 and D_5 mRNA have been identified in the monkey and human PFC (J. H. Meador-Woodruff et al., 1996; M. S. Lidow et al., 1998). Despite the unavailability of a ligand which can distinguish between D_1 and D_5, differences have emerged. For example, D_5 has higher constitutive activity (M. Tiberi and M. G. Caron, 1994) and a 10-fold higher affinity for dopamine (R. K. Sunahara et al., 1991; R. L. Weinshank et al., 1991); D_1 interacts with the NMDA receptor (F. J. Lee et al., 2002), while D_5 interacts $GABA_A$ subunits (F. Liu et al., 2000); D_5 regulates acetylcholine release in the mouse hippocampus (F. Laplante et al., 2004); genetic deletion of D_1 impairs corticostriatal LTP, while blocking the remaining D_5 receptors impairs corticostriatal LTD (D. Centonze et al., 2003); and D_1 and D_5 have distinct effects on locomotion (G. Dziewczapolski et al., 1998; D. Centonze et al., 2003).

In both rats and monkeys, local and systemic PFC injection of D1R antagonists produced WM impairments, but D2R antagonists had no effect (T. Sawaguchi and P. S. Goldman-Rakic, 1991; A. F. Arnsten et al., 1994; J. K. Seamans et al., 1998). Moreover, excessive stimulation of PFC D1R also resulted in impaired WM (J. Zahrt et al., 1997). Together these results suggest that too little or too much D1R stimulation will result in poor WM performance (Fig. 1-3); and, if correct, the WM performance of animals with low PFC dopamine and D1R stimulation should be enhanced by D1R agonists, and vice versa. This hypothesis has been directly tested by Floresco and Phillips (2001). Rats were trained on an eight-arm radial maze with a delay period of 30 minutes as a test of WM. During this 30 minute delay period, PFC dopamine levels increased. The rats that performed well at a 30 minute delay were then tested at a 4 hour delay. The rats' WM performance, as well as PFC dopamine levels, fell significantly. If there is an inverted-U relationship between WM performance and PFC D1R stimulation, addition of a D1R agonist at the 30 minute delay should impair the rats' WM performance, but addition of a D1R agonist at the 4 hour delay should improve the rats' WM performance. Indeed, a local injection of D1R agonist impaired the performance after a short delay but enhanced performance after a long delay which was concomitant with low PFC dopamine levels (S. B. Floresco and A. G. Phillips, 2001). Thus, across species and methods of administration, the evidence is strong that the D1R is the main dopamine receptor family mediating the inverted-U relationship between PFC dopamine levels and WM performance.

D1R Stimulation and Delay Cells

If delay cells are indeed the cellular correlate of WM, one would hypothesize that their spatial tuning would also be impaired at high and low levels of D1R stimulation. The first evidence supporting this hypothesis came in 1995 again from the Goldman-Rakic laboratory. Tuned pyramidal delay cells lost their spatial tuning and their temporal activity profiles when high injection currents of a D1R agonist or antagonist were used, but their tuning was enhanced when a lower injection current of the D1R antagonist was used (G. V. Williams and P. S. Goldman-Rakic, 1995). A recent study from Vijayraghavan and colleagues (2007) has demonstrated that increasing D1R agonist injection currents improve the spatial tuning of a pyramidal delay cell only until a certain point at which the spatial and temporal tuning are abolished. Combined, these studies demonstrate that too much D1R stimulation and no D1R stimulation impair the spatial and temporal tuning of pyramidal delay cells, just like the relationship between D1R stimulation and WM performance. Thus, studying how variable levels D1R stimulation might influence the activity of a pyramidal cell can shed light on how variable levels of D1R stimulation are affecting WM performance.

D_1 and D_5 in Dorsolateral Prefrontal Circuitry

Activation of D1R typically enhances the excitability of a neuron (reviewed in J. K. Seamans and C. R. Yang, 2004). Although there is no currently available drug which can distinguish D_1 from D_5, the D_5 receptor has a 10-fold higher affinity for dopamine than does the D_1 receptor (R. K. Sunahara et al., 1991; R. L. Weinshank et al., 1991). This key difference, coupled with the knowledge of their precise localization, may shed light on the mechanism which drives the inverted-U relationship between D1R

stimulation and WM ability. There have been few reports to date regarding the localization of D_1 and D_5 to specific components of PFC circuitry, but they do suggest that D_1 and D_5 have distinct localizations throughout the PFC neuropil (C. Bergson et al., 1995b; E. C. Muly et al., 1998; C. D. Paspalas and P. S. Goldman-Rakic, 2005). In Chapters 2 and 3 of this dissertation, I have quantitatively determined the localization of both D_1 and D_5 across the neuropil of the PFC and within PV and CR interneurons, and then used this information, coupled with previous electrophysiological and pharmacological data, to propose a model to explain the inverted-U relationship.

D1R Signal Transduction

Because the D1R a metabotropic, they use a signal transduction cascade (Fig. 1-4). The basic scheme of D1R signal transduction involves the coupling of D1R to $G_{\alpha s}$ to activate adenylyl cyclase (AC) which produces cyclic AMP (cAMP) which, in turn, activates protein kinase A (PKA). PKA can then phosphorylate a variety of substrate proteins, including the related proteins inhibitor-1 (I-1) and dopamine- and cAMP-regulated phosphoprotein, 32 kDa (DARPP-32). When I-1 is phosphorylated at threonine 35 (Thr35), or DARPP-32 is phosphorylated at threonine 34 (Thr34), they become potent inhibitors of protein phosphatase 1 (PP1), a serine/threonine phosphatase (F. L. Huang and W. H. Glinsmann, 1976; H. C. Hemmings, Jr. et al., 1984). Active PP1 can dephosphorylate any number of downstream effectors, including glutamate receptors (G. L. Snyder et al., 1998; Z. Yan et al., 1999), $GABA_A$ receptors (Z. Yan and D. J. Surmeier, 1997; J. Flores-Hernandez et al., 2000), calcium channels (D. J. Surmeier et al., 1995) and cAMP response element-binding (CREB) (D. Genoux et al., 2002). Many of

the functional outcomes of D1R stimulation depend on I-1, DARPP-32 and PP1 (P. Greengard et al., 1999; Z. Yan et al., 1999; J. Flores-Hernandez et al., 2000; G. L. Snyder et al., 2000; J. Flores-Hernandez et al., 2002). Thus, it is important to determine their localization throughout the dlPFC to compare with D_1 and D_5.

Inhibitor-1 and DARPP-32

I-1 and DARPP-32 are two phosphoproteins which share many properties: both are heat and acid stable (F. L. Huang and W. H. Glinsmann, 1976; S. I. Walaas et al., 1983), both share a high degree of amino acid sequence homology (A. Aitken et al., 1982; K. R. Williams et al., 1986), and both become potent inhibitors of PP1 when phosphorylated at Thr35 or Thr34, respectively (G. A. Nimmo and P. Cohen, 1978; H. C. Hemmings, Jr. et al., 1984). In the striatum, these proteins are crucial for mediating the downstream effects of D1R stimulation. For example, D1R agonist prevents the "rundown" of AMPA receptor current in striatal neurons. This effect is mimicked by Thr34 phosphorylated DARPP-32 (Z. Yan et al., 1999). D1R activation in neostriatal neurons also results in increased phosphorylation of the $GABA_A$ receptor, which enhances GABA currents. In DARPP-32 knockout mice, this effect of D1R agonists on GABA currents was diminished (J. Flores-Hernandez et al., 2000). Changes in I-1 and DARPP-32 also affect animal behavior. Mice with a deletion of DARPP-32 or a deletion of I-1 have decreased conditioned place preference to cocaine (V. Zachariou et al., 2002). However, some differences between the two have emerged. I-1 and DARPP-32 have different distributions in cortical and non-cortical tissues (H. C. Hemmings, Jr. and P. Greengard, 1986; E. L. Gustafson et al., 1991; H. C. Hemmings, Jr. et al., 1992), they are differentially regulated by kinases other than PKA (F. Desdouits et al., 1995; C. Nguyen

et al., 2007a), and genetic deletion of DARPP-32, but not I-1, affects lordosis (S. K. Mani et al., 2000). Because of their importance to the functional outcomes of D1R activation, it will be important to determine their localization across PFC neuropil and within PV and CR interneurons to compare with that of the D1R, and these experiments are described in Chapters 4 and 5 of this dissertation.

Protein Phosphatase 1

Protein phosphatase-1 (PP1) is a serine/threonine phosphatase involved in many cellular processes including glycogen metabolism, RNA transcription, protein synthesis, cellular division, and apoptosis (reviewed in J. B. Aggen et al., 2000; P. T. Cohen, 2002; H. Ceulemans and M. Bollen, 2004). In neurons, PP1 influences neurite outgrowth (C. J. Oliver et al., 2002), synapse formation (F. Malchiodi-Albedi et al., 1997) and neurotransmission (reviewed in P. Greengard et al., 1999; N. E. Price and M. C. Mumby, 1999; R. J. Colbran, 2004). PP1 regulates the coupling of D1 to $G_{\alpha s}$ (X. Zhen et al., 2001) and regulates AMPA (Z. Yan et al., 1999; G. L. Snyder et al., 2000), NMDA (G. L. Snyder et al., 1998) and $GABA_A$ receptors (J. Flores-Hernandez et al., 2000), as well as calcium currents (D. J. Surmeier et al., 1995). PP1 is also critical for synaptic plasticity, especially long-term depression (R. M. Mulkey et al., 1994; W. Morishita et al., 2001).

PP1 consists of a catalytic subunit that can interact with over 50 regulatory or scaffolding proteins, and these binding partners specify localization, substrate selectivity and/or overall activity (P. T. Cohen, 2002). For example, spinophilin (P. B. Allen et al., 1997), neurabin (H. Nakanishi et al., 1997) and yotiao (J. W. Lin et al., 1998) are three neuronal PP1 scaffolding proteins. Scaffold-mediated localization of PP1 plays an

important role in the control of NMDA currents (R. S. Westphal et al., 1999) and dopaminergic regulation of AMPA currents (Z. Yan et al., 1999). The distribution of spinophilin and neurabin in primate prefrontal cortex (PFC) overlaps considerably, but not completely. Both scaffolding proteins are concentrated in spines but are also found to a lesser extent in dendrites, glia and preterminal axons. However, only neurabin is found in axon terminals. Conversely, spinophilin, but not neurabin, is located within parvalbumin-containing interneurons (E. C. Muly et al., 2004c; E. C. Muly et al., 2004a). These data highlight the potential functional importance of PP1 localization in neuronal signal transduction, and suggest a complex and highly specific targeting of PP1 to a variety of neuronal compartments.

There are four isoforms of PP1: PP1α, PP1β, PP1γ1 and PP1γ2. These isoforms differ in scaffolding protein binding preference (L. B. MacMillan et al., 1999; R. T. Terry-Lorenzo et al., 2002; L. C. Carmody et al., 2004), regulation by protein kinase C (N. Takizawa et al., 1997) and protein expression levels in response to neurodegenerative-like cellular stress (F. C. Amador et al., 2004). PP1γ2 is specifically localized to the testes (H. Shima et al., 1993), and PP1β is enriched in muscle (G. Moorhead et al., 1998), though it has been identified in the brain (S. Strack et al., 1999; J. R. Bordelon et al., 2005). It is PP1α and PP1γ1 which are highly enriched in the brain and appear to be specifically enriched in dendritic spines, the major postsynaptic element in the brain (E. F. da Cruz e Silva et al., 1995; C. C. Ouimet et al., 1995; E. C. Muly et al., 2001). Furthermore, a quantitative electron microscopic study has shown that the D_1 receptor has access to both PP1α and PP1γ1 in pyramidal cell spines (E. C. Muly et al., 2001). However, it is unknown how prevalent they are in PV and CR interneurons. In

Chapters 4 and 5 of this dissertation I describe their localization throughout the dlPFC neuropil, and their prevalence in PV and CR interneurons to compare with I-1, DARPP-32 and the D1R.

Figure 1-1

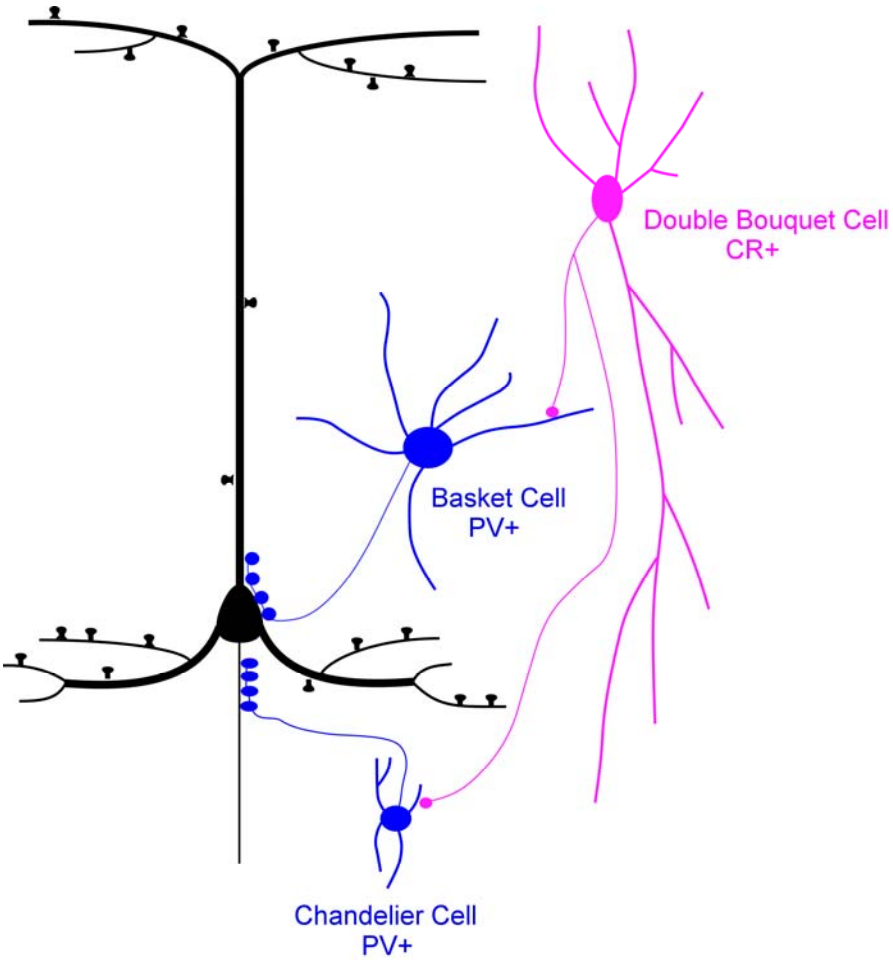

Figure 1-1. Schematic representation of the connections between pyramidal cells (black), PV interneurons (blue) and CR interneurons (pink). The pyramidal cell is the output neuron of the dlFPC, and its dendrites contain spines. PV-containing interneurons are basket cells and chandelier cells. Basket cells terminate on the perisomatic region of pyramidal cells, whereas chandelier cells terminate on the initial axon segment of pyramidal cells. CR-containing interneurons are typically double-bouquet neurons which have vertically orientated dendrites. CR interneurons terminate onto other interneurons, including PV interneurons.

Figure 1-2

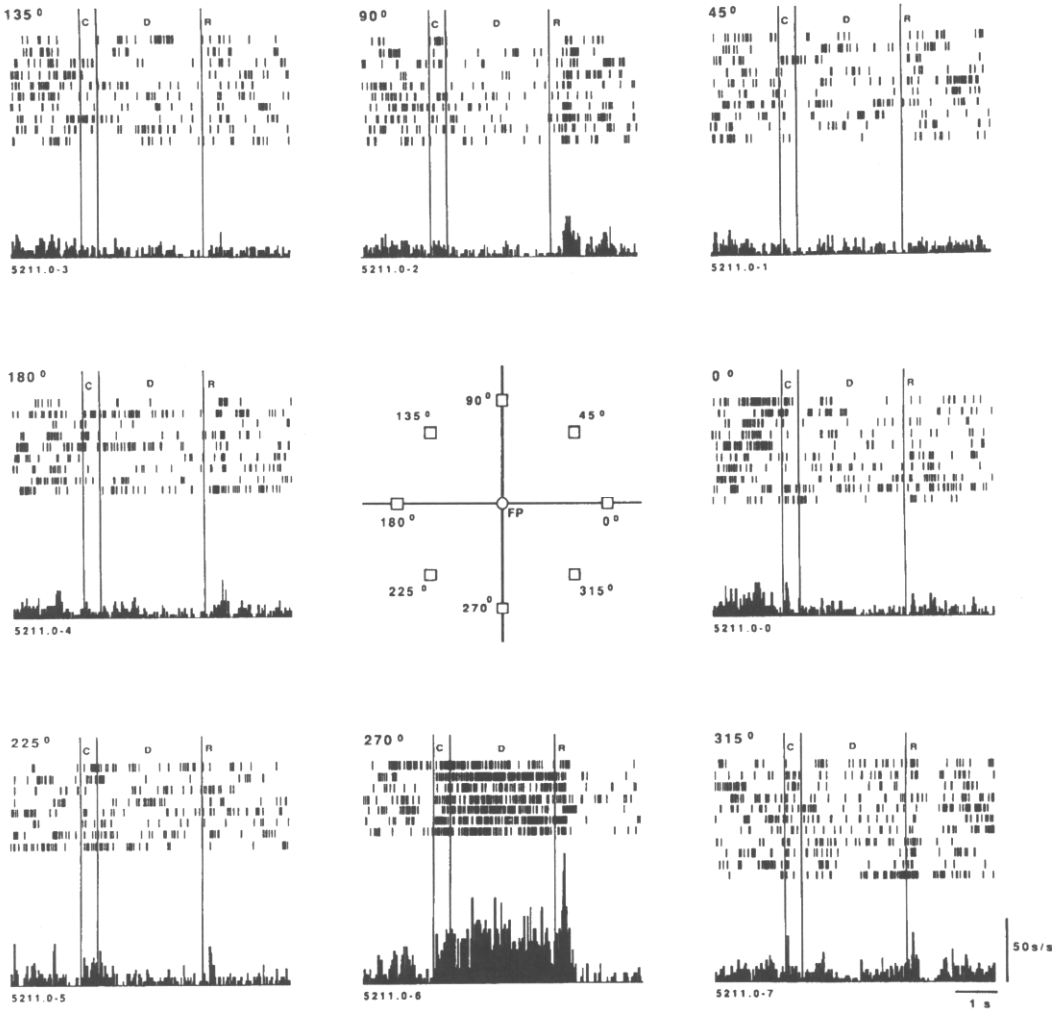

Figure 1-2. Example of a spatially and temporally tuned dlPFC pyramidal delay cell. This particular cell only responds during the delay period when the monkey has to remember a stimulus in the 270^{o} position. Abbreviations: C- cue, D- delay, R- response. Adapted from Funahashi et al. J Neurophisiology 1989: 331-349.

Figure 1-3

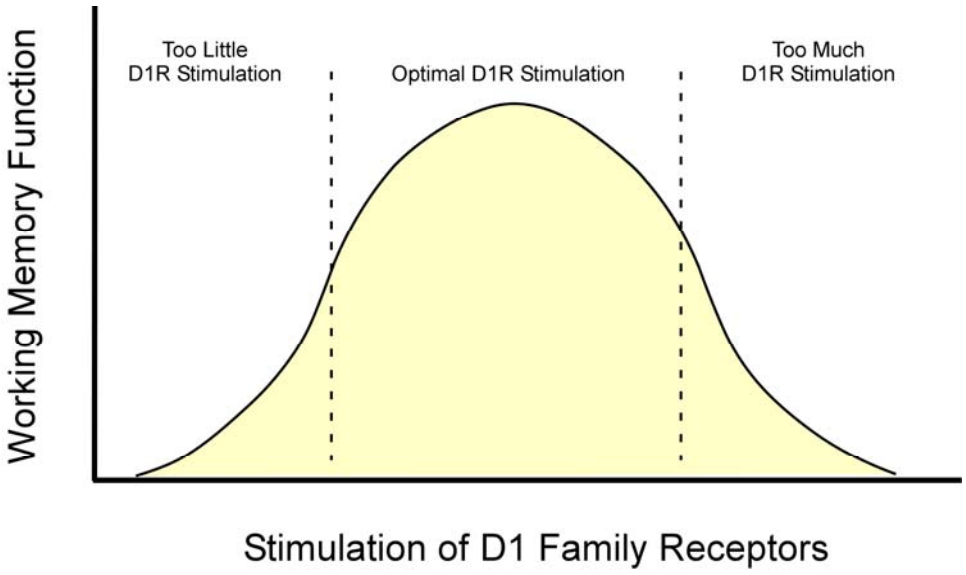

Figure 1-3. Graphical representation of the relationship between dlPFC D1R stimulation and WM ability. When there is too little available dopamine, and thus too little D1R stimulation, WM is poor. Similarly, when there is too much dopamine, and thus too much D1R stimulation, WM is also poor. It is intermediate levels of D1R stimulation that result in optimal WM performance.

Figure 1-4

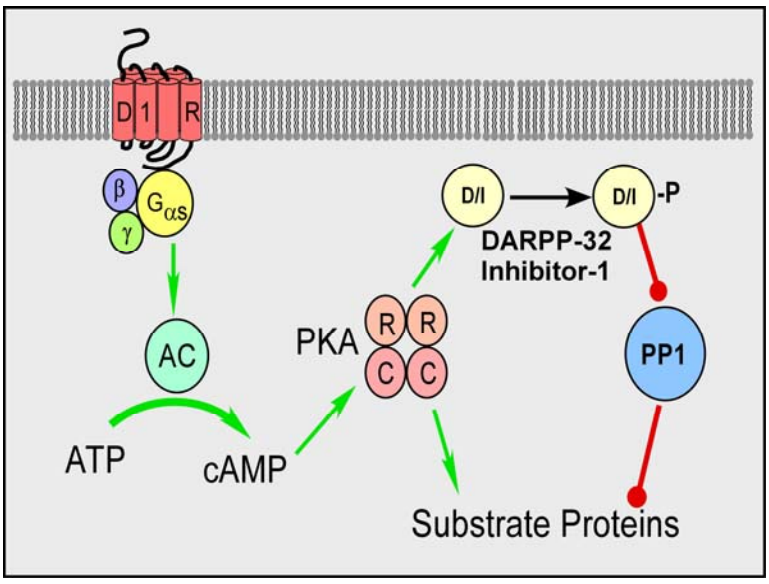

Figure 1-4. Schematic representation of D1R signal transduction pathway. Green arrows indicate activation steps, and red arrows indicate inhibitory steps. Abbreviations: AC- adenylyl cyclase, ATP- adenosine triphosphate, R- regulatory PKA subunit, C- catalytic PKA subunit.

Chapter 2

Localization of D_1 and D_5 in the neuropil of *Macaca mulatta* prefrontal cortical area 9

Adapted from Bordelon-Glausier JR, Khan ZU and Muly EC "Quantification of D_1 and D_5 dopamine receptor localization in layers I, III and V of *Macaca mulatta* prefrontal cortical area 9: co-expression in dendritic spines and axon terminals." J Comp Neurol. (2008) June 20; 508(6): 893-905

Introduction

Dopaminergic neurotransmission in the prefrontal cortex (PFC) is required to perform working memory (WM) tasks (T. J. Brozoski et al., 1979). In fact, depletion of dopamine in the PFC impairs WM almost as severely as PFC ablation (T. J. Brozoski et al., 1979). Though dopamine can signal via five distinct receptor subtypes (reviewed in C. Missale et al., 1998), the D1 family of dopamine receptors (D1R) is the most crucial for mediating dopamine's effects on WM ability (T. Sawaguchi and P. S. Goldman-Rakic, 1991, 1994; T. Sawaguchi, 2001a). Intriguingly, there is a complex relationship between D1R stimulation and WM performance, such that too little or too much D1R activation results in impaired WM abilities (reviewed in P. S. Goldman-Rakic et al., 2000). Given the importance of D1R activity for proper PFC functioning, it is critical to fully understand their roles within PFC cortical circuitry.

There are two subtypes of D1R, D_1 and D_5 (D. K. Grandy et al., 1991; R. K. Sunahara et al., 1991; M. Tiberi et al., 1991). D_1 and D_5 share 80% homology in their transmembrane domain, and they both primarily couple to $G_{\alpha s}$ (J. W. Kebabian and D. B. Calne, 1979; M. Tiberi et al., 1991). Currently available pharmacological tools do not differentiate D_1 and D_5. However, evidence for important functional differences between them have emerged (M. Tiberi and M. G. Caron, 1994; G. Dziewczapolski et al., 1998; F. Liu et al., 2000; F. J. Lee et al., 2002; D. Centonze et al., 2003; F. Laplante et al., 2004), including a 10-fold higher affinity for dopamine exhibited by the D_5 receptor (R. K. Sunahara et al., 1991; R. L. Weinshank et al., 1991). Intriguingly, there is a complex relationship between D1R stimulation and WM performance, such that too little or too much D1R activation results in impaired WM abilities (reviewed in P. S. Goldman-Rakic

et al., 2000). The mechanism which underlies this "inverted-U" relationship is unknown, but differences in D_1 and D_5 localization across the PFC neuropil may contribute.

I began studying D_1 and D_5 localization by determining a localization profile for each D1R in layers I, III and V across all components of the neuropil in prefrontal cortical area 9. Moreover, to determine if dopaminergic neurotransmission via the D1R can occur at distinct or overlapping axo-spinous synapses, I determined the extent of their co-localization to spines and axon terminals. In order to better correspond to the available physiological data, I performed these experiments in layer III, area 9 of macaque PFC. The data demonstrate that the D_1 and D_5 receptors are not restricted to spines and dendrites, respectively. Moreover, the data shows that they co-localize within dendritic spines and axon terminals such that the D_5 receptor is always present with the D_1 receptor in these elements, but not vice versa.

Materials and Methods

Antisera

Two antibodies were used in this study. The rat anti- D_1 antiserum (Sigma-Aldrich, St. Louis, MO, #D187) was prepared against a 97 amino acid synthetic peptide corresponding to the C-terminus of the human D_1 receptor. The antiserum stains 2 major bands at 40-45 and 65-75 kD (S. M. Hersch et al., 1995), and all staining at the light and electron microscopic levels was abolished when the antiserum was preincubated with 0.5mg/ml of D_1-GST fusion protein (J. F. Smiley et al., 1994). The D_5 antiserum was a rabbit polyclonal antiserum raised against residues 428-438 of the D_5 receptor. This sequence is common to both rat and human D_5 receptors. This antiserum reacts to D_5-

expressing recombinant Sf9 cells but not Sf9 cells expressing D_1, D_2, D_3 or D_4 (Z. U. Khan et al., 2000). Western blot in macaque PFC, striatum and hippocampus labeled a single band with a molecular weight of approximately 53-54 kD (Fig. 2-1A), in line with the predicted molecular weight of the D_5 receptor of approximately 53 kD (R. K. Sunahara et al., 1991; M. Tiberi et al., 1991). Finally, immunohistochemical staining of macaque PFC was abolished when the antiserum was pre-incubated with the cognate peptide (Fig. 2-1B,C)

Western blotting

Tissue from one male *Macaca mulatta* monkey, who was 1.13 years old at the time of sacrifice, was used for immunoblotting. The Western blotting was performed as described previously (E. C. Muly et al., 2004b). Briefly, the animal was sacrificed by pentobarbital overdose (100 mg/kg), and blocks of various brain regions were frozen. Samples of PFC, striatum and hippocampus were dounce homogenized in buffer containing 140 mM KCl, 10 mM glucose, 1.2 mM $MgCl_2$, 10mM HEPES, pH 7.4, with a cocktail of protease inhibitors added. The homogenate was centrifuged, pellet discarded, and the supernatant was assayed for protein concentrations using a colormetric assay (Bio-Rad Laboratories, Hercules, CA). The samples were subjected to sodium dodecyl sulfate-polyacrylamine gel electrophoresis. Each lane was loaded with 20 μg of protein sample, and the gel was run for 50 minutes at 200 V. The gel was then transferred to PVDF membrane. The membrane was rinsed, blocked, and probed with rabbit anti-D_5 (used at 1:300). After rinsing, the membrane was incubated with horseradish peroxidase (HRP)-conjugated secondary antibody (HRP-goat anti-rabbit IgG, 1:10000, Bio-Rad). Labeling was revealed by chemiluminescence. A ladder of markers was used to estimate

the molecular weight of the labeled bands (SeeBlue plus 2, Invitrogen). Images of the Western blots in TIFF format were imported into an image processing program (Canvas v.8, Deneba) where the image was cropped and labels were added.

Animals and preparation of tissue for immunohistochemistry

Tissue from eight *Macaca mulatta* monkeys was used for this study. The care of the animals and all anesthesia and sacrifice procedures in this study were performed according to the National Institutes for Health Guide for the Care and Use of Laboratory Animals and were approved by the Institutional Animal Care and Use Committee of Emory University. The animals were sacrificed with an overdose of pentobarbital (100mg/kg) and then perfused with a flush of Tyrode's solution. The flush was followed by 3 to 4 liters of fixative solution of 4% paraformaldehyde/0.1-0.2% glutaraldehyde/0-0.2% picric acid in phosphate buffer (0.1M, pH 7.4; PB). The brain was blocked and post-fixed in 4% paraformaldehyde for 2-24 hours. Coronal, 50 μm thick vibratome sections of prefrontal cortical area 9 (A. Walker, 1940) were cut and stored frozen at -80^{o}C in 15% sucrose until immunohistochemical experiments were performed.

Single-label immunohistochemistry

Single-label immunoperoxidase labeling was performed using rat anti-D_1 at a 1:500 dilution or rabbit anti-D_5 antisera at 1:500. The single-label immunoperoxidase labeling for D_1 and D_5 was performed as described previously (E. C. Muly et al., 1998). Briefly, sections were thawed, incubated in blocking serum (3% normal goat serum, 1% bovine serum albumin, 0.1% glycine, 0.1% lysine in 0.01 M phosphate buffered saline, pH 7.4) for 1 hour and then placed in primary antiserum diluted in blocking serum. After 36 hours at 4^{o}C, the sections were rinsed and placed in a 1:200 dilution of biotinylated donkey ant-rat IgG (Jackson Immuno Research, West Grove, PA) for D_1 or goat anti-

rabbit IgG (Vector, Burlingame, CA) for D_5 for 1 hour at room temperature. The sections were then rinsed, placed in avidin-biotinylated peroxidase complex (ABC) (ABC Elite, Vector, Burlingame, CA) for 1 hour at room temperature, and then processed to reveal peroxidase using 3,3'-diaminobenzidine (DAB) as the chromagen. Sections were then post-fixed in osmium tetroxide, stained *en bloc* with uranyl acetate, dehydrated, and embedded in Durcupan resin (Electron Microscopy Sciences, Fort Washington, PA). Selected regions were mounted on blocks, and ultrathin sections were collected onto pioloform-coated slot grids and counterstained with lead citrate. Control sections processed as above except for the omission of the primary immunoreagent, did not contain DAB label upon electron microscopic examination.

Six *Macaca mulatta* monkeys in total were processed for D_1 layers I, III and V, with four in each condition. Four of the six were female, and the age range was 2.14 - 14.75 years. No differences in receptor localization related to monkey age were observed. Four monkeys were processed for D_5 layers I and III, and two were male. The monkeys ranged from 2.14 - 9 years of age, again no differences in receptor localization related to monkey age were observed. Three monkeys were processed for D_5 layer V, two of which were males. The monkeys ranged from 2.14 - 4.5 years of age.

Double-label immunogold/DAB immunohistochemistry

To examine the possibility of co-localization of the two D1R subtypes, I performed double-label immunogold/DAB experiments. In one condition D_1 was labeled with immunogold, and D_5 was labeled with DAB. In a second condition the chromagens were reversed. PFC tissue sections from area 9 were thawed and rinsed in PBS. They were incubated in blocking serum (3% normal goat serum, 1% bovine serum albumin,

0.1% glycine, 0.1% lysine and 0.5% fish gelatin in 0.01 M phosphate buffered saline, pH 7.4) for one hour and then placed in the primary antiserum diluted at the same concentrations as the single label experiments overnight at 4^{o}C. The sections were removed from the primary antiserum, rinsed in PBS and placed in secondary antiserum (1nm gold conjugated goat anti-rat, used at 1:100, Nanoprobes, Yaphank, NY and biotinylated goat anti-rabbit, used at 1:200, Jackson Immuno Research, West Grove, PA; 1nm gold conjugated goat anti-rabbit, used at 1:100, Nanoprobes, Yaphank, NY and biotinylated donkey anti-rat, used at 1:200, Jackson Immuno Research, West Grove, PA) overnight at 4^{o}C. The tissue was then rinsed in PBS, placed in 2% glutaraldehyde for 20 minutes, rinsed in PBS, rinsed in 2% acetate buffer, silver-intensified for four minutes (HQ silver, Nanoprobes, Yaphank, NY), then rinsed in acetate buffer and in PBS. The sections were incubated in ABC overnight at 4^{o}C and reacted in the same manner as the single-label material.

Double-label cocktail immunohistochemistry

In order to quantify the extent of co-localization of D_1 and D_5, tissue sections were incubated in a cocktail of the primary immunoreagents rat anti-D_1 and rabbit anti-D_5 at a dilution of 1:500 and compared to tissue sections that were incubated with rat anti-D_1 alone or rabbit anti-D_5 alone at a dilution of 1:500. Four *Macaca mulatta* monkeys in total were used for these experiments, with three monkeys processed for each condition. Three of the four monkeys were male, and the monkeys ranged from 2.83 – 9 years of age. This cocktail procedure has been described in detail (E. C. Muly et al., 2001), and has been used in subsequent studies (W. Lei et al., 2004; D. A. Mitrano and Y. Smith, 2007). Briefly, the tissue sections in the cocktail condition were incubated with both

primary antisera, then in a cocktail of biotinylated secondary IgGs and in ABC to reveal D_1 and D_5. DAB was used as the chromagen for both D_1 and D_5. The D_1 alone and D_5 alone conditions were processed as described above.

Analysis of material

To determine the localization profile, blocks of tissue from layers I, III and V of cortical area 9 were made and cut in ultrathin sections that were examined using a Zeiss EM10C electron microscope. Regions of the grids containing neuropil were selected based on the presence of label and adequate ultrastructural preservation. Fields of immunoreactive elements in the neuropil were randomly selected, and images were collected at a magnification of 31,500 using a Dualvision cooled CCD camera (1300 x 1030 pixels) and Digital Micrograph software (version 3.7.4, Gatan, Inc., Pleasanton, CA). Images selected for this dissertation were saved in TIFF format and imported into an image processing program (Canvas 8; Deneba Software, Miami, FL). The contrast was adjusted, and the images were cropped to meet size requirements.

On each micrograph, DAB-labeled profiles were identified and classified as spines, dendrites, terminals, axons, glia or unknown based on ultrastructural criteria (A. Peters et al., 1991). Profiles were identified as spines based on size (0.3 - 1.5 μm in diameter), presence of spine apparatus, absence of mitochondria or microtubules and, in some cases, the presence of asymmetric synaptic contacts. Dendrites were identified by their larger size (0.5 μm or greater in diameter), presence of microtubules, mitochondria and, in some cases, synaptic contacts. Axon terminals were characterized by the presence of numerous vesicles, mitochondria and occasionally a pre-synaptic specialization. Pre-terminal, unmyelinated axons were identified by their small size (0.1 – 0.3 μm in

diameter), regular round shape and occasional presence of synaptic vesicles or neurofilaments. Glial profiles were identified based on their unusual shape, which appears to fill in the space between nearby profiles and a relatively clear cytoplasm which occasionally contained numerous glial filaments and mitochondria. Profiles that could not be clearly characterized based on these criteria were considered unknown profiles. Profiles that could not be clearly characterized based on these criteria were considered unknown profiles. The number of immunoreactive profiles was tabulated and the distributions (excluding the unknown profiles) compared with a Chi-square analysis.

For D_1 a total of 295 micrographs representing 1,800 μm^2 of layer I were analyzed across four monkeys. Five hundred twenty-eight labeled profiles were counted, and each monkey contributed 123-147 profiles. Three hundred sixty micrographs representing 2196 μm^2 of layer III were analyzed across four monkeys. Five hundred forty-four labeled profiles were counted. Three of the monkeys contributed 100-141 labeled profiles each, and one monkey contributed 263. Two hundred ninety-five micrographs representing 1,800 μm^2 of layer V were analyzed across four monkeys. Five hundred sixteen labeled profiles were counted, and each monkey contributed 108-177 labeled profiles.

For D_5 a total of 290 micrographs representing 1769 μm^2 of layer I were analyzed across four monkeys. Four hundred and seventy labeled profiles were counted. Two of the monkeys contributed 116 labeled profiles each, one contributed 70 labeled profiles, and one contributed 168 labeled profiles. Three hundred forty micrographs representing 2074 μm^2 of layer III were analyzed across four monkeys. Four hundred ninety-eight labeled profiles were counted, and each monkey contributed 104-149 labeled profiles.

Finally, 316 micrographs representing 1,928 μm^2 of layer V were analyzed across three monkeys. Four hundred eighty-nine labeled profiles were counted, and they contributed 73, 205 and 211 labeled profiles each.

Analysis of the immunogold/DAB material was performed on blocks from layer III of area 9. I examined ultrathin sections from the surface of each block where both immunoperoxidase label and immunogold label were visible. Because immunogold label can be noisy, the very surface of each block where non-specific gold particles tend to accumulate was avoided. The immunogold label in a given structure was compared to the surrounding background level of immunogold labeling, as well as the size of the silver intensified gold particles. If the profile qualitatively contained more immunogold label than the background level, the immunogold labeling was deemed acceptable.

Blocks of tissue from layer III cortical area 9 were made for the D_1/D_5 cocktail condition, D_1 alone and D_5 alone conditions. Fields of the neuropil were randomly selected, and images were collected at a magnification of 20,000. An ANOVA sample size analysis (SigmaStat, Version 2.03, SPSS Inc.) indicated that the minimum sample size required to have a statistical power of 80% and a minimum detectable difference in group means of seven was 239 images; therefore, we analyzed 239 images in the D_1 alone condition, 297 images in the D_5 alone condition and 279 images in the D_1/D_5 cocktail condition. In each experimental condition, the number of micrographs analyzed from each monkey was similar. On each micrograph, spines and axon terminals were identified using the previously described ultrastructural criteria (A. Peters et al., 1991), then classified as immunopositive or immunonegative, and the percentage of identified spines or terminals that were immunopositive was calculated. The mean percentage of

immunopositive spines and axon terminals were tabulated for each condition and compared across antigen conditions using an ANOVA. The results are reported as mean ± standard error.

Results

Laminar and subtype specific variation in subcellular distributions of D1R

The localization of D_1 and D_5 in the PFC has been previously described in detail at the light microscopic level (C. Bergson et al., 1995a; C. Bergson et al., 1995b; E. C. Muly et al., 1998; Z. U. Khan et al., 2000). Briefly, D_1 immunolabeling is found in the Golgi apparatus of labeled perikarya and extends into the proximal dendrites. D_5 immunolabeling is also present in the cell soma and strongly labels dendrites. At the electron microscopic level, we identified label for both D_1 and D_5 in the soma. D_1-immunoreactivity (-IR) was associated with internal membranes, namely the Golgi apparatus (Fig. 2-2A). D_5-IR was also associated with internal membranes of the soma (Fig. 2-2B), as well as the plasma membrane (Fig. 2-2C).

I examined the localization of D_1 and D_5 in *Macaca mulatta* PFC neuropil in layers I, III and V of prefrontal cortical area 9 to determine if their localization patterns differ across cortical layers. Each receptor was seen in spines, dendrites, axon terminals, pre-terminal axons and glia in each cortical layer (Figs. 2-3 and 2-4); however, the degree to which each receptor was localized in these compartments appeared to differ. Accordingly, I quantified the distribution of each receptor in three different layers of PFC to create a localization profile for each receptor. The pattern of D_1 localization in various cellular compartments in layers I, III and V differed significantly (Fig. 2-5A; $\chi^2 = 41.728$;

$p<.0001$). Post-hoc testing revealed that D_1 was more frequently identified in spines of layer III than layers I or V, in pre-terminal axons of layer V than layers I or III and in glia of layer I than layers III or V. In addition, the pattern of D_5 localization in cellular compartments in layers I, III and V differed significantly (Fig. 2-5B; $\chi^2= 45.986$; $p<.0001$). Post-hoc testing revealed that D_5 was more frequently identified in dendrites of layer III than layer I, in axon terminals of layer I than layers III and V, in pre-terminal axons of layer V than layers I and III and in glia of layer I than layers III and V. Thus, in layer III, both D1R subtypes are enriched in dendritic structures where they can modulate the response of neurons.

The distributions of D_1 and D_5 observed in the laminar analyses appeared to be markedly different, and I tested this by comparing the distributions of D_1 and D_5 in layer III of area 9. Layer III was chosen for the remaining experiments because it is a major site of cortical integration (K. S. Rockland and D. N. Pandya, 1979; J. H. Maunsell and D. C. van Essen, 1983; M. F. Kritzer and P. S. Goldman-Rakic, 1995) and is altered in patients with schizophrenia (L. A. Glantz and D. A. Lewis, 2000; D. A. Lewis et al., 2003). Within layer III of PFC area 9, the patterns of D_1 and D_5 labeling differed significantly (Fig. 2-6; $\chi^2= 74.592$; $p<.0001$). Post-hoc testing revealed that D_1 immunoreactivity was more commonly found in spines and pre-terminal axons, while D_5 immunoreactivity was more commonly found in dendrites and glia.

Our quantitative analyses indicate that while the D_1 receptor is found in spines to a greater extent than D_5, both D_1 and D_5 are found to a large degree in both dendritic spines and shafts. Thus, once activated by dopamine, both are well positioned to modulate inputs to dendritic spines as well as the propagation of these signals through the

dendritic shafts to the cell soma. Furthermore, while less prominent, both D1R subtypes are positioned to play a role in modulating presynaptic actions.

Distribution of D_1 and D_5 in cortical spines and axon terminals

The quantitative analyses show that both receptors are present in spines and axon terminals and, as such, are positioned to mediate dopaminergic modulation of axo-spinous inputs to pyramidal cells both pre- and postsynaptically. An important question is whether the D_1 and D_5 receptors are located in the same or different populations of spines and axon terminals. Because of their different affinities for dopamine and the dose-response relationship of D1R stimulation and working memory function, we hypothesized that D_1 and D_5 receptors would be found in different populations of dendritic spines and axon terminals. In order to test this hypothesis, I used a double-label approach in which one receptor was revealed with pre-embedding immunogold and the other with DAB. Contrary to the hypothesis, I found spines containing both immunogold and DAB, and double labeled spines and axon terminals could be identified regardless of which chromagen was utilized (Fig. 2-7). These experiments suggest that D_1 and D_5 are co-localized in dendritic spines of prefrontal cortical area 9. However, there are reasons to be cautious in interpreting these experiments. While the different labels are distinguishable when examined with the electron microscope, pre-embedding immunogold labeling is less sensitive than immunoperoxidase labeling due to limited penetration of 1nm gold conjugates as well as the instability of silver intensifier in osmium treated material. This is especially problematic when lower abundance antigens are examined, such as dopamine receptors in neocortex, as compared to calcium-binding proteins (A. Galvan et al., 2006). In addition, it is our experience that immunoperoxidase

labeling is less robust in tissue that has been previously silver intensified. However, if silver intensification is performed after the immunoperoxidase reaction, it can nonspecifically deposit onto DAB, as demonstrated by the use of silver solutions to intensify DAB labeling (J. F. Smiley and P. S. Goldman-Rakic, 1993; R. Teclemariam-Mesbah et al., 1997). Thus it is very difficult to interpret the significance of single-labeled profiles in this double-labeled material. For these reasons, the extent of co-localization of the two receptors cannot be determined using these methods.

In order to quantify the degree to which the two receptors co-localize in spines and axon terminals, I used a cocktail labeling approach which has been successfully used to identify overlapping distributions of proteins (E. C. Muly et al., 2001; D. A. Mitrano and Y. Smith, 2007) as well as distinct distributions (W. Lei et al., 2004). The advantage of this procedure is that the labeling method used for both receptors (immunoperoxidase labeling) has the best and equal sensitivity and penetration (F. G. Wouterlood et al., 1993; A. Galvan et al., 2006). Material labeled with antiserum to D_1, D_5 or a cocktail of antisera to both receptors was randomly imaged, and the percentage of spines and terminals labeled for each receptor individually as well as for the two receptors combined was calculated. These values were then compared using an ANOVA. The percentage of spines in layer III of area 9 labeled individually for the two receptors or the cocktail differed significantly (Fig. 2-8A; $F_{2,812} = 8.418$, $p = .0002$), and post-hoc Scheffe tests confirmed that the percentage of spines labeled for D_5 was significantly less than for D_1 ($p = .0030$) and the cocktail ($p = .0016$). However, there was no significant difference between the percentage of spines labeled for D_1 or the cocktail of D_1 and D_5 ($p = .9996$). The finding that the percentage of spines labeled by D_1 and a cocktail of D_1 and D_5 is not

significantly different demonstrates that the D_5 receptor is found in a subpopulation of the D_1 positive spines. If D_1 and D_5 labeled separate populations of spines, the cocktail condition would label a higher percentage of spines than D_1 alone. This data indicates that both D_1 and D_5 are found together in approximately 14% of dendritic spines, and that D_1 is found in an additional 7% of prefrontal cortical area 9 layer III spines.

I also performed a double-label cocktail analysis for axon terminals in prefrontal cortical area 9 within layer III, as we had for dendritic spines. As seen in dendritic spine labeling, the percentage of axon terminals labeled for D_1, D_5 or the cocktail differed significantly (Fig. 2-8B; $F_{2,811} = 25.598$, $p<.0001$), and post-hoc Scheffe tests confirmed that the percentage D_5 labeled terminals was significantly less than D_1 ($p < .0001$) and the cocktail ($p < .0001$); however, there was no significant difference between D_1 and the cocktail ($p = .3396$). This data indicates that both D_1 and D_5 are found together in approximately 4% of axon terminals, and that D_1 is found in an additional 6% of prefrontal cortical area 9 layer III terminals

The synaptic type and postsynaptic structures of D1R-labeled axon terminals was examined. Of the 29 D_1 positive axon terminals which made identifiable synapses, 26 were asymmetric and three were symmetric. Twenty-three of the asymmetric synapses were onto unlabeled spines, while the remaining three were onto unlabeled dendrites. Two of the symmetric synapses were onto unlabeled dendrites, and the remaining D_1 positive axon terminal formed a symmetric synapse onto an unlabeled spine. Of the 24 D_5 positive axon terminals which made identifiable synapses, 23 were asymmetric and one was symmetric. Twenty-one of the asymmetric synapses were onto unlabeled spines, while the remaining two were onto unlabeled dendrites. The symmetric synapse was

formed onto a spine. Taken together, our data demonstrate that there are 3 populations of spines and axon terminals in area 9 of the macaque PFC defined by their presence or absence of D1R: those which contain both D_1 and D_5, those that contain only D_1 and those that contain neither D1R subtype.

Discussion

I have quantified the distributions of the D_1 and D_5 receptors within *Macaca mulatta* prefrontal cortical area 9 neuropil and determined their co-localization in dendritic spines and axon terminals. The data confirm the previously reported relative enrichment of D_1 in spines and D_5 in dendrites (C. Bergson et al., 1995b). However, my quantitative data indicate each receptor has a complex localization throughout the neuropil, including the D_1 receptor labeling spines and dendrites at equivalent frequencies. Furthermore, there is laminar specificity in the distributions of the two D1R subtypes in macaque prefrontal cortical area 9, a region where they are critical for working memory function. These laminar differences suggest a potential circuit specificity in their actions. Finally, a key finding of the current study is that the D1R are extensively co-localized to area 9 prefrontal cortical pyramidal cell spines and axon terminals, such that D_5 is always localized with D_1. This final result demonstrates that dopaminergic activation of the two D1R can modulate overlapping populations of synapses both presynaptically on terminals and postsynaptically on dendritic spines.

One finding of these studies is that the distribution of each D1R subtype differs across the area 9 cortical layers. The six layers of neocortex are heterogeneous in their cellular makeup, extrinsic and intrinsic connections (C. D. Gilbert, 1983; H. A. Swadlow,

1983); and these laminar differences are likely related to the observed differences in D1R localization. For example, the increased D1R labeling of glia in layer I compared to layers III and V may reflect the increased presence of glia in layer I versus other layers (S. M. Dombrowski et al., 2001). The extent of glial labeling observed in our study (10-25%) was unexpected; however, the presence of dopamine receptors, including D_1 and D_5, in cortical and striatal glial cells is well documented (P. Zanassi et al., 1999; B. Reuss and K. Unsicker, 2001; V. Brito et al., 2004; I. Miyazaki et al., 2004; U. Kumar and S. C. Patel, 2007), though one study did not find D_5 glial labeling in rat tissue (B. J. Ciliax et al., 2000). Dopamine has been shown to increase intracellular calcium levels in cortical glial cells (B. Reuss et al., 2001; B. Reuss and K. Unsicker, 2001), an effect which is blocked by pre-treatment with atypical neuroleptics (B. Reuss and K. Unsicker, 2001). The D1R agonist SKF 38393 stimulates G-protein coupling in rat spinal white matter (V. V. Venugopalan et al., 2006); induces cAMP production in rat, monkey and human striatal glia (R. J. Vermeulen et al., 1994) and rat cortical glia (P. Zanassi et al., 1999); and increases PKA activity in striatal glia (A. Li et al., 2006). Additionally, brain-derived neurotrophic factor specifically stimulates D_5 expression in mouse striatal astrocyte cultures (V. Brito et al., 2004). Moreover, recent research suggests methamphetamine has significant effects on gliogenesis in the medial PFC of rats (C. D. Mandyam et al., 2007). Thus, while research is on-going regarding glial D1R, a picture is emerging that dopaminergic agents and D1R activity in glia play a role in proper CNS functioning and can be disregulated in many CNS diseases (reviewed in N. J. Maragakis and J. D. Rothstein, 2006).

The D_5 receptor is present in layer I axon terminals to a greater extent than in layers III and V. While our data do not address the source of these axon terminals, layer I in particular receives input from the intralaminar thalamic nuclei (E. G. Jones, 1975; E. Rausell and C. Avendano, 1985) which expresses the D_5 receptor in rat, monkey and human brain (B. J. Ciliax et al., 2000; S. M. Clinton et al., 2005). The layer I D_5 positive terminals identified in the current study form asymmetric synapses predominately onto unlabeled dendritic spines, as would be expected from thalamic nuclei which also predominately form asymmetric axo-spinous synapses. Interestingly, lesions of the intralaminar nuclei in rats causes specific deficits in memory tasks (R. G. Mair et al., 1998), and D_5 receptors on the axon terminals from these nuclei may contribute to D1R modulation of cognition. D_1 and D_5 were also present in pre-terminal axons of layer V more so than layers I and III. The enrichment of these receptors in pre-terminal axons may represent a reservoir of D1R (D. Shakiryanova et al., 2006) destined for the axon terminals of corticostriatal or corticocortical projections.

Perhaps the most striking finding of the quantitative laminar analyses undertaken in this study is that D_1 labeled spines and D_5 labeled dendritic shafts are particularly common in prefrontal cortical area 9 layer III compared to layers I and V. Layer III is a major site of cortical integration (K. S. Rockland and D. N. Pandya, 1979; J. H. Maunsell and D. C. van Essen, 1983; M. F. Kritzer and P. S. Goldman-Rakic, 1995), and prefrontal cortical layer III pyramidal cells are modulated by dopamine and D1R antagonists (D. A. Henze et al., 2000; N. N. Urban et al., 2002). Furthermore, patients with schizophrenia show specific alterations in layer III (L. A. Glantz and D. A. Lewis, 2000; D. A. Lewis et al., 2003). The enrichment of D1R subtypes at sites of postsynaptic integration suggests

that D1R activity plays a particularly important role in modulating responses in layer III of the PFC.

Comparing the localization of D_1 and D_5, we show that the D_1 receptor antiserum labels spines more frequently than D_5, and the D_5 receptor antiserum labels dendrites more frequently than D_1. However, it is important to note that the D_1 receptor labels dendritic shafts at equivalent and greater frequencies than it labels dendritic spines across layers I, III and V. Electrophysiological studies have emphasized the importance of D1R dendritic localization in modulating PFC input in a spatially-dependent manner (J. K. Seamans and C. R. Yang, 2004). For example, activation of D1R on apical dendrites attenuates high-threshold Ca^{2+} spikes, thus attenuating the effects of inputs to these apical dendrites (C. R. Yang and J. K. Seamans, 1996). Our present study indicates that both the D_5 and D_1 receptors are present in dendritic shafts, and therefore both may be modulating ionic conductances on pyramidal cell dendrites. While we have not directly addressed whether both the D1R are expressed on the dendrite plasma membrane, studies in the rodent basal ganglia and basolateral amygdala and monkey PFC demonstrate the presence of the D_1 receptor on the plasma membrane of dendritic shafts (B. Dumartin et al., 2000; C. D. Paspalas and P. S. Goldman-Rakic, 2005; V. M. Pickel et al., 2006; Y. Hara and V. M. Pickel, 2007).

D1R activation in the PFC is critical for WM performance (reviewed in P. S. Goldman-Rakic, 1995); and D1R activation has a dose-dependent relationship with WM ability and neuronal activity, such that low levels of D1R activation results in low ability and activity, medium levels of D1R activation result in optimal WM ability and higher activity, and high levels of D1R activation result in diminished WM ability and lower

activity (S. Vijayraghavan et al., 2007). In this context, it is particularly germane to note that D_5 has been reported to have a 10- fold greater affinity for dopamine; however, the individual contributions of D_1 and D_5 to WM processes cannot be determined with currently available pharmacological tools. We have found that the D_1 receptor is located in approximately 20% of PFC spines (C. Bergson et al., 1995b; E. C. Muly et al., 2001), and that the D_5 receptor is located in approximately 14% of PFC spines. We expected the D1R subtypes to be found in different populations of spines, similar to the selective localization of the D_5, but not the D_1 or D_2 receptors, in the vicinity of subsurface cisterns of cell bodies in the macaque PFC (C. D. Paspalas and P. S. Goldman-Rakic, 2004). However, using a cocktail of the D_1 and D_5 antibodies, we have determined that the D_5 receptor is present in a subpopulation of those spines that contain the D_1 receptor. This observation has a number of implications regarding the dose-dependent relationship between D1R activation and PFC functioning. First, the spines with both D1R subtypes will have a larger dynamic response range to varying dopamine concentrations than spines expressing only D_1. However, it remains unknown whether the responses to D_1 and D_5 stimulation are simply additive within a spine, or if they result in distinct actions. Both receptors couple through G_s, therefore increasing levels of dopamine should result in a larger cAMP response. Additionally, there is growing evidence that G-protein coupled receptors can signal via heterodimers or oligomers (M. Bouvier, 2001; S. C. Prinster et al., 2005), including a D_1-D_2 heterodimer (M. Dziedzicka-Wasylewska et al., 2006). The quantitative cocktail and immunogold/DAB data demonstrate that D_1-D_5 heterodimers are possible (Fig. 2-6B). Biochemical studies will be required to determine if such interactions occur in the primate PFC.

Alternately, there is evidence that the two D1R subtypes can couple to different G- proteins (K. Kimura et al., 1995; A. Sidhu et al., 1998; Q. Wang et al., 2001), can differentially signal via protein kinase C and phospholipase C (P. Y. Yu et al., 1996; M. Paolillo et al., 1998; A. Jackson et al., 2005; X. Zhen et al., 2005) and are physically linked to different effector proteins (F. Liu et al., 2000; F. J. Lee et al., 2002). Moreover, precise targeting of signal transduction proteins via scaffolds has been shown to play an important role in neuronal signaling (R. S. Westphal et al., 1999; Z. Yan et al., 1999; G. Chen et al., 2004). These factors raise the possibility that D_1 and D_5 could induce distinct intracellular signals within the same spine, contributing to the complex relationship between D1R and WM. Indeed, the group I metabotropic glutamate receptors 1 and 5 are frequently co-localized, even though they both classically signal via the same second messenger cascade. Using subtype-specific pharmacological tools, it is now known that activation of each receptor leads to discrete neuronal responses when the two are co-localized (reviewed in O. Valenti et al., 2002; O. V. Poisik et al., 2003).

Electrophysiological studies indicate that activation of pre-synaptic D1R generally decreases excitatory and inhibitory neurotransmission (T. Momiyama and J. A. Sim, 1996; J. Behr et al., 2000; W. J. Gao et al., 2001; C. E. Young and C. R. Yang, 2005). Twenty-six of the 29 D_1-only containing axon terminals made asymmetric synapses; and 11.5% (3 of 26) of these D_1-positive axon terminals making asymmetric synapses targeted dendrites, while the remainder formed asymmetric synapses onto spines. This data is in strong agreement with a previously published study of D_1-positive axon terminals in the macaque PFC which found that 11.7% of D_1-positive axon terminals formed asymmetric synapses onto dendrites (C. D. Paspalas and P. S.

Goldman-Rakic, 2005). It is important to recognize that the data reported here on the distribution of D1R in the neuropil primarily reflects the distribution of these receptors in the most common cellular element in the PFC, which is the pyramidal projection neuron. Because certain populations of interneurons also show tuned delay responses during WM tasks (S. G. Rao et al., 1999, 2000), have been shown to contain the D_1 receptor (E. C. Muly et al., 1998) and can strongly modulate pyramidal cell output (J. S. Lund and D. A. Lewis, 1993; J. DeFelipe, 1997; A. V. Zaitsev et al., 2004; G. Gonzalez-Burgos et al., 2005a); determining the localization of D1R to specific classes of interneurons will prove to be helpful in understanding the circuitry mechanisms of D1R activation on neural activity.

Figure 2-1

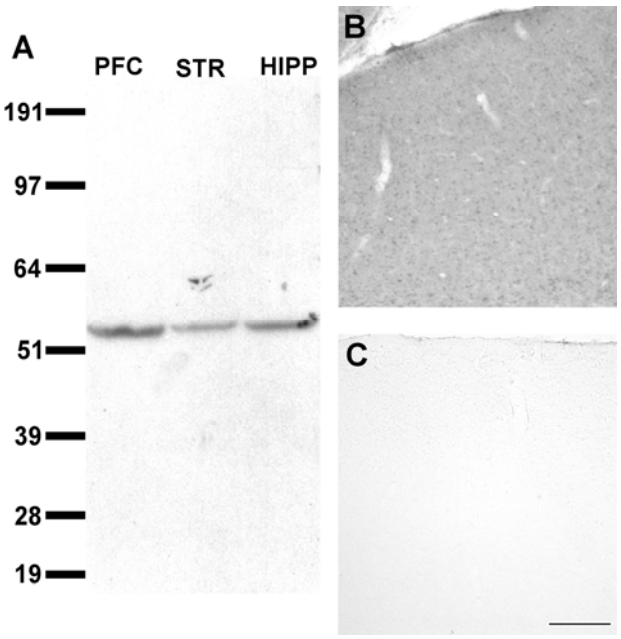

Figure 2-1. A: Western blot of *Macaca mulatta* prefrontal cortex (PFC), striatum (STR) and hippocampus (HIPP) showing that the D_5 antibody reacts only with a single protein band at a molecular weight of approximately 53 kD. **B:** Light electron microscopic image of typical D_5 staining in macaque PFC. **C:** D_5 staining is abolished in macaque PFC when the antiserum was pre-incubated with the cognate peptide. Scale bar is 200 μm.

Figure 2-2

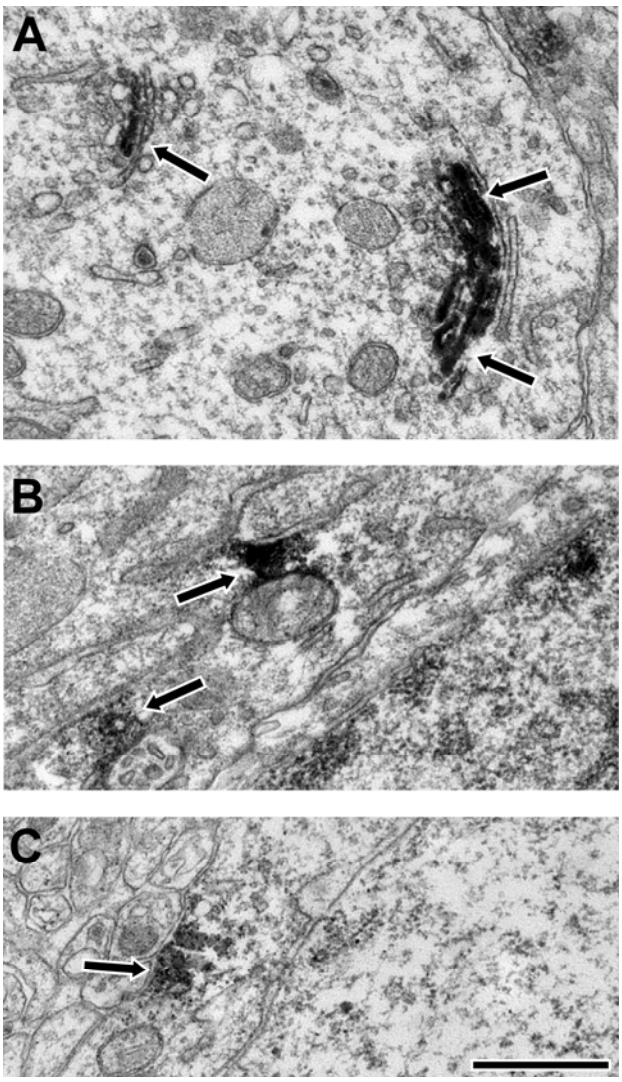

Figure 2-2. Electron micrographs illustrating typical somatic labeling. D_1 diaminobenzidine label (arrows) was limited to the Golgi apparatus in cell bodies (**A**), while D_5 immunoreactivity was associated with internal membranes such as the endoplasmic reticulum (**B**) as well as the plasma membrane (**C**). Scale bar is 500 nm.

Figure 2-3

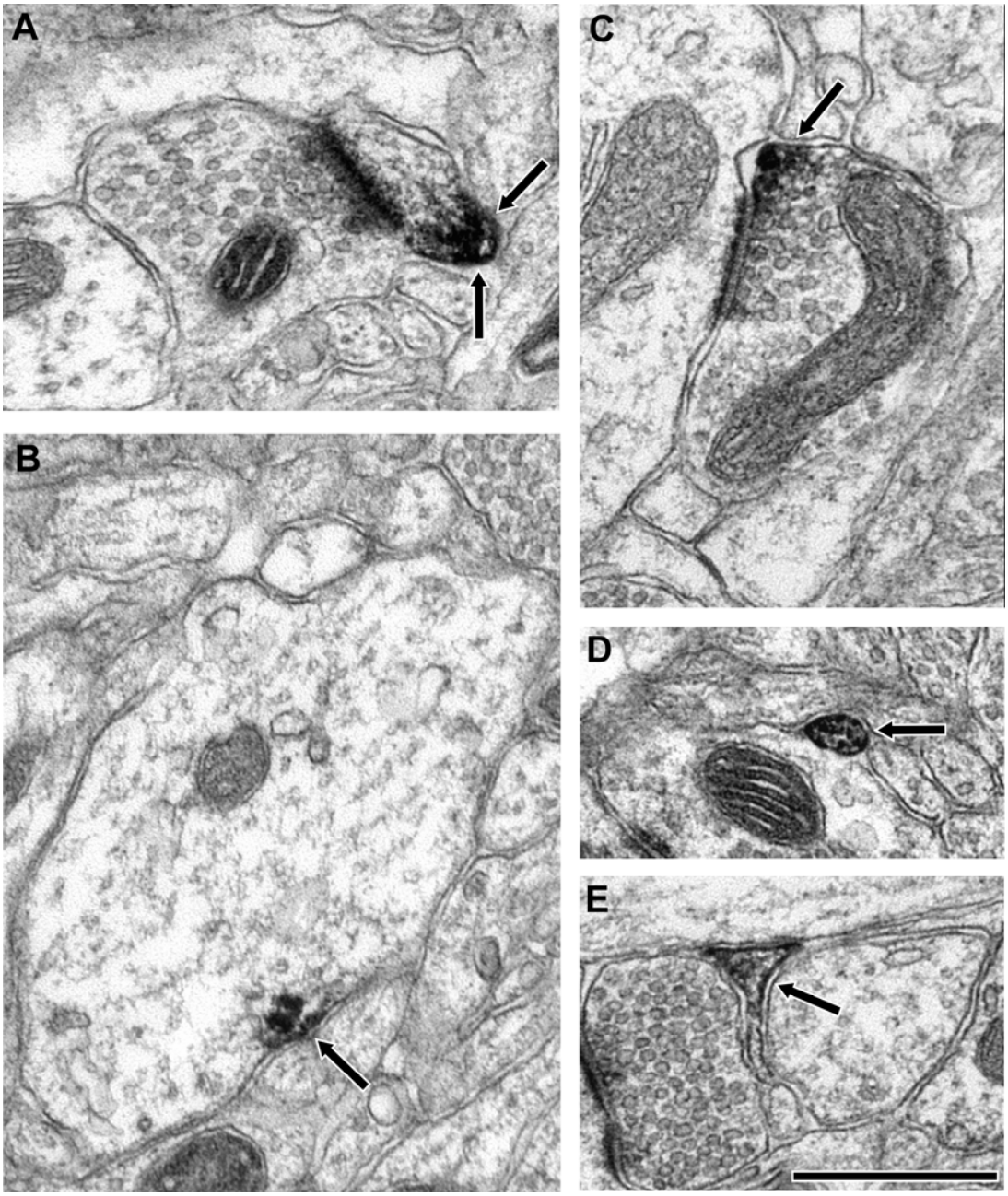

Figure 2-3. Electron micrographs illustrating examples of D_1 immunoreactivity in PFC area 9 neuropil. Diaminobenzidine label (arrows) was identified in spines (**A**), dendrites (**B**), axon terminals (**C**), pre-terminal axons (**D**) and glia (**E**) in each layer examined. Scale bar is 500 nm.

Figure 2-4

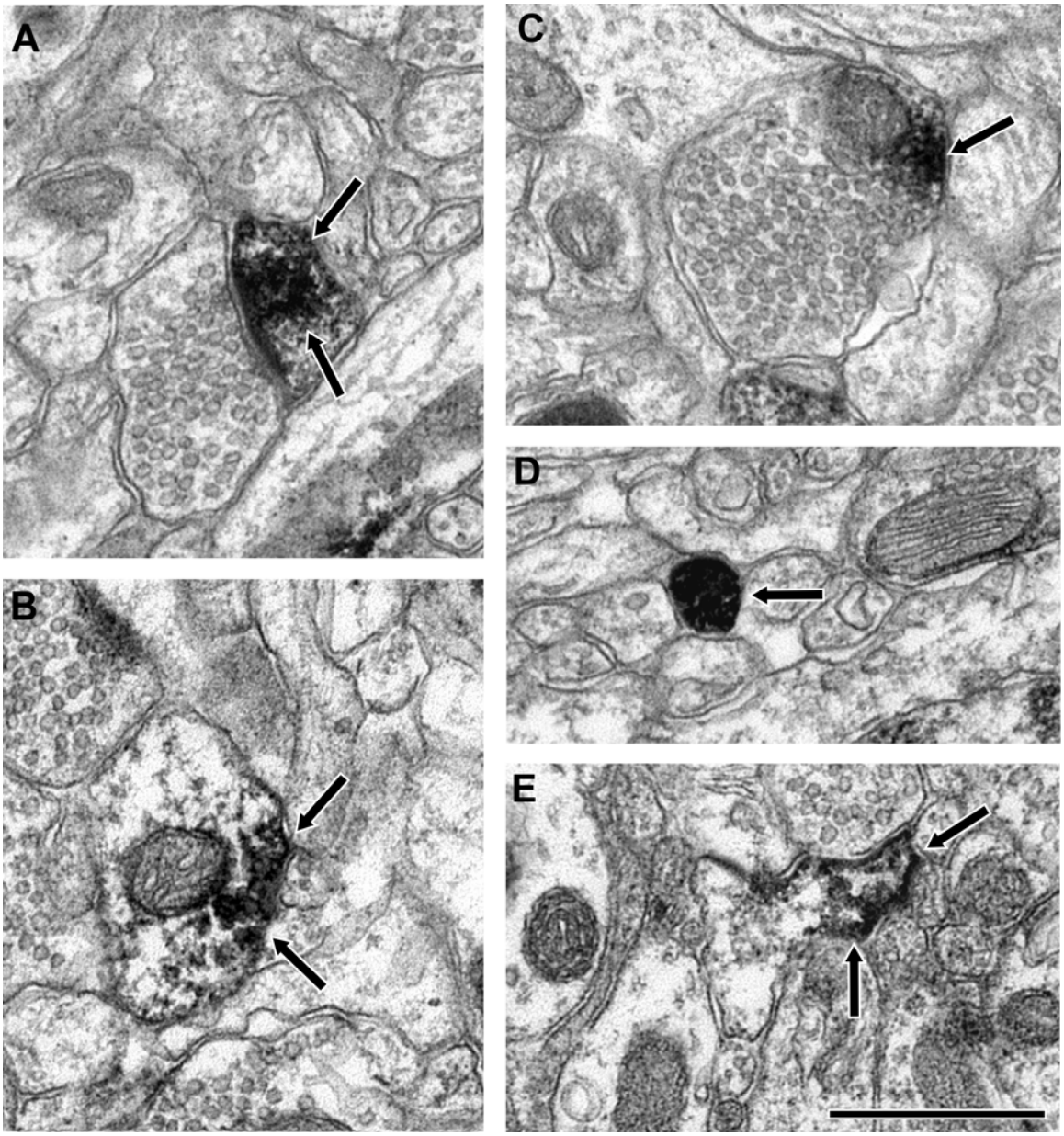

Figure 2-4. Electron micrographs illustrating examples of D_5 immunoreactivity in PFC area 9 neuropil. Diaminobenzidine label (arrows) was identified in spines (**A**), dendrites (**B**), axon terminals (**C**), pre-terminal axons (**D**) and glia (**E**) in each layer examined. Scale bar is 500 nm.

Figure 2-5

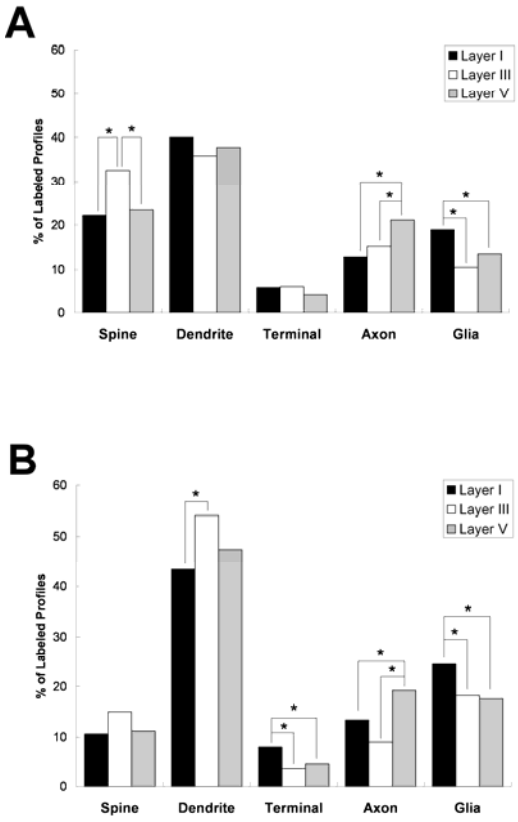

Figure 2-5. A: A histogram showing the relative abundance of D_1 in layers I, III and V in area 9 of the PFC. In layer I 528 profiles in 295 micrographs were examined; in layer III 544 profiles in 360 micrographs were examined; and in layer V 516 profiles in 295 micrographs were examined. The distribution of the D_1 receptor differed significantly across layers (χ^2= 41.728; p<.0001). **B:** A histogram showing the relative abundance of D_5 in layers I, III and V in area 9 of the PFC. In layer I 470 profiles in 290 micrographs were examined; in layer III 498 profiles in 340 micrographs were examined; and in layer V 489 profiles in 316 micrographs were examined. The distribution of the D_5 receptor differed significantly across layers (χ^2= 45.986; p<.0001). Comparisons that are significantly different by post-hoc tests are indicated by an asterisk.

Figure 2-6

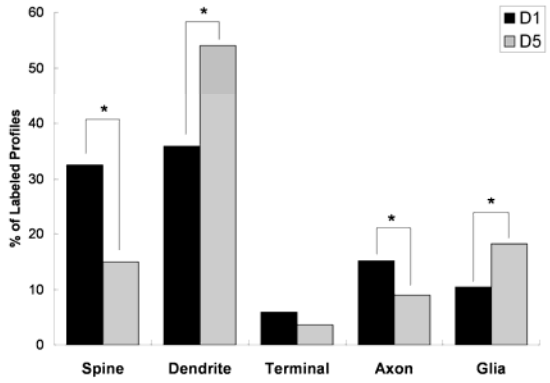

Figure 2-6. A histogram comparing the relative abundance of D_1 and D_5 in layer III of area 9 of the PFC. The distribution of D_1 and D_5 differed significantly in layer III (χ^2= 74.592; p<.0001). Post-hoc testing revealed that spines and pre-terminal axons were more commonly labeled for D_1, while dendrites and glia were more commonly labeled for D_5. Comparisons that are significantly different by post-hoc tests are indicated by an asterisk.

Figure 2-7

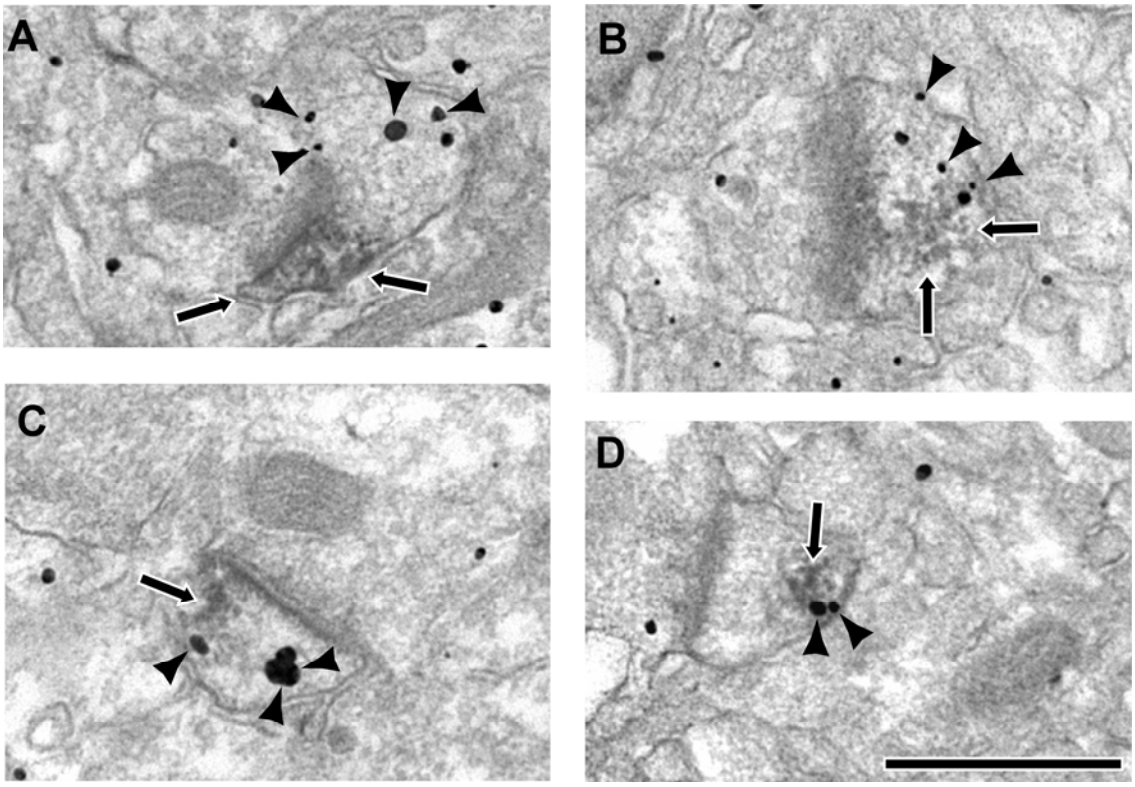

Figure 2-7. Electron micrographs of double-label immunogold (arrowheads) and DAB (arrows) images of D_1 and D_5 in PFC. **A, B:** Dendritic spines immunogold labeled for D_1 and DAB labeled for D_5. **C, D:** Dendritic spines immunogold labeled for D_5 and DAB labeled for D_1. Scale bar is 500 nm.

Figure 2-8

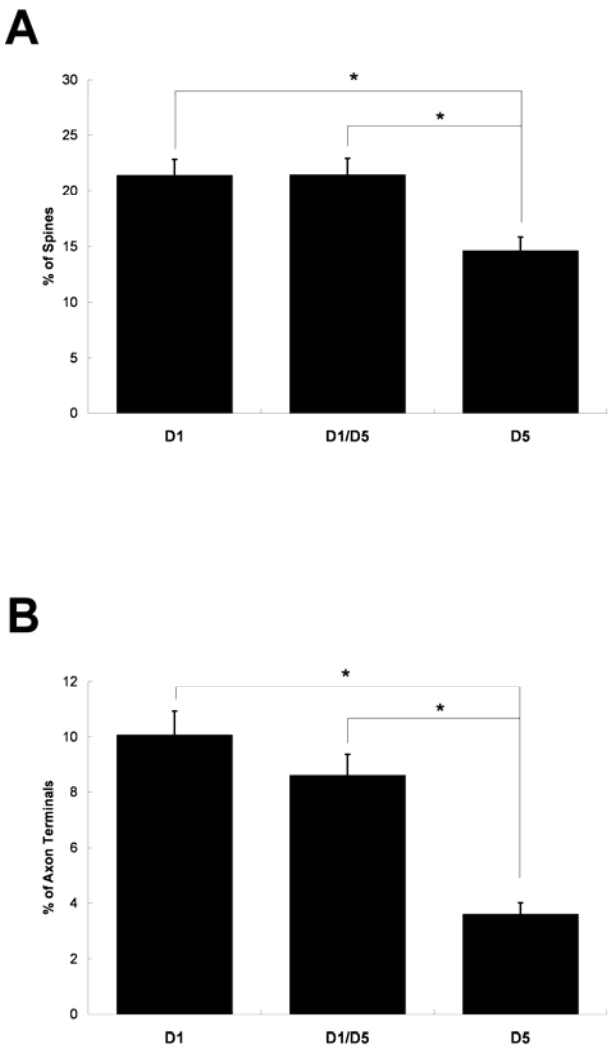

Figure 2-8. A: A histogram showing the percentage of PFC area 9 layer III spines labeled by D_1, by D_5 or by both D_1 and D_5. For the D_1 alone condition, 239 micrographs containing 1,053 spines were analyzed. For the D_5 alone condition, 297 micrographs containing 1,284 spines were analyzed. For the D_1/D_5 cocktail condition, 279 micrographs containing 1,258 spines were analyzed. ANOVA analysis revealed that the percentage of spines labeled for D_1 (21.38 ± 1.438), D_5 (14.635 ± 1.211) or by both D_1 and D_5 (21.438 ± 1.487) differed significantly ($F_{2,812} = 8.418$, $p = .0002$), and post-hoc

Scheffe tests confirmed that the percentage of D_5 labeled spines was significantly less than D_1 ($p = .0030$) and the cocktail ($p = .0016$). However, there was no significant difference between D_1 and the cocktail ($p = .9996$). These data demonstrate that the D_5 dopamine receptor is found in a subset of the D_1 labeled spines. **B:** A histogram showing the percentage of axon terminals labeled by D_1, by D_5 or by both D_1 and D_5 in layer III area 9 the PFC. For the D_1 alone condition, 239 micrographs containing 2,033 axon terminals were analyzed. For the D_5 alone condition, 297 micrographs containing 2,483 axon terminals were analyzed. For the D_1/D_5 cocktail condition, 279 micrographs containing 1,842 axon terminals were analyzed. ANOVA analysis revealed that the percentage of axon terminals labeled for D_1 (10.066 ± 0.858), D_5 (3.595 ± 0.411) and by both D_1 and D_5 (8.620 ± 0.756) differed significantly ($F_{2,811} = 25.598$, $p<.0001$), and post-hoc Scheffe tests confirmed that the percentage D_5 labeled terminals was significantly less than D_1 ($p < .0001$) and the cocktail ($p < .0001$). However, there was no significant difference between D_1 and the cocktail ($p = .3396$). These data indicate the D_5 dopamine receptor is found in a subset of the D_1 labeled axon terminals. Comparisons that are significantly different by post-hoc Scheffe tests are indicated by an asterisk.

Chapter 3

Localization of D_1 and D_5 in parvalbumin and calretinin interneurons in *Macaca mulatta* prefrontal cortical area 9

Adapted from Bordelon-Glausier JR, Khan ZU and Muly EC "Dopamine D_1 and D_5 receptors are localized to discrete populations of interneurons in primate prefrontal cortex." Submitted J Neurosci

Introduction

The cellular correlate of working memory (WM) is proposed to be individual pyramidal cells which respond to discrete cues selectively during the delay period of WM tasks (reviewed in P. S. Goldman-Rakic, 1995). Both the activity and the accuracy, or tuning, of these "delay cells" is modulated by activation of D1 family of dopamine receptors (D1R) in a dose-dependent manner (G. V. Williams and P. S. Goldman-Rakic, 1995; S. Vijayraghavan et al., 2007). Tuned delay activity has also been identified in putative inhibitory interneurons of the prefrontal cortex (PFC) (F. A. Wilson et al., 1994; S. G. Rao et al., 1999), and blockade of GABAergic neurotransmission abolishes tuned neuronal responses (S. G. Rao et al., 2000). Given the importance of GABAergic and D1R activity for PFC functioning, it is important to determine if D1R are present on inhibitory interneurons.

Cortical interneurons can be subdivided by the presence of calcium-binding proteins such as parvalbumin (PV) and calretinin (CR) (F. Conde et al., 1994; Y. Gonchar and A. Burkhalter, 1997; Y. Kawaguchi and Y. Kubota, 1997). PV interneurons are chandelier and basket cells, which provide the strongest inhibition to pyramidal cells (S. M. Williams et al., 1992; G. Gonzalez-Burgos et al., 2005a). Calretinin (CR) interneurons comprise approximately 50% of the total interneuron population in monkey PFC (F. Conde et al., 1994). They typically exhibit double bouquet morphology and synapse onto other interneurons (P. L. Gabbott and S. J. Bacon, 1996; V. Meskenaite, 1997), which may result in the disinhibition of a pyramidal cell (X. J. Wang et al., 2004). The disparate effects PV and CR interneurons can have on pyramidal cell output identify

them as key circuit components underlying the inverted-U relationship between D1R activation and WM function.

Evidence for differences between the D_1 and D_5 dopamine receptors is amassing despite the lack of a pharmacological tool which can distinguish the two receptors. Perhaps the most important difference for understanding the dose-dependent relationship between D1R activation and WM performance/delay cell activity, is the 10-fold higher affinity for dopamine exhibited by the D_5 receptor (R. K. Sunahara et al., 1991; R. L. Weinshank et al., 1991). Activation of the D1R typically enhances the excitability of a neuron (reviewed in J. K. Seamans and C. R. Yang, 2004), and the higher affinity D_5 has for dopamine suggests it would be preferentially activated at low dopamine concentrations. Thus, understanding the localization of both receptors across the PV and CR interneuron populations in particular will shed light on which components of circuitry can be activated at varying concentrations of dopamine in the PFC.

A previous study has identified D_1 in PFC PV interneurons and, to a lesser extent, CR interneurons (E. C. Muly et al., 1998). In this chapter, I have used a quantitative electron microscopic (EM) approach to determine the subcellular distribution of D_1 and D_5 receptors in PV and CR interneurons. The findings demonstrate that D_1 and D_5 dopamine receptors are differentially localized to PV and CR interneurons; PV interneurons are mainly associated with D_1 receptors, while CR interneurons are mainly associated with D_5 receptors in area 9 of primate PFC.

Materials and Methods

Animals and preparation of tissue

Tissue from seven *Macaca mulatta* monkeys was used for this study. The care of the animals and all anesthesia and sacrifice procedures in this study were performed according to the National Institutes for Health Guide for the Care and Use of Laboratory Animals and were approved by the Institutional Animal Care and Use Committee of Emory University. The animals were sacrificed with an overdose of pentobarbital (100mg/kg) and then perfused with a flush of Tyrode's solution. The flush was followed by 3 to 4 liters of fixative solution of 4% paraformaldehyde/0.1-0.2% glutaraldehyde/0-0.2% picric acid in phosphate buffer (0.1M, pH 7.4; PB). The brain was blocked and post-fixed in 4% paraformaldehyde for 2-24 hours. Coronal, 50 μm thick vibratome sections of prefrontal cortical area 9 (A. Walker, 1940) were cut and stored frozen at -80^{o}C in 15% sucrose until immunohistochemical experiments were performed.

Double-Label Immunohistochemistry

To examine the presence of D_1 and D_5 in cortical interneurons, double label experiments were performed. A pre-embedding immunogold/DAB protocol was used in which immunogold was used to label parvalbumin (PV) or calretinin (CR), and D_1 or D_5 was labeled with DAB. The methods used have been described previously (E. C. Muly et al., 1998). Briefly, sections were incubated overnight in a cocktail of primary immunoreagents (rat anti-D_1, 1:500, Sigma-RBI, St. Louis, MO; or rabbit anti-D_5, 1:500, Z. Khan; and mouse anti-PV, 1:10,000, Sigma-RBI; or mouse anti-CR, 1:10,000, Swant, Switzerland), and then incubated overnight in a cocktail of secondary antisera (biotinylated donkey anti-rat at 1:200, Jackson ImmunoResearch, West Grove, PA; or biotinylated goat anti-rabbit at 1:200, Vector, Burlingame, CA; and 1 nm gold-conjugated goat anti-mouse at 1:200, Nanoprobes, Yaphank, NY). The sections were then silver-

intensified (Nanoprobes, Yaphank, NY), incubated in ABC reagent (Vector, Burlingame, CA) and reacted with DAB. Control sections, in which one of the two primary immunoreagents was omitted, showed no evidence either for nonspecific deposition of gold particles or for nonspecific deposition of DAB onto previously developed gold particles.

Analysis of Material

At least two blocks from each of the 3-4 animals in each type of double label experiment were examined. The blocks were made from layer III of cortical area 9; ultrathin sections were cut and examined using a Zeiss EM10C electron microscope. Regions of the grids containing neuropil were selected for analysis based ultrastructural preservation and adequate DAB staining amongst the immunogold labeling. Electron micrographs of immunogold-containing dendrites and axon terminals (immunoreactive for PV or CR) were taken, and these profiles were then examined for the presence of immunoperoxidase label (D_1 or D_5). Images were collected at a magnification of 31,500 using a Dualvision cooled CCD camera (1300 x 1030 pixels) and Digital Micrograph software (version 3.7.4, Gatan, Inc., Pleasanton, CA). For D_1/PV a total of 423 micrographs from four monkeys representing 2580 μm^2 were analyzed. For D_1/CR a total of 330 micrographs from three monkeys representing 2013 μm^2 were analyzed. For D_5/PV a total of 411 micrographs from four monkeys representing 2507 μm^2 were analyzed. For D_5/CR a total of 434 micrographs from four monkeys representing 2647 μm^2 were analyzed. The percentage of PV and CR profiles which contained label for either D_1 or D_5 was tabulated and compared with a Chi-square analysis. All p-values are reported as Fisher's exact p-value.

To assess if variations in DAB labeling across individual experiments could contribute to false-negative results, the percentage of axon terminals which were immunoreactive for D_1 or D_5 was calculated across experimental conditions. In both the PV and CR double-labeled experiments, the percentage of D_1 and D_5 DAB labeled terminals differed by only 1%, and the percentage of D_1 or D_5 DAB labeled terminals differed by approximately 2% between the PV and CR conditions. Thus, the quality of immunoperoxidase label was equivalent in both types of double-label experiments.

Images containing PV- or CR-labeled dendrites were further analyzed to determine if they were synaptically contacted by axon terminals and, if so, whether the axon terminal displayed D_1 or D_5 immunoreactivity. Synapses were identified as asymmetric or symmetric based on ultrastructural criteria (A. Peters, 1987).

Results

Localization of D_1 and D_5 in PV- and CR-labeled cell bodies

While the primary goal of this study was to determine the extent of D1R localization in the dendritic and axonal arbors of cortical interneurons, we also examined PV and CR immunogold-labeled cell bodies for the presence of D_1 and D_5 DAB label. As previously reported (E. C. Muly et al., 1998), PV-labeled cell bodies were commonly immunoreactive for D_1. On the other hand, CR-labeled cell bodies were commonly immunoreactive for D_5. The D_1 labeling pattern within PV somas was similar to that seen in pyramidal cell somas (J. F. Smiley et al., 1994; J. R. Bordelon-Glausier et al., In Press) that is, D_1-immunoreactivity (IR) was principally located on the Golgi apparatus (Fig. 3-1A), though labeling with other internal membranes was also identified (Fig. 3-

1B). D_5 labeling within CR cell bodies was also consistent with that observed in pyramidal cell somas (J. R. Bordelon-Glausier et al., In Press), being associated with a variety of internal membranes (Fig. 3-1C).

Co- localization of D_1 or D_5 in PV interneurons

To determine the extent to which either D1R subtype is present in PV-containing prefrontal interneuron dendrites or axon terminals, I performed double-label experiments. PV-containing dendrites in PFC are non-pyramidal local circuit interneurons (S. M. Williams et al., 1992; J. S. Lund and D. A. Lewis, 1993); however, PV-containing axon terminals may arise from two sources: PV interneurons and thalamocortical axons. PV-IR thalamocortical terminals are found primarily in deep layer III and layer IV and make asymmetric synapses (M. Giguere and P. S. Goldman-Rakic, 1988; D. S. Melchitzky et al., 1999). In our blocks, taken primarily from superficial layer III, we identified 347 PV-labeled terminals, of which 117 made identifiable synapses. Only four of these 117 synapses were asymmetric, while the other 113 displayed symmetric specializations (Fig. 3-2D), indicating that our sample of PV-labeled terminals is almost entirely from interneuron axons.

Dendrites (Fig. 3-2A-C) that contained immunogold label for PV were identified and then examined for the presence of DAB label for either D_1 or D_5. The frequency of PV-labeled dendrites that contain D_1 (17.4%, 54 of 309) was greater than the frequency of PV-labeled dendrites that contain D_5 (5.0%, 15 of 298), and this difference was statistically significant (Fig. 3-3; $\chi^2 = 23.309$, $p < 0.0001$). Axon terminals (Fig. 3-2D) that contained immunogold label for PV were also identified and then examined for the presence of DAB label for either D_1 or D_5. Similar to PV dendrites, the frequency of PV-

labeled axon terminals that contain D_1 (10.9%, 19 of 174) was greater than the frequency of PV-labeled axon terminals that contained D_5 (0.5%, 1 of 177), and this difference was also statistically significant ($\chi^2 = 17.508$, $p < 0.0001$). The percentage of PV-labeled terminals that contain D_1 is similar to that reported previously for randomly selected prefrontal terminals (10%), while the percentage of PV-labeled terminals that contain D_5 is smaller than that previously reported for randomly selected terminals (4%), suggesting a selective lack of D_5 in PV terminals (J. R. Bordelon-Glausier et al., In Press). In material double-labeled for PV and D_1, there was a trend toward an increased frequency of D_1 labeling in dendrites compared to axon terminals, but this difference was not statistically significant ($\chi^2 = 3.730$, $p = 0.0535$). These results indicate that the D_1 receptor is the predominate type of D1R localized to PV interneurons of the primate PFC, and it is found with similar frequency in the dendritic and axonal arbor of these cells.

Co-localization of D_1 or D_5 in CR interneurons

We next performed double-label experiments to determine the frequency of the D1R in CR interneuron dendrites and axon terminals. CR cells in the PFC are non-pyramidal local circuit interneurons that frequently display double-bouquet morphology and are densest in layers I-IIIa (F. Conde et al., 1994). Dendrites (Fig. 3-4A, B) and axon terminals (Fig. 3-4C, D) containing immunogold label for CR were identified. We examined 203 CR-IR axon terminals, and 45 were making identifiable synapses. Of these, 93.3% (42 of 45) were making symmetric synapses, and 6.7% (3 of 45) were making asymmetric synapses. This data indicates that the vast majority of the CR-IR terminals sampled originate from inhibitory interneurons, which is in strong agreement

with a previous report that 93% of CR-IR terminals in superficial cortical layers form symmetric synapses (D. S. Melchitzky et al., 2005).

I quantified the extent to which CR-IR dendrites and terminals also contained D_1-IR or D_5-IR. In contrast to what we observed for PV-labeled dendrites, the frequency of CR-labeled dendrites that contained D_5 (14.9%, 48 of 323 dendrites) was greater than the frequency of CR dendrites that contained D_1 (4.6%, 13 of 282 dendrites). This difference was statistically significant (Fig. 3-5; $\chi^2 = 17.450$, $p < 0.0001$). Neither D_1-IR (1.3%, 1 of 77) nor D_5-IR (5.75%, 8 of 139) was commonly observed in CR-labeled axon terminals, and the number of observations of CR-labeled axon terminals in the D_1 double label experiment was not sufficient to allow a valid statistical comparison between D_1/CR and D_5/CR axon terminal frequencies. When comparing the distribution of D_5-IR in CR-labeled profiles, the D_5 receptor is more prevalent in CR dendrites than axon terminals ($\chi^2 = 7.564$, $p = 0.006$). These results indicate that D_5 is the predominant D1R localized to CR interneurons, and it is more frequently localized to the postsynaptic dendrites of CR interneurons.

D1R immunoreactivity in terminals contacting PV and CR dendrites

D1R have been identified on axon terminals in the current and previous studies (E. C. Muly et al., 1998; C. D. Paspalas and P. S. Goldman-Rakic, 2005; J. R. Bordelon-Glausier et al., In Press). Electrophysiological studies indicate that D1R ligands can have presynaptic effects on pyramidal cell-fast spiking cell pairs (G. Gonzalez-Burgos et al., 2005b) and fast spiking- fast spiking interneuron pairs (S. K. Towers and S. Hestrin, 2008). Therefore, we analyzed the prevalence of D1R-IR on axon terminals contacting PV- and CR-labeled dendrites. On average, 47% (219 of 482) of PV-labeled dendritic

profiles received synapses, and in some instances more than one. Of the axon terminals contacting PV dendrites, 91% (282 of 312) formed asymmetric synapses. On the other hand, 35% (171 of 484) of CR-labeled dendrites received one or more synapses, and 74% (155 of 209) of these synapses were asymmetric. These results are consistent with a previous report examining local axon termination onto PV and CR interneurons which found that PV dendrites receive a higher density of excitatory inputs than CR dendrites (D. S. Melchitzky and D. A. Lewis, 2003). In material double-labeled for D_1 and PV, only 1.2% (2 of 165) of terminals synapsing onto PV-labeled dendrites contained label for D_1. One D_1-IR axon terminal made an asymmetric synapse, while the other was symmetric. In material double-labeled for D_5 and PV, 4.1% (6 of 147) of terminals synapsing onto PV-labeled dendrites contained label for D_5, and each of these synapses were asymmetric. In material double-labeled for D_1 and CR, none of the terminals synapsing onto CR-labeled dendrites contained label for D_1 (0 of 81). Finally, in material double-labeled for D_5 and CR, 3.1% (4 of 128) of terminals synapsing onto CR-labeled dendrites contained label for D_5. Two of the synapses were asymmetric, and the remaining two were symmetric. These results suggest that D1R are found on axon terminals that synapse onto inhibitory interneurons. The frequency with which these terminal profiles contain D1R is relatively small, and at this time the small sample size does not allow us to compare the frequency with which D_1- or D_5-IR is found on these terminal profiles.

Discussion

In the current chapter, I determined the localization of the D_1 and D_5 dopamine receptors in two different classes of interneurons defined by their content of parvalbumin (PV) or calretinin (CR) within layer III of prefrontal cortical area 9 in *Macaca mulatta* monkeys. The D_1 receptor is the major D1R subtype in PV interneurons where it is present at similar frequencies in dendrites and axon terminals. D_5 is the predominant D1R subtype in CR interneurons, where it is found mainly in dendrites. D1R were also identified on axon terminals contacting PV- and CR-labeled dendrites. Though their total number was relatively small, the data suggests there could be a limited presynaptic D1R effect for inputs to PV and CR interneurons, or that the effect is limited to a subset of these interneurons.

Inhibitory neurotransmission influences prefrontal function both at the behavioral and cellular level. Activation or inhibition of GABAergic signaling can impair WM performance, and blockade of inhibitory neurotransmission abolishes pyramidal delay cell activity (T. Sawaguchi et al., 1988, 1989; S. G. Rao et al., 2000; T. Sawaguchi and M. Iba, 2001). Furthermore, inhibitory interneurons have been shown to display tuned delay activity similar to pyramidal delay cells (S. G. Rao et al., 1999), and it has been proposed that they contribute to the specificity of pyramidal delay cells (S. G. Rao et al., 1999; G. Gonzalez-Burgos et al., 2005a). Stimulation of D1R enhances the excitability of GABAergic neurons and pyramidal cells by augmenting glutamate currents and various ionic conductances (reviewed in C. R. Yang et al., 1999; J. K. Seamans and C. R. Yang, 2004). Thus, an interaction between D1R signaling and GABAergic neurotransmission may contribute to the inverted-U relationship.

Interneurons are a diverse group of cells, displaying various morphologies, electrophysiological properties and synaptology (see reviews J. DeFelipe, 1997; H. Markram et al., 2004). Importantly, PV and CR interneurons have very different postsynaptic targets. PV interneurons primarily synapse onto cell bodies, axon initial segments and the proximal dendritic shafts of pyramidal cells (J. DeFelipe et al., 1989; D. A. Lewis and J. S. Lund, 1990; S. M. Williams et al., 1992; Y. Kawaguchi, 1995), and activation of PV interneurons prevents action potentials in the pyramidal cells they innervate (A. M. Thomson et al., 1996; G. Tamas et al., 1997; Z. Xiang et al., 2002; G. Gonzalez-Burgos et al., 2005a; N. V. Povysheva et al., 2006; A. R. Woodruff and P. Sah, 2007). On the other hand, CR interneurons primarily synapse onto other interneurons, including those containing PV (P. L. Gabbott and S. J. Bacon, 1996; A. I. Gulyas et al., 1996; V. Meskenaite, 1997). PV interneurons do receive symmetric inputs (S. M. Williams et al., 1992), and inhibitory post-synaptic currents in PV interneurons are faster, have higher amplitude and are more frequent than in other types of interneurons (A. Bacci et al., 2003). Taken together, these data indicate that PV and CR interneurons have discrete roles in controlling pyramidal cell output.

I have shown that the D1R subtypes are differentially distributed between PV and CR interneurons. Differential receptor expression across interneuron subtypes has been reported previously (P. Vissavajjhala et al., 1996; R. L. Jakab and P. S. Goldman-Rakic, 2000; G. Nyiri et al., 2003; P. Somogyi et al., 2003; Y. P. Deng et al., 2007), and receptor heterogeneity could contribute to the varied electrophysiological responses seen in interneurons (J. R. Geiger et al., 1995; A. Bacci et al., 2003; J. H. Goldberg et al., 2003). There is growing evidence for functional differences between D_1 and D_5 (M. Filip et al.,

2000; A. I. Hersi et al., 2000; A. E. Kudwa et al., 2005; N. Granado et al., 2008), and one difference that is particularly relevant for understanding the dose-dependent relationship between D1R stimulation and WM performance/delay cell tuning is the 10-fold higher affinity for dopamine exhibited by the D_5 receptor (R. K. Sunahara et al., 1991; R. L. Weinshank et al., 1991; M. Tiberi and M. G. Caron, 1994). The preferential expression of D_1 in PV interneurons and D_5 in CR interneurons suggests that as the concentration of dopamine in the PFC changes, different populations of interneurons are modulated through D1R stimulation. Future electrophysiological studies examining the effect D1R activation on interneurons has on pyramidal cell output will be invaluable in interpreting these EM observations.

Figure 3-1

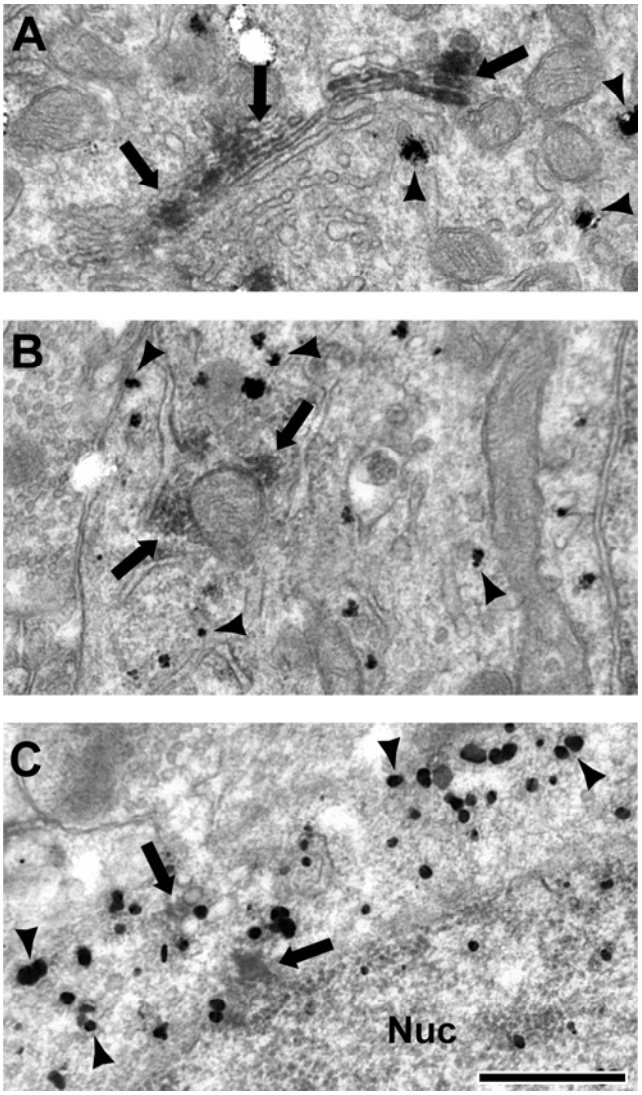

Figure 3-1. Electron micrographs of cell bodies immunogold labeled for PV or CR (black arrowheads) which also contain DAB label (black arrows) for D_1 and D_5. In PV somas, the stereotypical D_1 staining of the Golgi apparatus was identified *(A)*, as well as labeling associated with other internal membrane structures, including endoplasmic reticulum and mitochondria *(B)*. In CR somas, D_5 staining was associated with internal membranes *(C)*. Nucleus (Nuc). Scale bar is 500 nm.

Figure 3-2

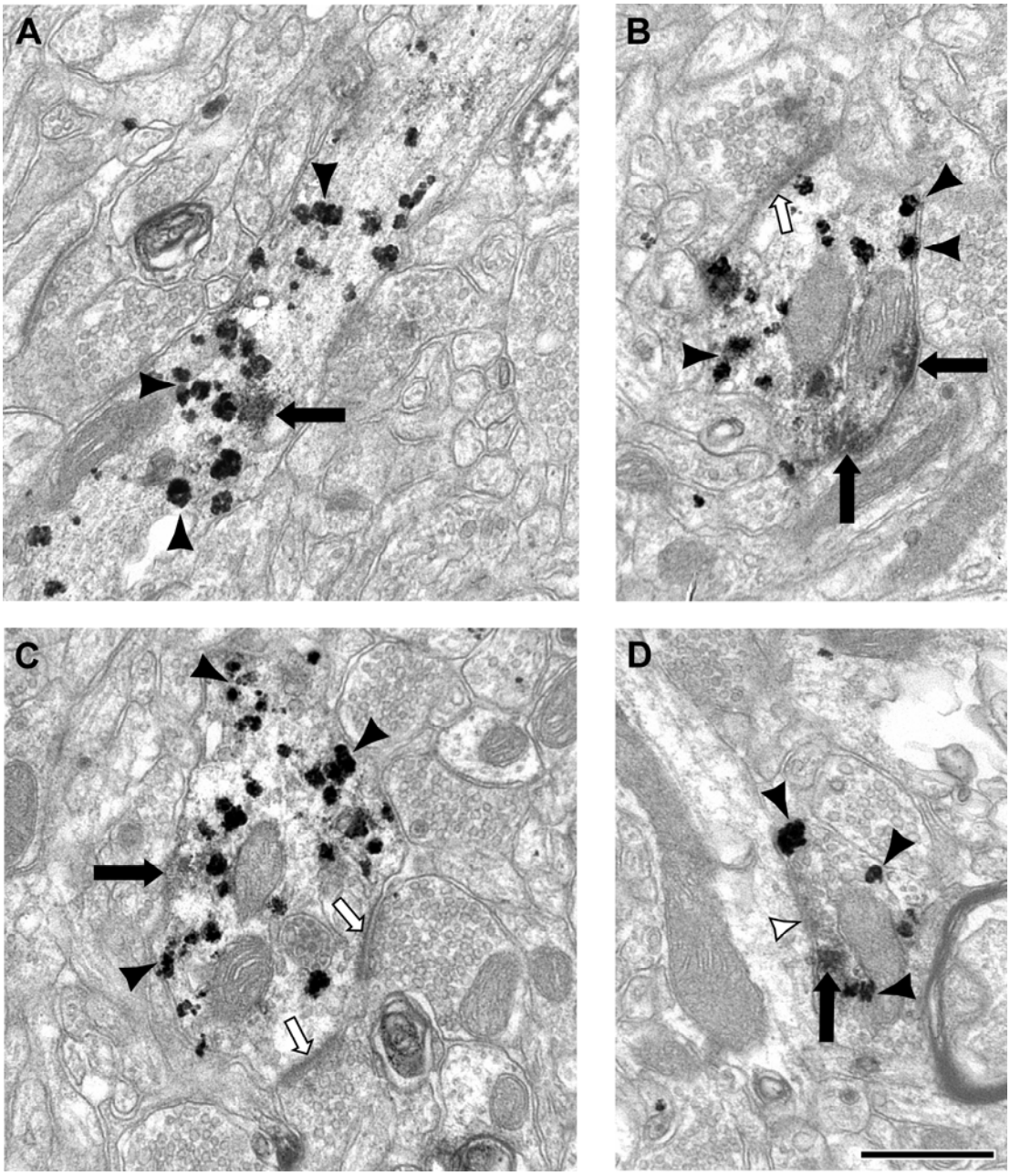

Figure 3-2. Electron micrographs of dendrites (*A*-*C*) and an axon terminal (*D*) labeled for parvalbumin with immunogold (black arrowheads) and D_1 with DAB (black arrows). PV-labeled dendrites often received asymmetric synapses (white arrows). PV-labeled axon terminals were typically observed to make symmetric synaptic contacts onto unlabeled dendrites (white arrowhead). Scale bar is 500 nm.

Figure 3-3

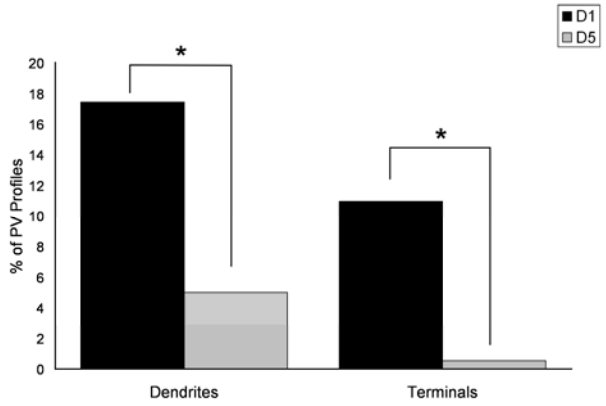

Figure 3-3. A histogram showing the percentage of PV-labeled dendrites and axon terminals that also contained immunoreactivity for D_1 and D_5. In tissue double-labeled for D_1 and PV, 313 PV-IR dendrites and 173 axon terminals in total were counted. In tissue double-labeled for D_5 and PV, 309 dendrites and 174 axon terminals in total were counted. The frequency of D_1/PV dendrites (17.5%) and axon terminals (10.9%) is greater than the frequency of D_5/PV dendrites (5.0%) and axon terminals (0.56%). Within D_1/PV neurons, the difference in the frequency of D_1 labeling in dendrites compared to axon terminals was not statistically significant.

Figure 3-4

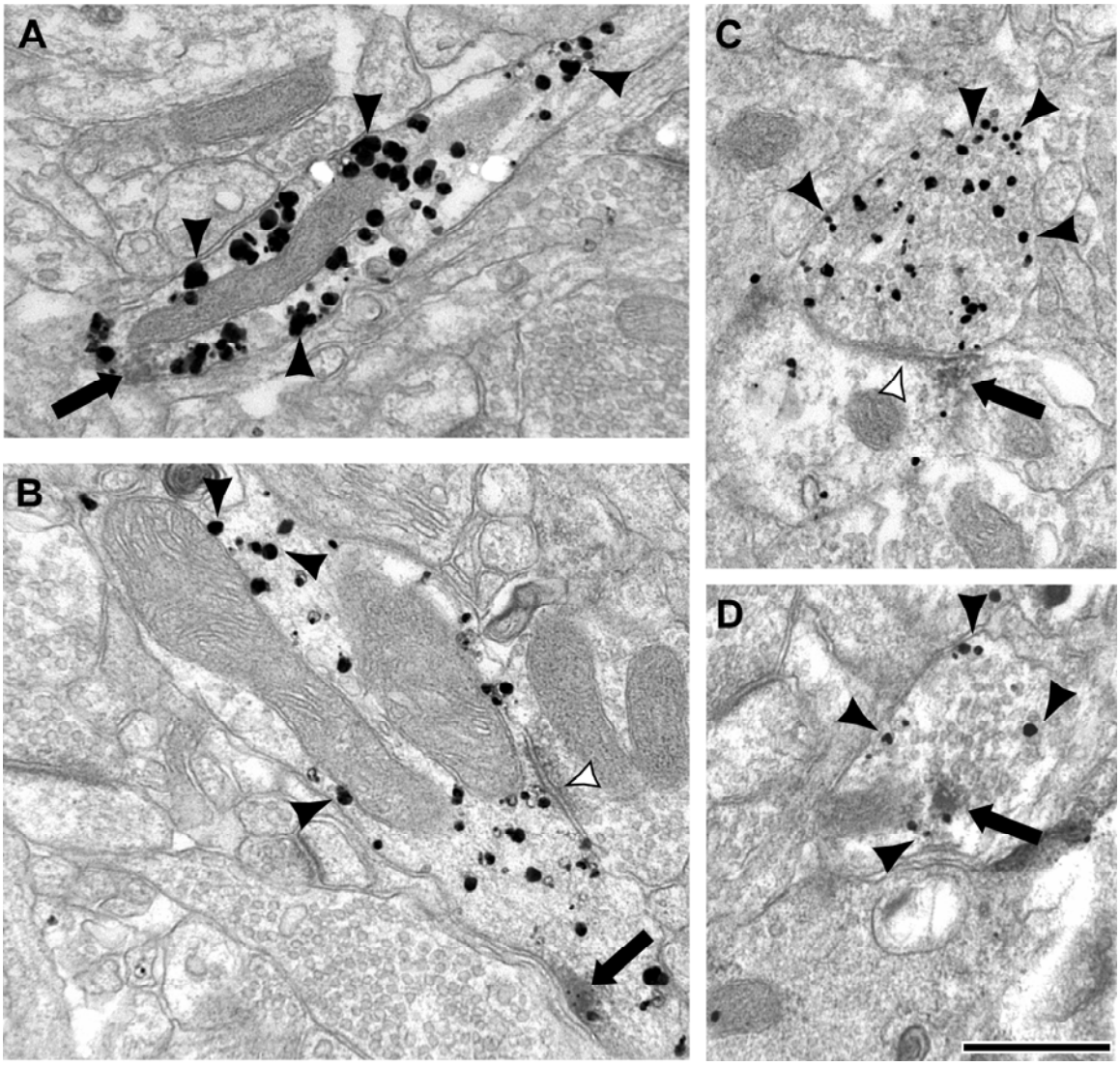

Figure 3-4. Electron micrographs of dendrites (*A* ,*B*) labeled with immunogold (black arrowheads) for CR and DAB (black arrows) for D_5. *C*: CR immunogold-labeled axon terminal making a symmetric synapse (white arrowhead) onto a single-labeled D_5 DAB labeled dendrite. D: CR immunogold-labeled axon terminal also containing D_5 DAB label. Scale bar is 500 nm.

Figure 3-5

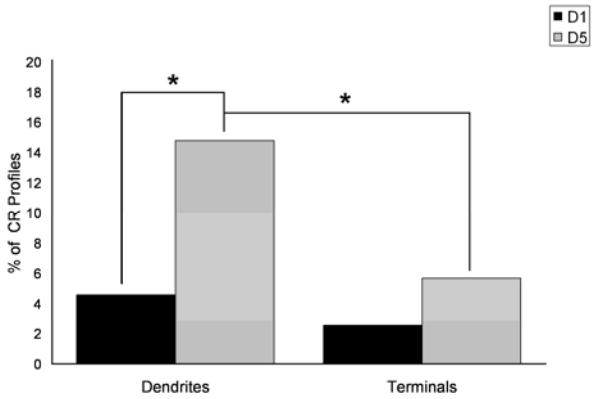

Figure 3-5. A histogram showing the percentage of CR-labeled dendrites and axon terminals that also contained immunoreactivity for D_1 and D_5. In the D_1/CR condition, 281 dendrites and 77 axon terminals in total were counted. In the D_5/CR condition, 323 dendrites and 139 axon terminals in total were counted. The frequency of D_5/CR dendrites (14.8%) is greater than the frequency of D_1/CR dendrites (4.6%). The number of CR-IR axon terminals in the D_1 double label condition was not sufficient to permit a valid statistical analysis between D_1/CR and D_5/CR. The D_5 receptor is more prevalent in CR dendrites (14.8%) than in CR axon terminals (5.7%).

Chapter 4

Localization of Inhibitor-1, DARPP-32, Protein Phosphatase-1α and Protein Phosphatase-1γ1 in the neuropil of *Macaca mulatta* prefrontal cortical area 9

Portions adapted from Bordelon JR, Smith Y, Nairn AC, Colbran RJ, Greengard P, Muly EC (2005) "Differential Localization of Protein Phosphatase-1α, β and γ1 Isoforms in Primate Prefrontal Cortex." Cer Cor 15(12): 1928-1937.

Introduction

The effects of D1 family of dopamine receptor (D1R) activation depend on a complex signal transduction pathway (Fig. 1-4). The basic scheme of D1R signal transduction involves the coupling of D1R to $G_{\alpha s}$ to activate adenylyl cyclase (AC) which produces cyclic AMP (cAMP) which, in turn, activates protein kinase A (PKA). PKA can then phosphorylate a variety of substrate proteins, including the related proteins inhibitor-1 (I-1) and dopamine- and cAMP-regulated phosphoprotein, 32 kDa (DARPP-32). When I-1 is phosphorylated at threonine 35 (Thr35), or DARPP-32 is phosphorylated at threonine 34 (Thr34), they become potent inhibitors of protein phosphatase 1 (PP1), a serine/threonine phosphatase (F. L. Huang and W. H. Glinsmann, 1976; H. C. Hemmings, Jr. et al., 1984). Active PP1 can dephosphorylate any number of downstream effectors, including glutamate receptors (G. L. Snyder et al., 1998; Z. Yan et al., 1999), $GABA_A$ receptors (Z. Yan and D. J. Surmeier, 1997; J. Flores-Hernandez et al., 2000), calcium channels (D. J. Surmeier et al., 1995) and cAMP response element-binding (CREB) (D. Genoux et al., 2002).

Many of the functional consequences of D1R activation rely on PP1 activity. For example, D1R agonist prevents the "rundown" of AMPA receptor current in striatal neurons. This effect is mimicked by inhibition of PP1 with okadaic acid or phosphorylated DARPP-32, illustrating the importance of the signal transduction cascade to D1R signaling (Z. Yan et al., 1999). D1R agonists increase the phosphorylation of the NMDA receptor NR1 subunit in wildtype but not DARPP-32 knockout mice, indicating the importance of DARPP-32 and PP1 for functional consequences of D1R activation (G. L. Snyder et al., 1998). D1R activation in neostriatal neurons also results in increased

phosphorylation of the $GABA_A$ receptor, which enhances GABA currents. In DARPP-32 knockout mice, this effect of D1R agonists on GABA currents was diminished (J. Flores-Hernandez et al., 2000), again illustrating the importance of PP1 and its inhibitors in controlling the functional outcome of D1R stimulation. Taken together, these data suggest that activation of a receptor can result in different functional outcomes based on the availability of its signal transduction proteins. Therefore, I have determined the localization of I-1, DARPP-32, and two PP1 isoforms in the neuropil of prefrontal cortical area 9 to compare with D_1 and D_5.

There have been few immunohistochemical studies examining the localization of I-1 and DARPP-32 in the cortex. Qualitative studies of the rat, cat and ferret cortex suggest that I-1 is almost exclusively found in dendrites with no labeling in dendritic spines (P. R. Lowenstein et al., 1995), suggesting that DARPP-32 may be the major PFC PP1 inhibitor. However, studies in adult monkeys have shown weak DARPP-32 labeling in the PFC (B. Berger et al., 1990; C. C. Ouimet et al., 1992), suggesting I-1 as the major PFC PP1 inhibitor. My previous data (Chapter 2) indicates that D_1 and D_5 are located on all components of the neuropil, but they are preferentially localized to dendritic spines and shafts. Thus, if either or neither I-1 or DARPP-32 are present in spines, dendrites or axon terminals of the PFC, the D_1 and D_5 dopamine receptors must use a different signal transduction cascade than what has been identified in the striatum (P. Greengard et al., 1999). To begin determining if the D1R have access to I-1 or DARPP-32 in the PFC, I obtained their localization profile across the PFC neuropil. In Chapter 2, I demonstrated that the D_1 receptor is present in about 20% of spines, while the D_5 receptor is present in about 14% of spines, and that the D_5 receptor is always present with D_1. A previous

study in our laboratory determined that PP1α and PP1γ1 are present in 73% and 37% of spines, respectively, and that the D_1 receptor has access to both isoforms in pyramidal cell spines (E. C. Muly et al., 2001). However, it is unknown whether I-1 and DARPP-32 are as prevalent in PFC pyramidal cell spines as PP1α and PP1γ1. Therefore, I determined the percentage of PFC spines which express I-1 and DARPP-32 to compare with the percentage containing D_1 and D_5.

PP1 exists in multiple isoforms (P. T. Cohen, 1988; V. Dombradi et al., 1990; K. Sasaki et al., 1990), and these isoforms differ in their localization in neurons (S. Strack et al., 1999; E. C. Muly et al., 2001). PP1 can bind to over 50 regulatory or scaffolding proteins, and this largely determines its substrate specificity and localization (J. B. Aggen et al., 2000; P. T. Cohen, 2002; H. Ceulemans and M. Bollen, 2004). There is evidence that some scaffolding proteins have PP1 isoform binding preferences (L. B. MacMillan et al., 1999; R. T. Terry-Lorenzo et al., 2002; L. C. Carmody et al., 2004), suggesting that PP1 isoforms are differentially regulated and localized within PFC circuitry. Indeed, an electron microscopic (EM) examination of the PP1α and PP1γ1 isoforms demonstrated that these two isoforms are localized to populations of PFC spines such that a spine can contain only PP1α, both PP1α and PP1γ1 or neither isoform (E. C. Muly et al., 2001). This data demonstrated that signaling environments can differ even within a single type of neuropil component. Because the D_1 and D_5 receptors are located every component of the neuropil, it is important to ascertain where PP1 is present in the PFC neuropil. I have chosen to examine the PP1α and PP1γ1 isoforms for 2 main reasons: 1) emerging biochemical evidence demonstrates PP1 isoform-specific neuronal actions (M. H. Brush et al., 2003; T. S. Tang et al., 2003), and 2) they are the PP1 isoforms which seem to be

critical for postsynaptic neurotransmission (G. L. Snyder et al., 1998; Z. Yan et al., 1999; G. L. Snyder et al., 2000). To determine where PP1α and PP1γ1 are throughout the PFC neuropil, I obtained a localization profile for each isoform.

Methods and Materials

Antisera

Four antibodies were used in these studies: rabbit anti-inhibitor-1, mouse anti-DARPP-32, rabbit anti-PP1α and anti-PP1γ1. The rabbit anti-inhibitor-1 was kindly provided by Dr. Angus Nairn, the mouse anti-DARPP-32 was kindly provided by Dr. Hugh Hemmings, and the rabbit-anti PP1α and PP1γ1 antisera were kindly provided by Dr. Paul Greengard. The rabbit anti-inhibitor-1 antibody was raised against I-1 from rabbit skeletal muscle. This antibody does not recognize DARPP-32 on immunoblot, and I-1-IR is not seen in immunohistochemical reactions when the I-1 antibody is preadsorbed with I-1 protein (E. L. Gustafson et al., 1991). The mouse anti-DARPP-32 antibody was raised against purified bovine DARPP-32 (H. C. Hemmings, Jr. and P. Greengard, 1986), and does not produce labeling in DARPP-32 knock-out mice (A. A. Fienberg and P. Greengard, 2000). The rabbit anti-PP1α antiserum was prepared a 15 amino acid C terminal sequence, and the anti-PP1γ1 antiserum was prepared against a 32 amino acid C terminal sequence. Each antiserum stains a major band around 37kDa, which is their predicted weight (Fig. 4-1C), and neither PP1 antibody cross-reacts with the other isoform (E. F. da Cruz e Silva et al., 1995).

Western blotting

Tissue from one male *Macaca mulatta* monkey, who was 1.04 years old at the time of sacrifice, was used for immunoblotting I-1 and DARPP-32. Tissue from one

female *Macaca mulatta* monkey, who was 1.08 years old at the time of sacrifice, was used for immunoblotting PP1α and PP1γ1. The Western blotting was performed as described previously (E. C. Muly et al., 2004b). Briefly, the animal was sacrificed by pentobarbital overdose (100 mg/kg), and blocks of various brain regions were frozen. Samples of PFC were dounce homogenized in buffer containing 140 mM KCl, 10 mM glucose, 1.2 mM $MgCl_2$, 10mM HEPES, pH 7.4, with a cocktail of protease inhibitors added. The homogenate was centrifuged, pellet discarded, and the supernatant was assayed for protein concentrations using a colormetric assay (Bio-Rad Laboratories, Hercules, CA). The samples were subjected to sodium dodecyl sulfate-polyacrylamine gel electrophoresis. Each lane was loaded with 20 μg of protein sample, and the gel was run for 50 minutes at 200 V. The gel was then transferred to PVDF membrane. The membrane was rinsed, blocked, and probed with rabbit anti-I1 (used at 1:2000), mouse anti-DARPP32 (used at 1:7500), rabbit anti-PP1α (used at 1:11,400), or rabbit anti-PP1γ1 (used at 1:2600). After rinsing, the membrane was incubated with horseradish peroxidase (HRP)-conjugated secondary antibody (HRP-goat anti-rabbit IgG, 1:10000, Bio-Rad; or HRP-goat anti-mouse IgG, 1:20000, Bio-Rad). Labeling was revealed by chemiluminescence. A ladder of markers was used to estimate the molecular weight of the labeled bands (SeeBlue plus 2, Invitrogen). Images of the Western blots in TIFF format were imported into an image processing program (Canvas 8, Deneba, Miami) where the image was cropped and labels were added.

Animals and preparation of tissue

Tissue from seven *Macaca mulatta* monkeys was used for this study. The care of the animals and all anesthesia and sacrifice procedures in this study were performed

according to the National Institutes for Health Guide for the Care and Use of Laboratory Animals and were approved by the Institutional Animal Care and Use Committee of Emory University. The animals were sacrificed with an overdose of pentobarbital (100mg/kg) and then perfused with a flush of Tyrode's solution. The flush was followed by 3 to 4 liters of fixative solution of 4% paraformaldehyde/0.1-0.2% glutaraldehyde/0-0.2% picric acid in phosphate buffer (0.1M, pH 7.4; PB). The brain was blocked and post-fixed in 4% paraformaldehyde for 2-24 hours. Coronal, 50 μm thick vibratome sections of prefrontal cortical area 9 (A. Walker, 1940) were cut and stored frozen at -80^{o}C in 15% sucrose until immunohistochemical experiments were performed.

Single-label immunohistochemistry

Single-label immunoperoxidase labeling was performed by using rabbit anti-inhibitor-1, mouse anti-DARPP-32, rabbit anti-PP1α or anti-PP1γ1 antisera. The antisera were used at the following dilutions: 1:15000 for I-1, 1:12000 for DARPP-32, 1:5700 for PP1α and 1:1300 for PP1γ1. The single-label immunoperoxidase labeling was performed as described previously (E. C. Muly et al., 1998). Briefly, sections were thawed, incubated in blocking serum (3% normal goat serum, 1% bovine serum albumin, 0.1% glycine, 0.1% lysine in 0.01 M phosphate buffered saline, pH 7.4) for 1 hour and then placed in primary antiserum diluted in blocking serum. After 36 hours at 4^{o}C, the sections were rinsed and placed in a 1:200 dilution of biotinylated goat anti-rabbit IgG (Vector, Burlingame, CA) or 1:20 biotinylated donkey anti-mouse IgG (Jackson Immuno Research, West Grove, PA) for 1 hour at room temperature. The sections were then rinsed, placed in avidin-biotinylated peroxidase complex (ABC Elite, Vector, Burlingame, CA) for 1 hour at room temperature, and then processed to reveal peroxidase

using 3,3'-diaminobenzidine (DAB) as the chromagen. Sections were then post-fixed in osmium tetroxide, stained *en bloc* with uranyl acetate, and then dehydrated, and embedded in Durcupan resin (Electron Microscopy Sciences, Fort Washington, PA). Selected regions were mounted on blocks, and ultrathin sections were collected onto pioloform-coated slot grids and counterstained with lead citrate. Control sections processed as above except for the omission of the primary immunoreagent, did not contain DAB label upon electron microscopic examination.

Four *Macaca mulatta* monkeys in total were processed for I-1 EM examination. Two were male, and two were female; the age range was 2-5.25 years of age. Four *Macaca mulatta* monkeys in total were processed for DARPP-32 EM examination. Three of the four were female, and the age range was 2-5.25 years. Three *Macaca mulatta* monkeys were processed for EM examination for PP1α and PP1γ1 each. All three were male, and the age range was 2-6.8 years.

One monkey was examined for the I-1 and DARPP-2 light microscopic (LM) examination. LM images were captured on a Leica DMRBE microscope using a Spot RT color digital camera (Diagnostic Instruments, Inc., Sterling Heights, MI) and Simple PCI imaging software (version 5.3, Hamamatsu Corp., Sewickley, PA). Images in TIFF format were imported into an imaging processing program (Canvas 8, Deneba Software, Miami). The contrast and brightness of the images was adjusted and labels were added.

Analysis of material

The single DAB-labeled material was analyzed as previously described (Chapter 2). Blocks of tissue from layer III of cortical area 9 were made and cut in ultrathin sections that were examined using a Zeiss EM10C electron microscope. Layer III was

chosen based on previous research in layers I, III and V demonstrating no effect of cortical layer on the extent of spine labeling for PP1α and PP1γ1 (E. C. Muly et al., 2001), and this layer is a major site of integration of inputs from different cortical areas (K. S. Rockland and D. N. Pandya, 1979; J. H. Maunsell and D. C. van Essen, 1983; M. F. Kritzer and P. S. Goldman-Rakic, 1995). Regions of the grids containing neuropil were selected based on the presence of label and adequate ultrastructural preservation. Fields of immunoreactive elements in the neuropil were randomly selected, and images were collected at a magnification of 31,500 using a Dualvision cooled CCD camera (1300 x 1030 pixels) and Digital Micrograph software (version 3.7.4, Gatan, Inc., Pleasanton, CA). For I-1, a total of 172 micrographs representing 1,050μm^2 were analyzed. Five hundred profiles were counted, and each monkey contributed 111-148 profiles. For DARPP-32, a total of 273 micrographs representing 1,665μm^2 were analyzed. Four hundred forty-five profiles were counted, and each monkey contributed 105-117 profiles. For PP1α, a total of 183 micrographs representing 1,117 μm^2 were analyzed. Five hundred forty-eight profiles were counted, and each monkey contributed 113, 115 and 340 profiles. For PP1γ1, a total of 279 micrographs representing 1,703 μm^2 were analyzed. Four hundred ninety-one profiles were counted, and each monkey contributed 152-191 profiles. On each micrograph, DAB-labeled profiles were identified and classified as spines, dendrites, terminals, axons, glia or unknown based on ultrastructural criteria (A. Peters et al., 1991) as previously described (Chapter 2). The number of immunoreactive profiles was tabulated and the distributions (excluding the unknown profiles) compared with a Chi-square analysis.

To determine the percentage of spines which contain I-1 or DARPP-32, fields of neuropil were randomly selected, and images were collected at a magnification of 20,000. An ANOVA sample size analysis (SigmaStat, Version 2.03, SPSS Inc.) indicated that the minimum sample size required to have a statistical power of 80% and a minimal detectable difference in the two group means of 5 was 129 images; therefore I analyzed 135 images from three monkeys in the I-1 condition and 134 images from three monkeys in the DARPP-32 condition. In each experimental condition, the number of micrographs analyzed from each monkey was similar. On each micrograph, spines were identified using the previously described ultrastructural criteria (A. Peters et al., 1991), then classified as immunopositive or immunonegative. The mean percentage of immunopositive spines was tabulated for both conditions and compared using an ANOVA. The results are reported as mean ± standard error.

Results

Western blot analysis of I-1 and DARPP-32

The relative abundance of I-1 and DARPP-32 in the PFC and striatum were examined using Western blotting procedures. As previously reported (C. C. Ouimet et al., 1984; A. C. Nairn et al., 1988), DARPP-32 is highly enriched in the striatum compared to the PFC (Fig. 4-1B). However, I-1 is present at similar levels in the PFC and the striatum (Fig. 4-1 A). Within the striatum, DARPP-32 appears to play a larger role than I-1 in inhibiting PP1. However, in the PFC, both I-1 and DARPP-32 are present at similar levels, suggesting that both may be equally influential in mediating the inhibition of PP1.

Light microscopic distribution of I-1 and DARPP-32

The localization of I-1 in the rat, cat and ferret frontal cortex has been previously described at the LM level (E. L. Gustafson et al., 1991; P. R. Lowenstein et al., 1995). Each study found somewhat different distributions of I-1-immunoreactive (IR) cells, though both identified I-1 in pyramidal and non-pyramidal cells. At the light microscopic level, I observed neuronal I-1 label in layers II-VI. The I-1 label produced a punctuate pattern throughout the neuropil, and labeled the nuclei of neurons (Fig. 4-2A). The LM localization of DARPP-32 has been previously characterized in the primate PFC (B. Berger et al., 1990). Briefly, DARPP-32-IR cell bodies were generally pyramidal or round in shape, and DARPP-32-IR glia were identified. My LM examination of DARPP-32 was consistent with this previous report. Neuronal labeling was identified in all layers, sans layer I. Most DARPP-32-IR neurons were pyramidal in shape with strongly labeled apical dendrites (Fig4-2B). Glial labeling was identified in layers I-VI (Fig. 4-2C) and the white matter (Fig. 4-2D).

Subcellular localization of I-1 and DARPP-32

While the primary goal of this study was to determine the subcellular localization of I-1 and DARPP-32 in the PFC neuropil, we also examined their localization within cell bodies. As suggesting in the LM observations, I-1-IR was more abundant in the nucleus (Fig. 4-3A), while DARPP-32-IR was also present in the somatic cytosol (Fig. 4-3B). Neither I-1 nor DARPP-32 appeared to be associated with any particular cell body organelle.

The precise subcellular localization of I-1 and DARPP-32 was then examined across the PFC neuropil. Each PP1 inhibitor was seen in dendritic spines, dendritic

shafts, axon terminals, pre-terminal axons and glia (Fig. 4-4). To explore differences in the neuropil distribution of I-1 and DARPP-32, I quantified the relative distribution of immunoreactive profiles to create a localization profile. I-1 and DARPP-32 immunoreactivity across neuropil elements differed significantly (Fig. 4-5; $\chi^2 = 41.237$; $p<.0001$). Post-hoc testing revealed that a significantly larger proportion of I-1 label was found in axon terminals (22.1%) than DARPP-32 (10.3%); and a significantly larger proportion of DARPP-32 label was found in glial profiles (22.7%) than I-1 (12.0%). This analysis illustrates that the distribution of I-1 and DARPP-32 differs across the neuropil in neuronal and non-neuronal compartments.

Western blot analysis of PP1α and PP1γ1

The relative abundance of PP1α and PP1γ1 in the PFC was examined using Western blotting procedures. Both isoforms are enriched in the PFC, though PP1α is present at higher levels than PP1γ1 (Fig. 4-1C).

Subcellular distribution of PP1α and PP1γ1

The localization of PP1α and PP1γ1 in the PFC has been previously described in detail at the light microscopic level (E. F. da Cruz e Silva et al., 1995; S. Strack et al., 1999; E. C. Muly et al., 2001). Briefly, PP1α and PP1γ1 immunolabeling is mainly found in small puncta, but PP1α is also expressed in neuronal nuclei.

I have used immunoperoxidase electron microscopy to more precisely determine the subcellular distribution of neuropil labeling for PP1α and PP1γ1. Each isoform was seen in dendritic spines, dendritic shafts, axon terminals, pre-terminal axons and glia (Fig. 4-6). To explore differences in the neuropil distribution of the three PP1 isoforms, we quantified the relative distribution of immunoreactive profiles. The relative

distribution of PP1α and PP1γ1 immunoreactivity across neuropil elements differed significantly (Fig. 4-7; χ^2= 25.069; p<.0001). Post hoc testing revealed that a significantly larger proportion of PP1α label was found in dendritic spines (65.7 %) than PP1γ1 (54.0%). PP1γ1 (19.8%) labeled a significantly larger percentage of glial processes than PP1α (10.4%). This analysis illustrates that the distribution of PP1α and PP1γ1 differs, but primarily in the extent of glial labeling. When glial labeling was excluded in a follow up analysis and only neuronal compartments were considered, the distribution of PP1α and PP1γ1 was not significantly different (χ^2=7.205, p=0.066).

Distribution of I-1 and DARPP-32 in spines

The quantitative analyses show that both I-1 and DARPP-32, like D_1 and D_5, are present in pyramidal cell spines and, as such, are positioned to mediate dopaminergic modulation of axo-spinous inputs to pyramidal cells. An important question is whether I-1 and DARPP-32 area also available to the D1R on PFC spines. To begin answering this question, I have determined the percentage of spines which contain I-1 and DARPP-32 in the macaque PFC. The percentage of spines in layer III of area 9 labeled individually for I-1 and DARPP-32 differed significantly (Fig. 4-8; $F_{1,710}$ = 4.340, p = .0382) such that I-1 labeled significantly more spines (7.7%) than did DARPP-32 (4.4%). This analysis indicates that, unlike for PP1α and PP1γ1, the D1R would have limited access to either I-1 or DARPP-32 on PFC pyramidal cell spines.

Discussion

This study represents an ultrastructural analysis that compares two sets of D1R signal transduction proteins: I-1 and DARPP-32, and PP1α and PP1γ1 in primate PFC.

In a Western blot analysis, both I-1 and DARPP-32 were present at similar levels in the PFC, while PP1α was present at slightly higher levels than PP1γ1. At the ultrastructural level, I-1 and DARPP-32 labeling was concentrated in dendritic shafts, while PP1α and PP1γ1 labeling was concentrated in pyramidal cell spines. Though PP1α and PP1γ1 label 73% and 37% of PFC spines, respectively, I-1 and DARPP-32 only label 7.7% and 4.4% of PFC spines, respectively. This differential localization of D1R signaling proteins may affect the functional outcome of D1R signaling in the PFC.

In the PFC, area 9 receives the highest density of dopaminergic input (D. A. Lewis et al., 1988; D. A. Lewis, 1992), and D1R signaling is critical for PFC functioning. Previous studies in rodents identified relatively weak I-1 and DARPP-32 staining in the frontal cortex (C. C. Ouimet et al., 1984; E. L. Gustafson et al., 1991; P. R. Lowenstein et al., 1995), and a qualitative electron microscopic analysis of cat cortex reported I-1 labeling in dendrites but not spines. This data suggested that D1R signaling in the PFC may be different than in the striatum. Across area 9 neuropil, I have observed I-1 and DARPP-32 in spines, dendrites, axon terminals, pre-terminal axons and glia. Both were enriched in dendrites relative to all other compartments; however, I-1 labeled axon terminals more frequently than did DARPP-32, and DARPP-32 labeled glial profiles more frequently than did I-1. What might these localization differences mean for PFC function? Although both DARPP-32 and I-1 are potent inhibitors of PP1 when phosphorylated at Thr34 and Thr35, respectively (H. C. Hemmings, Jr. et al., 1984), differences between the two are beginning to emerge. For example, cyclin-dependent kinase 5 (Cdk5) can phosphorylate DARPP-32 at Thr75, turning DARPP-32 into a PKA inhibitor (J. A. Bibb et al., 1999). However, Cdk5 phosphorylation of I-1 at serine (Ser)

6 or Ser67 enhances PKA signal (C. Nguyen et al., 2007b). I-1 can also be phosphorylated by PKC at Ser65 (B. Sahin et al., 2006); and extracellular signal-related kinase (ERK) activation depends on DARPP-32 availability, but not I-1 in the striatum (E. Valjent et al., 2005). Thus, the preferential availability of I-1 in axon terminals and DARPP-32 in glia may result in different functional outcomes.

Dendritic spines are the most frequently labeled neuropil element for PP1α and PP1γ1, while pre-terminal axons and axon terminals were least commonly labeled. Targeting of PP1 is accomplished by a variety of scaffolding proteins, two of which, spinophilin and neurabin, are also specifically enriched in spines (E. C. Muly et al., 2004c; E. C. Muly et al., 2004a) and selectively bind PP1α and PP1γ1 over other isoforms (L. B. MacMillan et al., 1999; R. T. Terry-Lorenzo et al., 2002; L. C. Carmody et al., 2004). Accordingly, neurabin-immunoreactive presynaptic profiles were also infrequently identified, and spinophilin is not found in axon terminals and rarely encountered in pre-terminal axons. Thus, it seems likely that the localization of spinophilin and neurabin underlies the selective localization of PP1α and PP1γ1 to dendritic spines.

Many receptors utilize I-1, DARPP-32, PP1α and PP1γ1 in the brain (P. Svenningsson et al., 1998; P. Svenningsson et al., 2002a; P. Svenningsson et al., 2002b; K. D. Yi et al., 2005; L. Lhuillier et al., 2007); and the activity and targeting of I-1, DARPP-32, PP1α and PP1γ1 modulates glutamatergic, GABAergic and calcium signaling (L. Y. Wang et al., 1994; R. S. Westphal et al., 1999; Z. Yan et al., 1999; T. S. Tang and I. Bezprozvanny, 2004; M. Terunuma et al., 2004). My EM studies indicate that I-1 and DARPP-32 are located in 8% and 4% of spines, respectively. However,

PP1α and PP1γ1 are present in 73% and 37% of spines, respectively (E. C. Muly et al., 2001). Combined, these data indicate that regulation of PP1 by I-1 or DARPP-32 is not the predominant method in the PFC. PP1 can be regulated by two basic mechanisms: inhibition by phosphoproteins or specific targeting by scaffolding proteins. Over 40 different phosphoproteins have been identified in the brain (S. I. Walaas et al., 1983), and many that are concentrated in the cortex have yet to be characterized. Thus, PP1 may be inhibited by some currently uncharacterized protein in the spines which do not contain I-1 or DARPP-32. Moreover, PP1 scaffolding proteins, like spinophilin and neurabin, are selectively concentrated in spines (E. C. Muly et al., 2004b; E. C. Muly et al., 2004a), and these scaffolding proteins can control the activity and/or the target protein of PP1 (Z. Yan et al., 1999; A. M. Brown et al., 2008). Indeed, availability of these PP1 scaffolds can even affect synaptic plasticity. For example, neurabin knockout mice demonstrate diminished corticostriatal LTP, but spinophilin knockout mice have intact corticostriatal LTP (P. B. Allen et al., 2006). Thus, while regulation of PP1 by DARPP-32 and I-1 in pyramidal cell spines is not the predominant mechanism in the PFC, it is unlikely that PP1 is totally unregulated in these spines.

In PFC spines, the D1R have access to both PP1α and PP1γ1 (Chapter 2; E. C. Muly et al., 2001). However, the prevalence of I-1 and DARPP-32 to spines is more restricted. At a maximum, 12% of PFC spines contain either I-1 or DARPP-32, while 20% contain D_1 and/or D_5. Therefore, the D1R must be signaling via different mechanisms in some spines of the dlPFC compared to the striatum. D1R may be utilizing additional phosphoproteins, like protein III (S. I. Walaas and P. Greengard, 1984), or may be signaling via other pathways like the ERK cascade (J. D. Runyan and P.

K. Dash, 2004; T. Nagai et al., 2007) in the spines which do not contain DARPP-32 or I-1. Indeed, there is emerging evidence suggesting that PFC D1R do not always utilize DARPP-32 in their signal transduction cascades. D1R activation enhanced the excitability of fast-spiking PFC interneurons in control and DARPP-32 knock-out mice (H. Trantham-Davidson et al., 2008), and DARPP-32 is required for ERK activation in the striatum but not the prefrontal cortex (E. Valjent et al., 2005). These data, combined with my own, begin to build a story indicating that the D1R may utilize different signal transduction pathways in the PFC than what has been determined in the striatum. Determining the differences between striatal and PFC D1R signaling via biochemical, electrophysiological and histological means will prove helpful in understanding neuroleptic and psychostimulant effects.

Figure 4-1

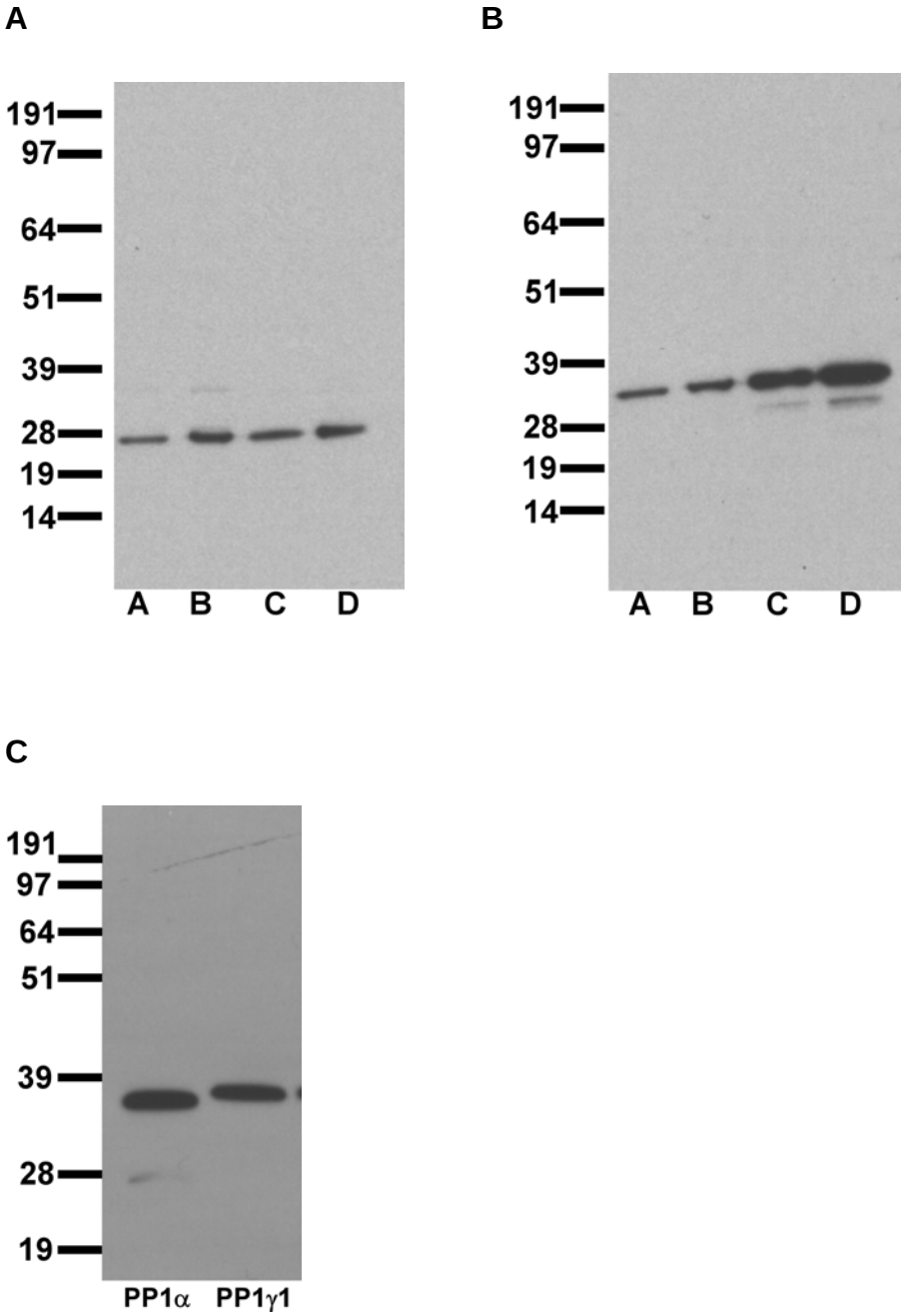

Figure 4-1. Immunoblots of I-1 (A), DARPP-32 (B) and PP1 isoforms (C). *A and B:* Lane A- 20 μg PFC protein. Lane B- 50μg PFC protein. Lane C- 5 μg striatum protein. Lane D- 10 μg striatum protein. *C:* 10 μg PFC protein.

Figure 4-2

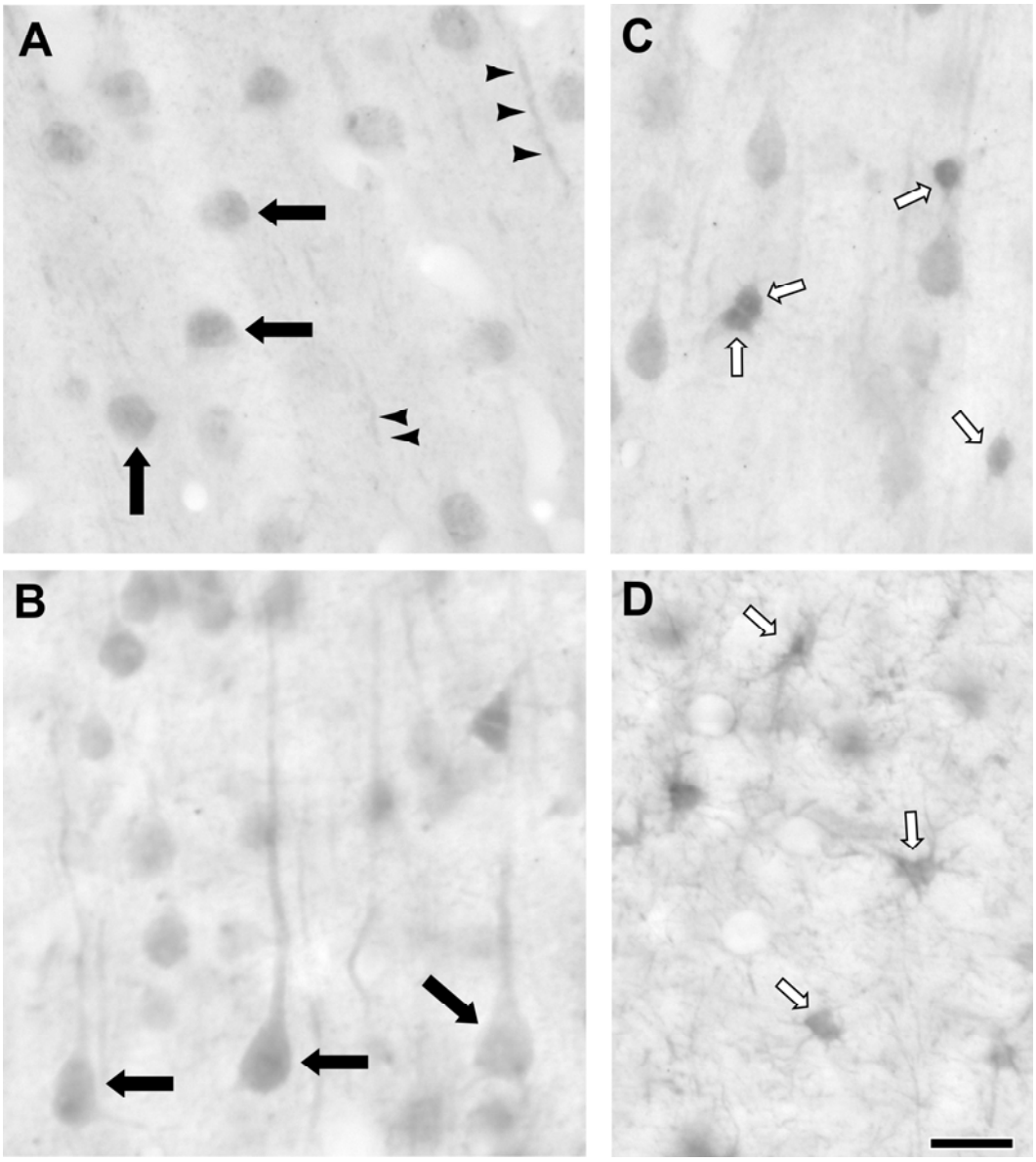

Figure 4-2. Light microscopic images of I-1 and DARPP-32 labeling in the macaque PFC. *A:* I-1 label stained the nucleus of neurons (black arrows) and the neuropil (black arrowheads). *B-D:* DARPP-32 label stained pyramidal cell bodies (B, black arrows) and glia in the grey (C, white arrows) and white matter (D, white arrows). Scale bar is 200μm.

Figure 4-3

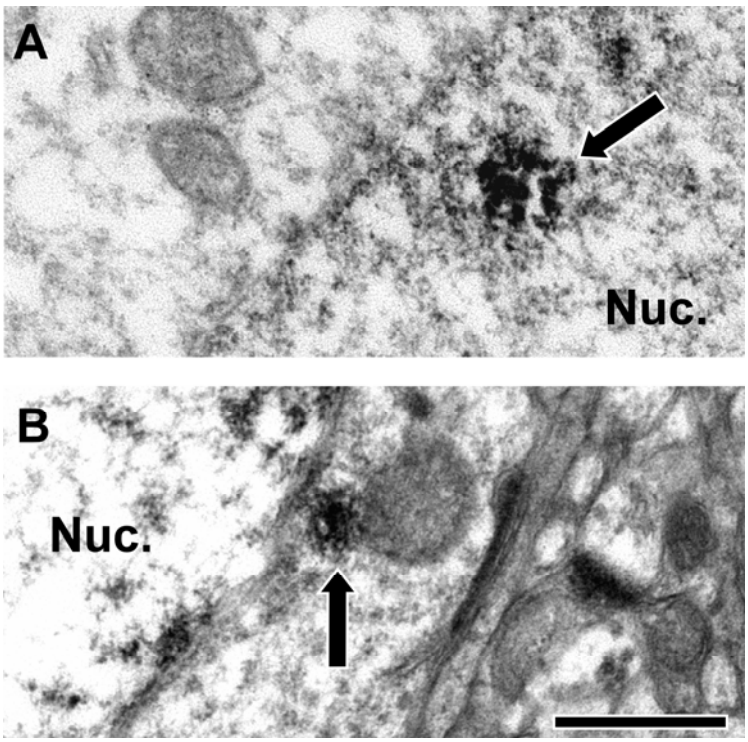

Figure 4-3. Electron micrographs of I-1 (A) and DARPP-32 (B) DAB label (arrows) in neuronal cell bodies. I-1 predominately labeled the nucleus (A), while DARPP-32 also labeled the somatic cytosol (B). Nuc- nucleus. Scale bar is 500 nm.

Figure 4-4

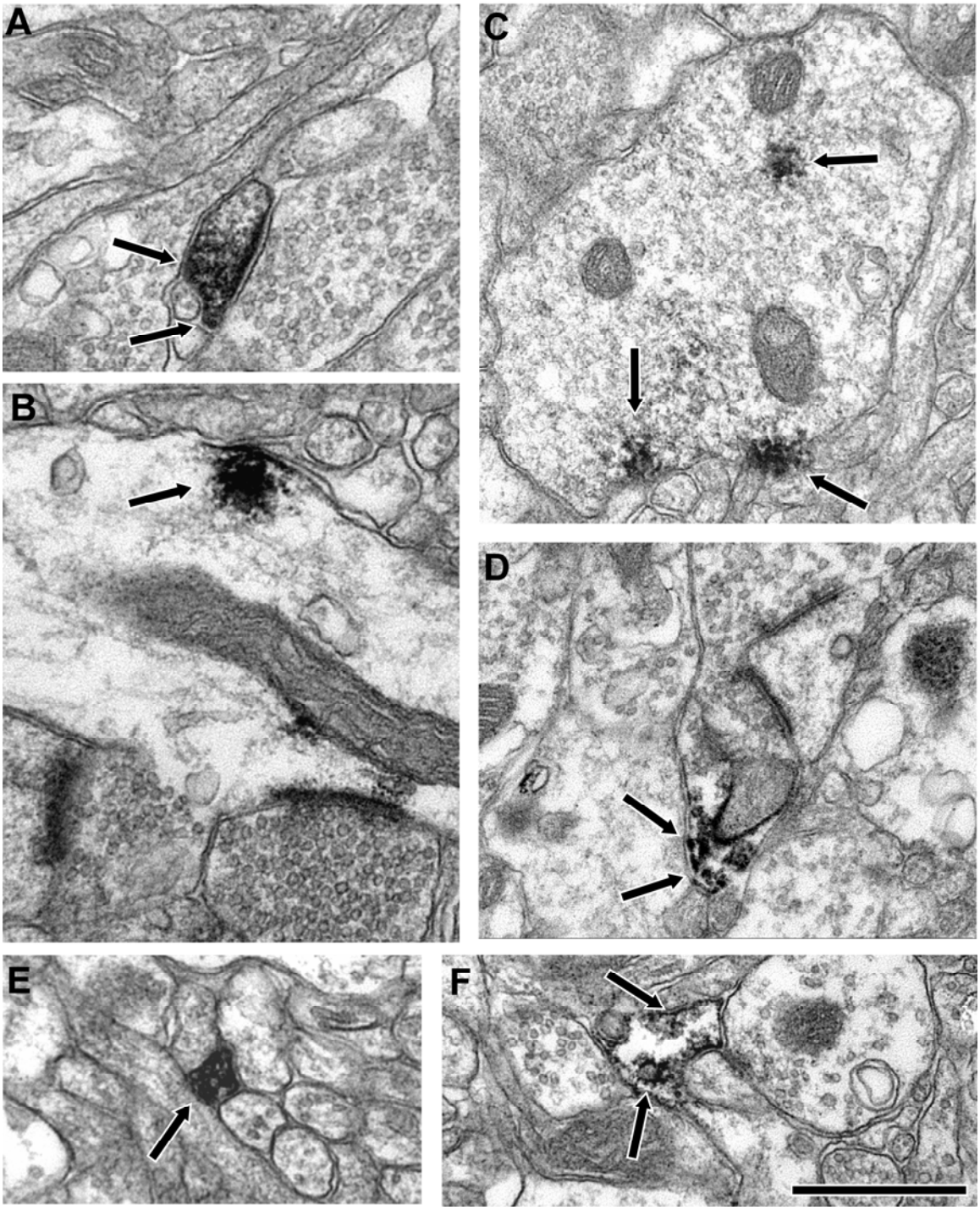

Figure 4-4. Electron micrographs illustrating the localization of I-1 and DARPP-32 in the neuropil of PFC. DAB label (arrows) was identified in spines (A; DARPP-32), and frequently identified in dendrites receiving synapses (B; DARPP-32) and those not

receiving synapses (C; I-1). I-1 labeled axon terminals (D) were commonly identified, and this example is making a perforated asymmetric synapse onto an unlabeled spine. DARPP-32 labeled pre-terminal axons (E) and glia (F) were commonly observed. Scale bar is 500 nm for A, B and E. Scale bar is 750 nm for C, D and F.

Figure 4-5

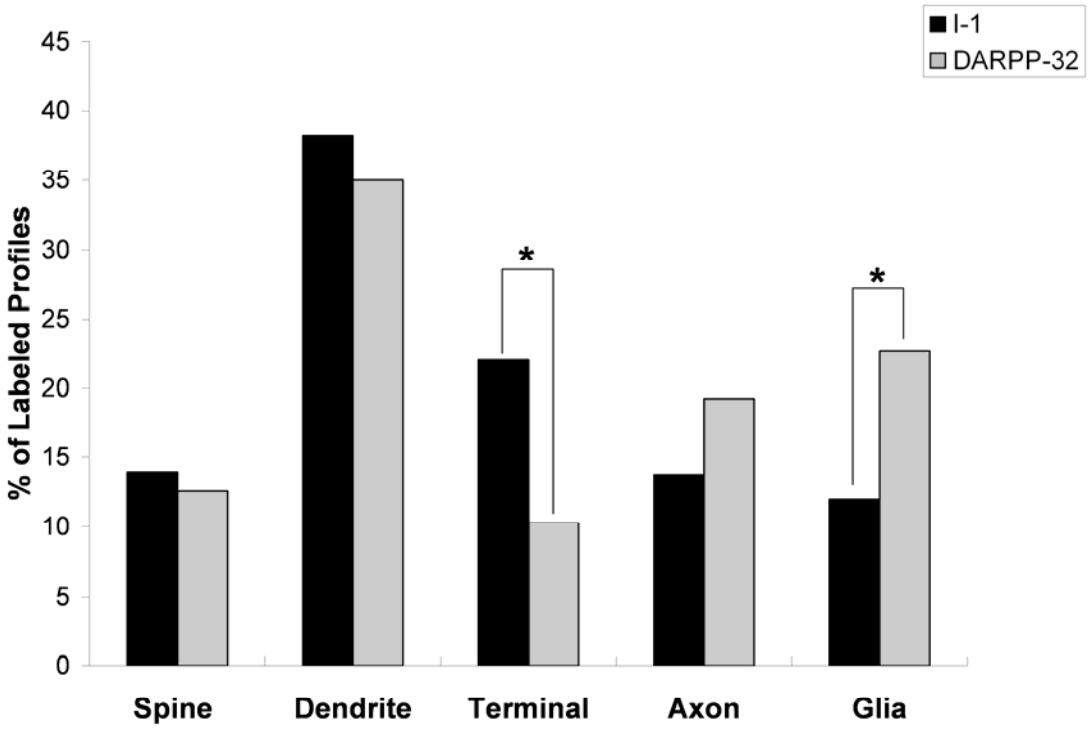

Figure 4-5. A histogram showing the relative abundance of labeled elements for I-1 and DARPP-32 in the neuropil of primate PFC. The distribution of immunoreactive profiles is significantly different between the isoforms (χ^2=41.237; p<.0001). Post hoc analysis revealed that a larger percentage of I-1 label is found in axon terminals, while DARPP-32 label is found more frequently in glia.

Figure 4-6

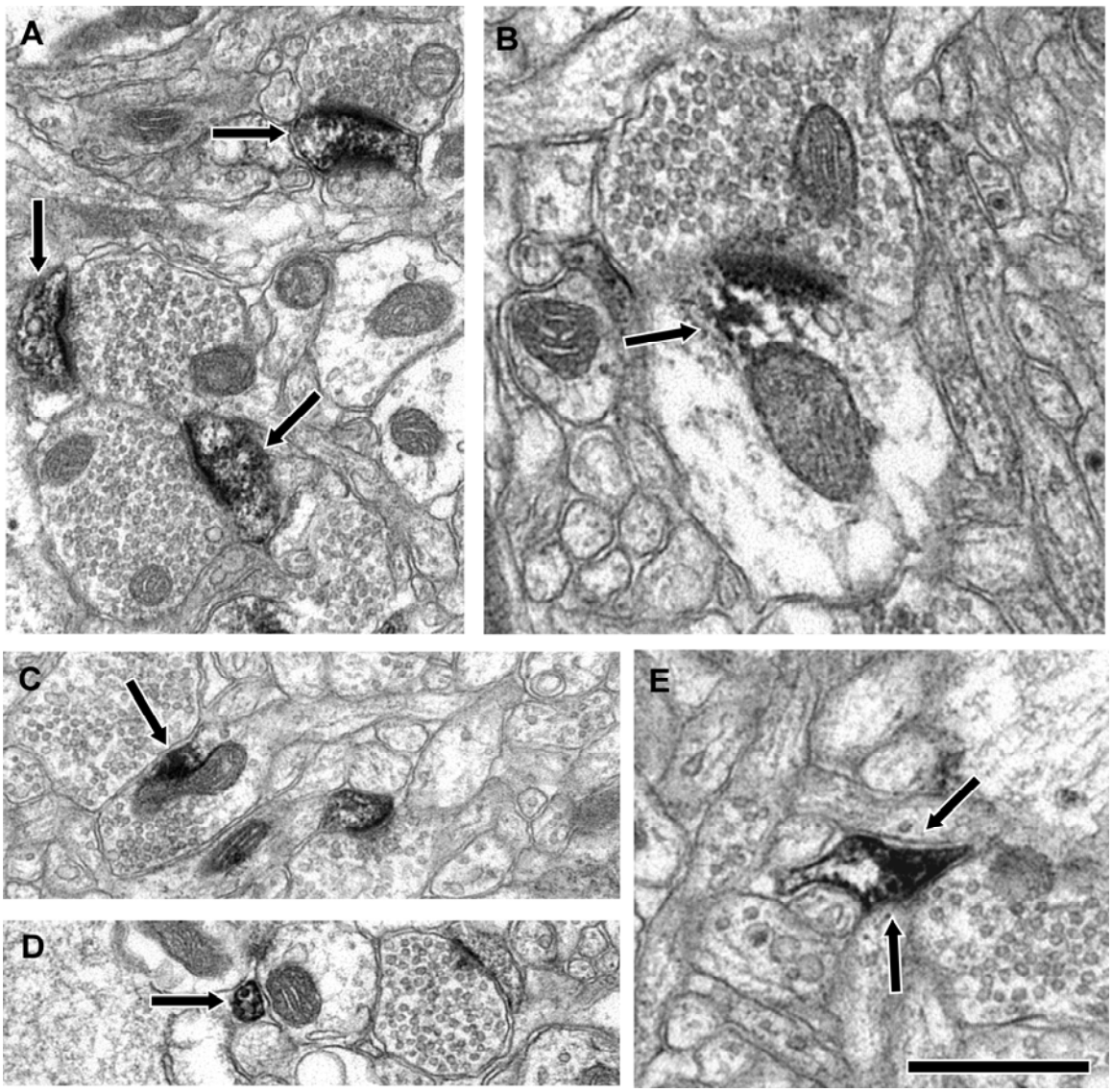

Figure 4-6. Electron micrographs illustrating the localization of PP1α and PP1γ1 in the neuropil of PFC. DAB label (arrows) was frequently identified in spines (A; PP1α), and commonly identified in dendrites (B; PP1γ1) for PP1α and PP1γ1. Labeled axon terminals (C; PP1γ1), pre-terminal axons (D; PP1α) and glia (E; PP1γ1) were also observed for all three isoforms. Scale bar is 500 nm for B and E; and 750 nm for A, C, and D.

Figure 4-7

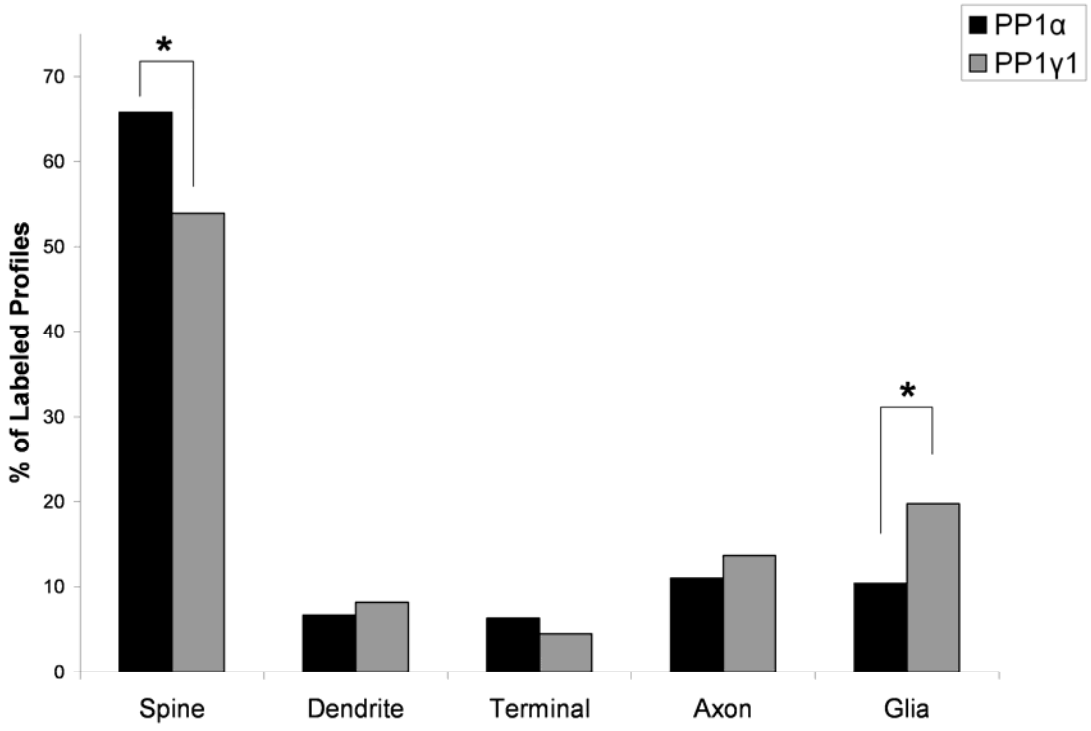

Figure 4-7. A histogram showing the relative abundance of PP1α and PP1γ1 in the neuropil of macaque PFC. The distribution of immunoreactive profiles is significantly different between the isoforms (χ^2=25.069; p<.0001). Post hoc analysis revealed that a larger percentage of PP1α label is found in spines, while PP1γ1 label is found more frequently in glia.

Figure 4-8

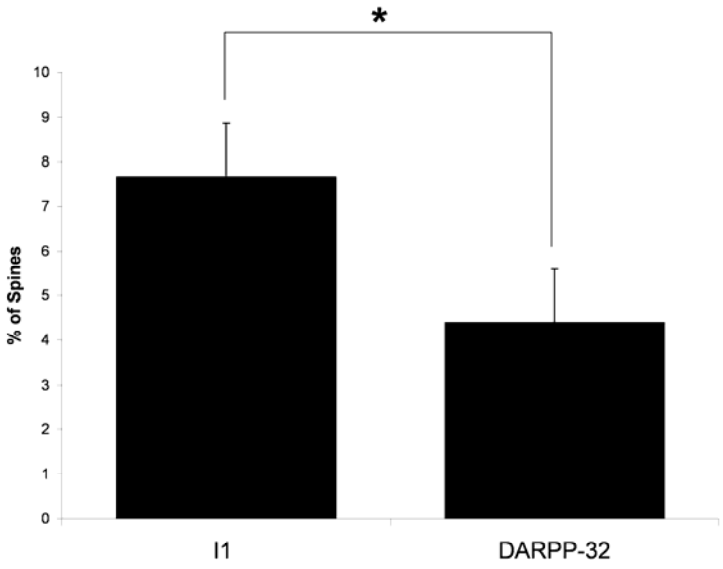

Figure 4-8. A histogram showing the percentage of area 9 pyramidal cell spines which contain I-1 or DARPP-32. ANOVA analysis revealed that I-1 labeled significantly more spines than did DARPP-32 ($F_{1,710} = 4.340$, $p = 0.0382$).

Chapter 5

Localization of inhibitor-1, DARPP-32, protein phosphatase-1α and protein phosphatase-1γ1 to parvalbumin and calretinin interneurons of *Macaca mulatta* prefrontal cortical area 9

Introduction

The dopamine D1 receptor family (D1R) is comprised of the D_1 and D_5 receptors (reviewed in C. Missale et al., 1998). Typically, the D1R couple to $G_{\alpha s}$ to stimulate adenylyl cyclase (AC), which produces cyclic AMP (cAMP) which, in turn, activates protein kinase A (PKA). PKA can then phosphorylate a variety of substrate proteins, including the related proteins inhibitor-1 (I-1) and dopamine- and cAMP-regulated phosphoprotein, 32 kDa (DARPP-32). When I-1 is phosphorylated at threonine 35 (Thr35), or DARPP-32 is phosphorylated at threonine 34 (Thr34), they become potent inhibitors of protein phosphatase 1 (PP1), a serine/threonine phosphatase (F. L. Huang and W. H. Glinsmann, 1976; H. C. Hemmings, Jr. et al., 1984). Active PP1 can dephosphorylate any number of downstream effectors, including glutamate receptors (G. L. Snyder et al., 1998; Z. Yan et al., 1999), $GABA_A$ receptors (Z. Yan and D. J. Surmeier, 1997; J. Flores-Hernandez et al., 2000), calcium channels (D. J. Surmeier et al., 1995) and cAMP response element-binding (CREB) (D. Genoux et al., 2002).

I-1 and DARPP-32 are heat and acid stable phosphoproteins which, when phosphorylated become potent inhibitors of PP1 (H. C. Hemmings, Jr. et al., 1984; K. R. Williams et al., 1986). PP1 exists in multiple isoforms (P. T. Cohen, 1988; V. Dombradi et al., 1990; K. Sasaki et al., 1990), and there is emerging evidence demonstrating PP1 isoform-specific actions. For example, PP1α modulates type 1 inositol 1,4,5-triphosphate receptors (IP_3R) (T. S. Tang et al., 2003; H. Tu et al., 2004), is targeted to the endoplasmic reticulum (M. H. Brush et al., 2003) and is absent in the anterior cingulated cortex of schizophrenia patients (D. Clark et al., 2006). I-1, DARPP-32, PP1α and PP1γ1 can be identified in each type of neuropil component (Chapter 4). However, I-

1 and DARPP-32 are concentrated in dendrites, while PP1α and PP1γ1 are concentrated in pyramidal cell spines. Interestingly, D1R have access to both PP1 isoforms in pyramidal cells spines, but do not always have access to I-1 or DARPP-32 in pyramidal cell spines (Chapter 4). This data is consistent with emerging data demonstrating that the D1R may signal via additional mechanisms in the prefrontal cortex (G. Chen et al., 2004; H. Trantham-Davidson et al., 2008). To further investigate this phenomenon, I have investigated the localization of I-1, DARPP-32, PP1α and PP1γ1 in parvalbumin (PV) and calretinin (CR) interneurons of the dorsolateral PFC (dlPFC).

Cortical interneurons are a diverse group of cells which can be identified based on molecular, electrophysiological and morphological measures (reviewed in J. DeFelipe, 1997; H. Markram et al., 2004). Interneurons containing the calcium-binding protein PV comprise approximately 25% of the dlPFC interneurons, have fast-spiking electrophysiological properties and are morphologically characterized as chandelier and basket cells. These interneurons provide the strongest inhibition to pyramidal cells (S. M. Williams et al., 1992; F. Conde et al., 1994; G. Gonzalez-Burgos et al., 2005a). Interneurons containing the calcium-binding protein CR interneurons comprise approximately 50% of the total interneuron population in monkey PFC (F. Conde et al., 1994). They typically exhibit double bouquet morphology and synapse onto other interneurons (P. L. Gabbott and S. J. Bacon, 1996; V. Meskenaite, 1997), which may result in the disinhibition of a pyramidal cell (X. J. Wang et al., 2004). PV and CR also differentially express the D1R, such that D_1 is predominately expressed on PV interneurons, and D_5 is predominately expressed on CR interneurons (Chapter 3). The disparate effects PV and CR interneurons can have on pyramidal cell output and their

differential expression of D1R identify them as key circuit components contributing to PFC function. Determining the prevalence of major D1R signaling proteins in these two interneuron populations will further enhance our knowledge regarding D1R signaling in the PFC.

In this chapter, I have used a quantitative electron microscopic (EM) approach to determine the prevalence and subcellular localization of I-1, DARPP-32, PP1α and PP1γ1 in PV and CR interneurons of area 9 in the *Macaca mulatta* PFC. The results demonstrate that PV interneurons predominately express I-1 and PP1α, while CR interneurons predominately express I-1, PP1α and PP1γ1.

Materials and Methods

Animals and preparation of tissue

Tissue from ten *Macaca mulatta* monkeys was used for this study. The care of the animals and all anesthesia and sacrifice procedures in this study were performed according to the National Institutes for Health Guide for the Care and Use of Laboratory Animals and were approved by the Institutional Animal Care and Use Committee of Emory University. The animals were sacrificed with an overdose of pentobarbital (100mg/kg) and then perfused with a flush of Tyrode's solution. The flush was followed by 3 to 4 liters of fixative solution of 4% paraformaldehyde/0.1-0.2% glutaraldehyde/0-0.2% picric acid in phosphate buffer (0.1M, pH 7.4; PB). The brain was blocked and post-fixed in 4% paraformaldehyde for 2-24 hours. Coronal, 50 μm thick vibratome sections of prefrontal cortical area 9 (A. Walker, 1940) were cut and stored frozen at -80^{o}C in 15% sucrose until immunohistochemical experiments were performed.

Double-Label Immunohistochemisty

To examine the presence of I-1, DARPP-32, PP1α and PP1γ1 in cortical interneurons, double label experiments were performed. A pre-embedding immunogold/DAB protocol was used in which immunogold was used to label parvalbumin (PV) or calretinin (CR), and I-1, DARPP-32, PP1α and PP1γ1was labeled with DAB. The methods used have been described previously (Chapter 2). PFC tissue sections from area 9 were thawed and rinsed in PBS. They were incubated in blocking serum (3% normal goat serum, 1% bovine serum albumin, 0.1% glycine, 0.1% lysine and 0.5% fish gelatin in 0.01 M phosphate buffered saline, pH 7.4) for one hour and then placed in the primary antiserum overnight at 4^{o}C. The following primary antisera were used: rabbit anti-I-1, 1:15000, Dr. Angus Nairn; mouse anti-DARPP-32, 1:12000, Dr. Hugh Hemmings; rabbit anti-PP1α, 1:5700, Dr. Paul Greengard, rabbit anti-PP1γ1, 1:1300, Dr. Paul Greengard; mouse anti-PV, 1:10,000, Sigma-RBI). The sections were removed from the primary antiserum, rinsed in PBS and placed in secondary antiserum (mouse or rabbit anti-CR, 1:10,000, Swant, Switzerland; mouse or rabbit anti-PV, 1:5000, Swant, Switzerland; and biotinylated goat anti-rabbit, 1:200, Vector, Burlingame, CA; or biotinylated donkey anti-mouse, 1:200, Jackson Immuno Research, West Grove, PA) overnight at 4^{o}C. The tissue was then rinsed in PBS, placed in 2% glutaraldehyde for 20 minutes, rinsed in PBS, rinsed in 2% acetate buffer, silver-intensified for four minutes (HQ silver, Nanoprobes, Yaphank, NY), then rinsed in acetate buffer and in PBS. The sections were incubated in ABC overnight at 4^{o}C and reacted in the same manner as the single-label material.

Analysis of Material

At least two blocks from each of the 2-4 animals in each type of double label experiment were examined. The blocks were made from layer III of cortical area 9; ultrathin sections were cut and examined using a Zeiss EM10C electron microscope. Regions of the grids containing neuropil were selected for analysis based ultrastructural preservation and adequate DAB staining amongst the immunogold labeling. Electron micrographs of immunogold-containing dendrites and axon terminals (immunoreactive for PV or CR) were taken, and these profiles were then examined for the presence of immunoperoxidase label (I-1, DARPP-32, PP1α or PP1γ1). Images were collected at a magnification of 31,500 using a Dualvision cooled CCD camera (1300 x 1030 pixels) and Digital Micrograph software (version 3.7.4, Gatan, Inc., Pleasanton, CA). For I-1/PV a total of 280 micrographs from three monkeys representing 1708 μm^2 were analyzed. For DARPP-32/PV a total of 185 micrographs from two monkeys representing 1129 μm^2 were analyzed. For PP1α /PV a total of 378 micrographs from four monkeys representing 2306 μm^2 were analyzed. For PP1γ1 /PV a total of 418 micrographs from four monkeys representing 2550 μm^2 were analyzed. For I-1/CR a total of 229 micrographs from three monkeys representing 1397 μm^2 were analyzed. For DARPP-32/CR a total of 156 micrographs from three monkeys representing 952 μm^2 were analyzed. For PP1α /CR a total of 282 micrographs from four monkeys representing 1720 μm^2 were analyzed. For PP1γ1 /CR a total of 279 micrographs from four monkeys representing 1702 μm^2 were analyzed. The percentage of PV and CR profiles which contained label for either I-1 or DARPP-32, and PP1α or PP1γ1 was tabulated and compared with Chi-square analysis. All p-values are reported as Fisher's exact p-value.

Results

Localization of I-1 and DARPP-32 in PV and CR interneurons

Dendrites and axon terminals that contained immunogold label for PV were identified, and then examined for the presence of DAB label for either I-1 or DARPP-32 (Fig. 5-1). The frequency of PV-labeled dendrites that contain I-1 (18.8%, 39 of 168) was greater than the frequency of PV-labeled dendrites that contain DARPP-32 (8%, 9 of 103), and this difference was statistically significant (Fig. 5-2; $\chi^2 = 6.638$, $p = 0.0131$). Axon terminals that contained immunogold label for PV were also identified and then examined for the presence of DAB label for either I-1 or DARPP-32. Similar to PV dendrites, the frequency of PV-labeled axon terminals that contain I-1 (10.9%, 16 of 131) was greater than the frequency of PV-labeled axon terminals that contained DARPP-32 (2.7%, 3 of 109), and this difference was statistically significant (Fig. 5-2; $\chi^2 = 6.297$, $p = 0.0147$). In material double labeled for PV and I-1, there was a trend toward increased frequency of I-1 labeling in dendrites compared to axon terminals, but this difference was not statistically significant ($\chi^2 = 4.146$, $p = 0.0524$). DARPP-32 is found at indistinguishable frequencies in PV dendrites and axon terminals ($\chi^2 = 3.170$, $p = 0.1351$). These results indicate that, of DARPP-32 and I-1, I-1 is the most prevalent PP1 inhibitor in PV dendrites and axon terminals.

Next, I identified dendrites and axon terminals which contained immunogold label for CR, then identified the percentage of those which contained DAB label for I-1 or DARPP-32 (Fig. 5-3). The frequency of CR-labeled dendrites that contained label for I-1 (23.2%, 46 of 152) was greater than the frequency of CR dendrites that contained label for DARPP-32 (8.9%, 12 of 123), and this difference was statistically significant

(Fig. 5-4; $\chi^2 = 11.481$, $p = 0.0006$). In CR axon terminals, I-1 labeling was more frequently identified (11.8%, 7 of 52) than DARPP-32 labeling (4.2%, 2 of 46). However, a valid statistical comparison could not be made because the number of expected observations of CR-labeled axon terminals in the DARPP-32 double label experiment was not sufficient. When comparing the distribution of I-1 labeling within CR interneurons, there was not a statistically significant difference in the frequency of dendritic and axon terminal labeling ($\chi^2 = 3.588$, $p = 0.0671$). Again, a valid statistical comparison could not be made to determine if DARPP-32 label was more prevalent in CR dendrites or axon terminals because the number of expected observations of CR-labeled axon terminals in the DARPP-32 double label experiment was not sufficient. In sum, these results indicate that, of DARPP-32 and I-1, I-1 is the predominant PP1 inhibitor in PV and CR interneurons.

Localization of PP1α and PP1γ1 in PV and CR interneurons

Dendrites and axon terminals which contained label for PV were identified and then examined for the presence of DAB label for either PP1α or PP1γ1 (Fig. 5-5). The frequency of PV-labeled dendrites that contain PP1α (21.4%, 63 of 231) was greater than the frequency of PV-labeled dendrites that contain PP1γ1 (6.6%, 21 of 295), and this difference was statistically significant (Fig. 5-6; $\chi^2 = 33.704$, $p < 0.0001$). In PV axon terminals, PP1α was more frequently identified (7.0%, 11 of 147) than PP1γ1 (2.4%, 4 of 166). However, a valid statistical comparison could not be made because the number of expected observations of PV-labeled axon terminals in the PP1α double label experiment was not sufficient. When comparing the distribution of PP1α within PV interneurons, PP1α labels significantly more dendrites than it does axon terminals ($\chi^2 = 14.743$, $p <$

0.0001). However, PP1γ1 labels PV dendrites and axon terminals at statistically indistinguishable frequencies ($\chi^2 = 2.228$, p = 0.1797). These data indicate that of PP1α or PP1γ1, PP1α is the predominant PP1 isoform in PV interneurons.

Dendrites and axon terminals which contained label for CR were identified and then examined for the presence of DAB label for either PP1α or PP1γ1 (Fig. 5-7). The frequency of CR-labeled dendrites that contain PP1α (10.3%, 21 of 184) was not statistically different than the frequency of CR-labeled dendrites that contain PP1γ1 (Fig. 5-8; 12.6%, 27 of 188; $\chi^2 = 0.503$, p = 0.5404). Similarly, in CR axon terminals, PP1α (6.1%, 6 of 98) and PP1γ1 (8.6%, 8 of 93) were identified at statistically indistinguishable frequencies ($\chi^2 = 0.432$, p = 0.5854). When comparing the distribution of PP1α within CR interneurons, PP1α labels dendrites and axon terminals at statistically indistinguishable frequencies ($\chi^2 = 1.443$, p = 0.2850), as does PP1γ1 ($\chi^2 = 1.009$, p = 0.4341). These data indicate that both PP1α and PP1γ1 are present at similar frequencies in CR interneurons.

Discussion

In the current chapter, I determined the localization of the key D1R signal transduction proteins I-1, DARPP-32, PP1α and PP1γ1 in two different classes of interneurons defined by their content of parvalbumin (PV) or calretinin (CR) within layer III of prefrontal cortical area 9 in *Macaca mulatta* monkeys. In PV interneurons, I-1 and PP1α are the predominant of the signal transduction proteins examined. However, in CR

interneurons, I-1, PP1α and PP1γ1 are the predominant of the signal transduction proteins examined. DARPP-32 was not frequently identified in either PV or CR interneurons.

What might the relative enhancement of I-1 and PP1α in PV interneurons mean for cAMP/PKA/I-1, DARPP-32/PP1 signaling? In the striatum, depolarization reduced Cdk5-phosphorylation of I-1 (C. Nguyen et al., 2007a). Similar to Thr35 phosphorylation of I-1, when I-1 is phosphorylated by Cdk5 it remains active, and the PKA signal can propagate (C. Nguyen et al., 2007b). However, Cdk5 phosphorylated DARPP-32 inhibits PKA (J. A. Bibb et al., 1999). Thus, the preferential localization of I-1 to PV interneurons may allow a longer and/or more robust I-1 response to depolarization and PKA activation. The localization and substrates for PP1 are largely determined by PP1-scaffolding proteins (reviewed in P. T. Cohen, 2002). Interestingly, spinophilin, a major PP1 scaffold, is also located in approximately 21% of PV dendrites (E. C. Muly et al., 2004a), and this may underlie the selective localization of PP1α to PV interneurons. PP1α is also selectively targeted to IP_3R, where it is important for initiating certain types of Ca^{2+} transients (T. S. Tang and I. Bezprozvanny, 2004). Though my data does not directly address whether I1 and PP1α are co-localized in PV interneurons, it does suggest that $G_{\alpha s}$ coupled receptors present on PV dendrites may have access to a "brake" (PP1) and accelerator (phosphorylated I-1).

In CR interneurons, I-1, PP1α and PP1γ1 are the most prevalent. Approximately 23% of post-synaptic CR dendritic profiles contain I-1, about 10% contain PP1α, and about 13% contain PP1γ1. This relationship is also seen in PV terminals where approximately 12% of CR axon terminal profiles contain I-1, about 6% contain PP1α, and about 7% contain PP1γ1. Although my data does not address whether the PP1

isoforms are co-localized in CR dendrites and axon terminals, it is interesting that adding the percentage of PP1α- and PP1γ1-labeled dendrites equals the percentage labeled by I-1, and the same is true for axon terminals. Thus, it is tempting to speculate that a CR dendrite or axon terminal would contain I-1 and PP1α, or I-1 and PP1γ1.

In Chapter 4, I identified via Western blotting and immunoelectron microscopic analysis that the $G_{\alpha s}$ signal transduction cascade in the PFC is different than what has been identified in the striatum, such that D1R cannot always utilize I-1 or DARPP-32 in pyramidal cell spines. Combined with the results from the current chapter, I have shown that signaling environments also differ between cell types within the PFC. In PFC pyramidal cell spines, D1R have little access to I-1 or DARPP-32, but always have access to PP1α and PP1γ1 (E. C. Muly et al., 2001). However, in PFC PV and CR interneurons I-1 and PP1α and PP1γ1 are abundant. Interestingly, the D_1 receptor labels PV dendrites at a similar frequency as does I-1 and PP1α, while the D_5 receptor labels CR dendrites at a similar frequency as does I-1, PP1α, and PP1γ1 (Fig. 5-9). Though my data cannot speak directly to whether the D1R are located on PV or CR dendrites which contain I-1, PP1α, and/or PP1γ1, it is likely that D_1 has access to I-1 and PP1α on some PV dendrites, while D_5 may have access to either I-1 and PP1α, or I-1 and PP1γ1 on some CR dendrites. In support of this idea, D1R signaling on PV interneurons does not require DARPP-32, but still signals via a $G_{\alpha s}$ mechanism (H. Trantham-Davidson et al., 2008), strongly suggesting that I-1 is the PP1 inhibitor in D1R-containing PV dendrites. This is in contrast to the signaling environment in pyramidal cell spines, where the D1R have sparse access to I-1 or DARPP-32, but always have access to both PP1α and PP1γ1.

Future studies directly testing the co-localization of the D1R with these signal transduction proteins in PV and CR interneurons, and examining the physiological consequences of variable signaling environments will prove useful in understanding D1R signaling in the PFC.

Figure 5-1

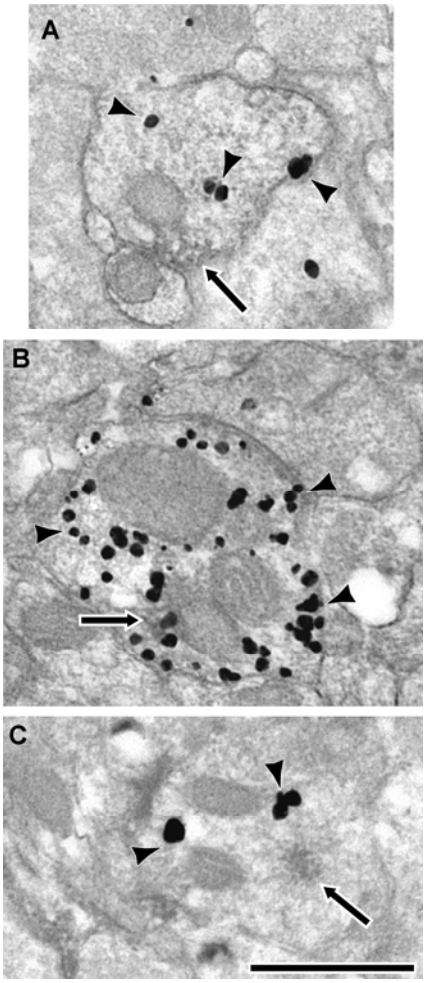

Figure 5-1. *A, B:* Electron micrographs of a dendrite (A) and an axon terminal (B) labeled with immunogold (black arrowheads) for PV and DAB (black arrows) for I-1. In B, the I-1/PV axon terminals is making a symmetric synapse onto a spine. *C:* Electron micrograph of a dendrite labeled with immunogold for PV and DAB for DARPP-32. Scale bare is 500 nm.

Figure 5-2

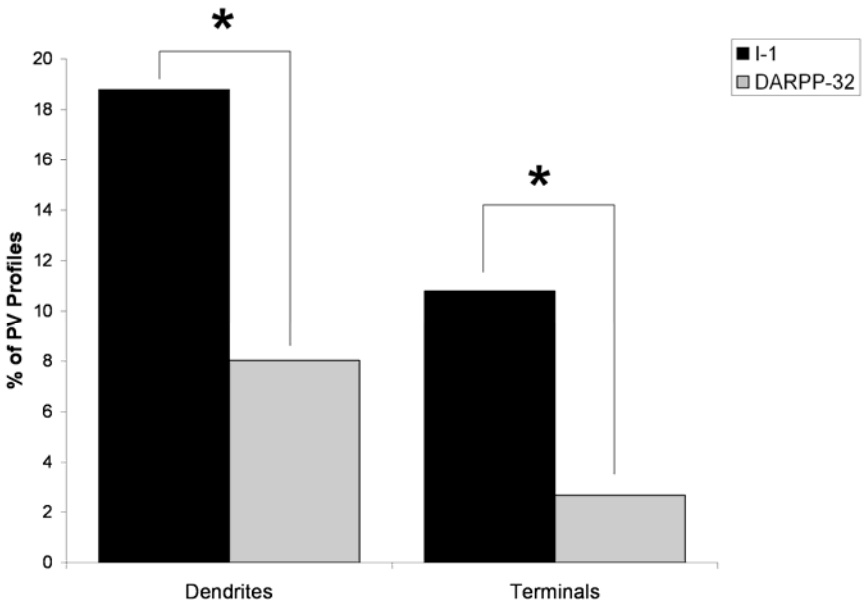

Figure 5-2. A histogram showing the percentage of PV-labeled dendrites and axon terminals that also contained immunoreactivity for I-1 and DARPP-32. The frequency of I-1/PV dendrites (18.8%) is greater than the frequency of DARPP-32/PV dendrites (8%). The frequency of I-1/PV axon terminals (10.9%) is greater than the frequency of DARPP-32/PV axon terminals (2.7%). Within I-1/PV labeled material and DARPP-32/PV labeled material there were no significant differences between dendritic and axon terminal labeling.

Figure 5-3

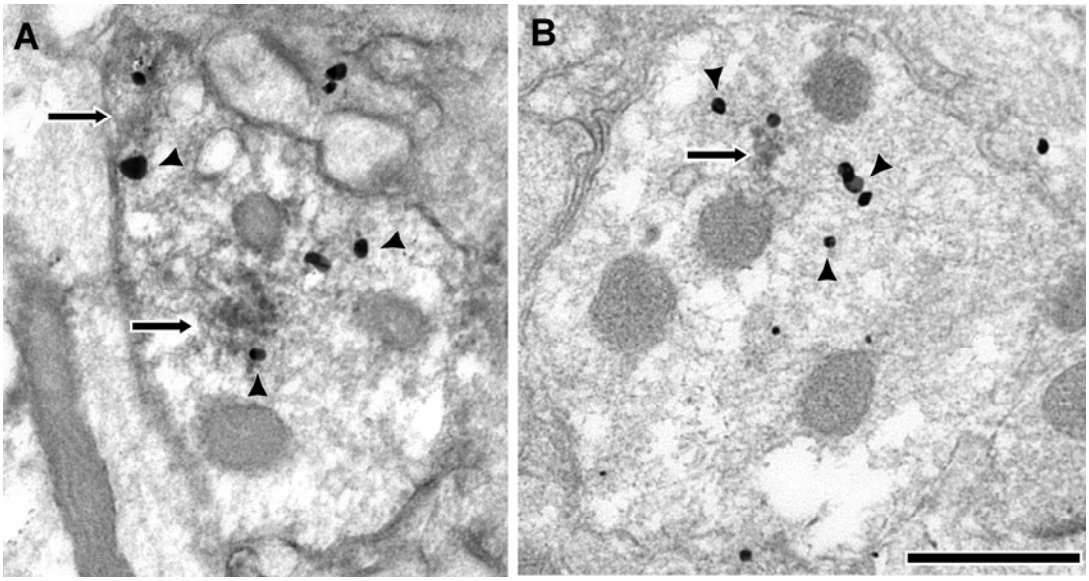

Figure 5-3. *A:* Electron micrograph of a dendrite immunogold labeled for CR (black arrowheads) and DAB labeled for I-1 (black arrows). *B:* Electron micrograph of a dendrite immunogold labeled for CR and DAB labeled for DARPP-32. Scale bar is 500 nm.

Figure 5-4

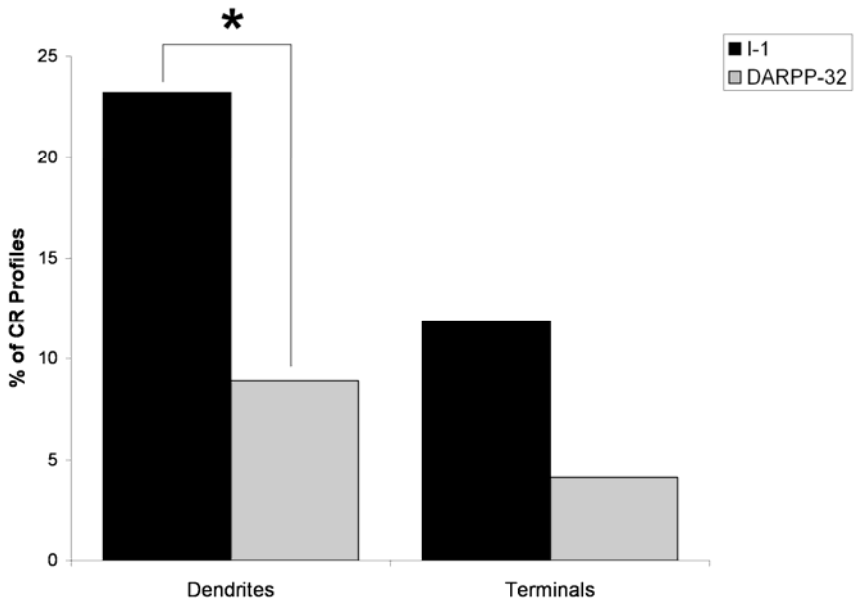

Figure 5-4. A histogram showing the percentage of CR-labeled dendrites and axon terminals that also contained immunoreactivity for I-1 and DARPP-32. The frequency of I-1/CR dendrites (23.2%) is greater than the frequency of DARPP-32/CR dendrites (8.9%). The number of expected observations of CR-labeled axon terminals in the DARPP-32 condition was not sufficient to perform a valid statistical comparison. Within I-1/CR material, there was no statistical difference in the frequency of dendritic or axon terminal labeling.

Figure 5-5

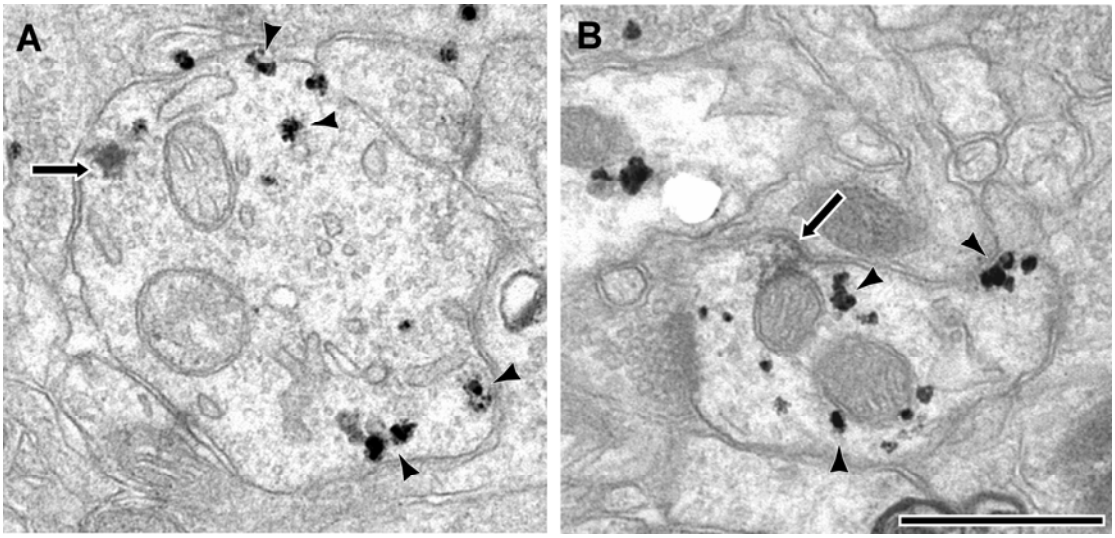

Figure 5-5. *A:* Electron micrograph of a dendrite labeled with immunogold (black arrowheads) for PV and DAB (black arrows) for PP1α. *B:* Electron micrograph of a dendrite labeled with immunogold (black arrowheads) for PV and DAB (black arrows) for PP1γ1. Scale bar is 500 nm.

Figure 5-6

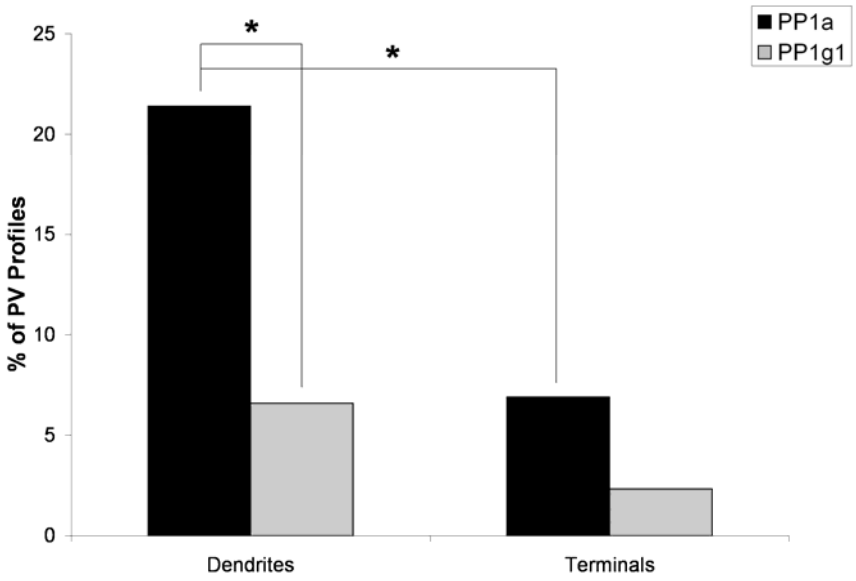

Figure 5-6. A histogram showing the percentage of PV-labeled dendrites and axon terminals that also contained immunoreactivity for PP1α and PP1γ1. The frequency of PP1α/PV dendrites (21.4%) is greater than the frequency of PP1γ1/PV dendrites (6.6%). The expected number of observations of PV-labeled axon terminals in the PP1α experiments was not sufficient to permit a valid statistical comparison. Within PP1α/PV double labeled material, PP1α labeled significantly more dendrites than it does axon terminals.

Figure 5-7

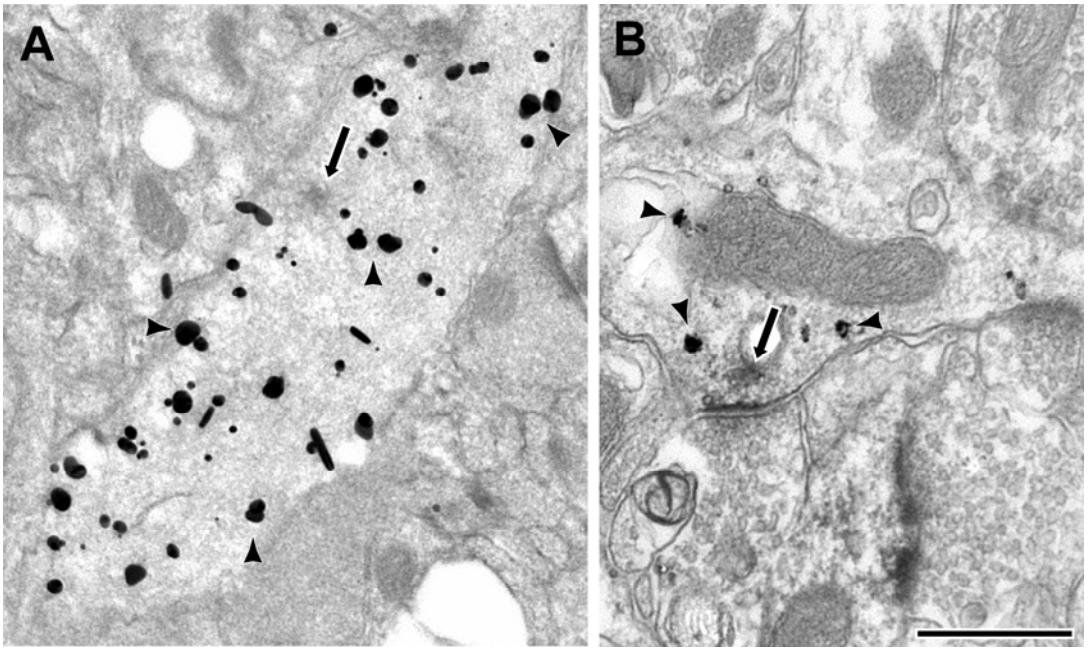

Figure 5-7. *A:* Electron micrograph of a dendrite labeled with immunogold (black arrowheads) for CR and DAB (black arrows) for PP1α. *B:* Electron micrograph of a dendrite labeled with immunogold (black arrowheads) for CR and DAB (black arrows) for PP1γ1. Scale bar is 500 nm.

Figure 5-8

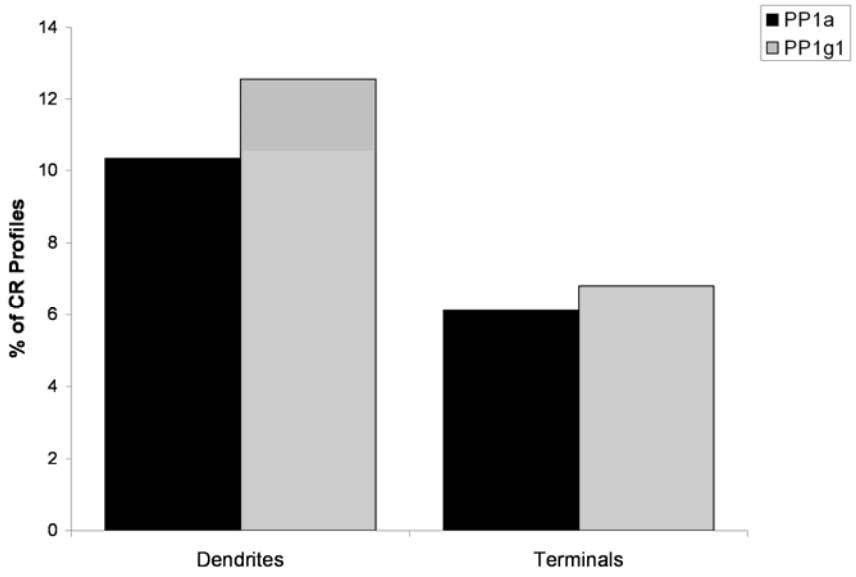

Figure 5-8. A histogram showing the percentage of CR-labeled dendrites and axon terminals that also contained immunoreactivity for PP1α and PP1γ1. There were no significant differences in the extent of CR dendritic or axon terminal labeling between PP1α and PP1γ1.

Figure 5-9

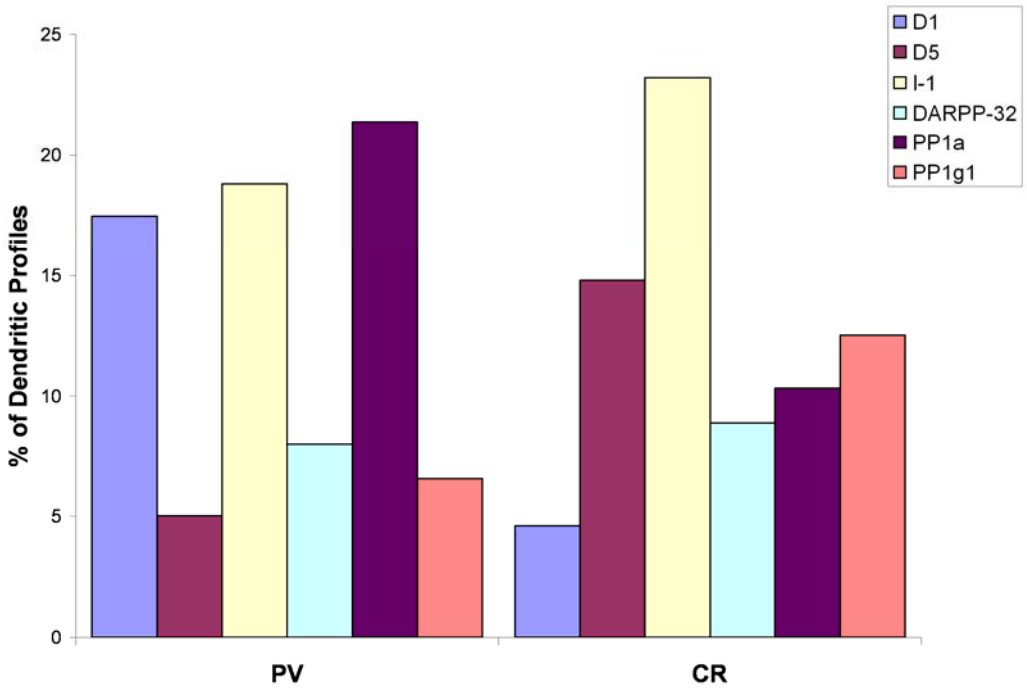

Figure 5-9. Histogram showing the percentage of PV and CR dendritic profiles labeled by the D_1, D_5, I-1, DARPP-32, PP1α and PP1γ1. In PV dendrites, D_1, I-1 and PP1α are most prevalent. On the other hand, D_5, I-1, PP1α and PP1γ1 predominant in CR dendrites.

Chapter 6

Concluding Remarks

Summary of Findings

Working memory (WM) is a core cognitive process that is severely impaired in individuals diagnosed with schizophrenia (reviewed in P. S. Goldman-Rakic, 1994). Because cognitive ability is the best predictor of employment, social integration and relapse (T. Wykes, 1994; M. F. Green, 1996; P. H. Lysaker et al., 1996; S. R. McGurk and H. Y. Meltzer, 2000; M. F. Green et al., 2004), it is important to understand how WM functions and how it is altered in schizophrenia. WM depends upon D1 dopamine receptor family (D1R) signaling in an intact dorsolateral prefrontal cortex (dlPFC) (reviewed in G. V. Williams and S. A. Castner, 2006). Interestingly, the relationship between D1R activation and WM ability is an inverted-U, such that too much or too little D1R stimulation impairs WM (reviewed in P. S. Goldman-Rakic et al., 2000). What might be underlying this relationship? I propose that the different molecular properties and anatomical localization of the D_1 and D_5 receptors, along with their signal transduction proteins, will shed light on this inverted-U relationship. To investigate this possibility, I have utilized immunoelectron microscopy to quantify the ultrastructural localization of D_1, D_5, inhibitor-1 (I-1), DARPP-32, PP1α and PP1γ1 in prefrontal cortical pyramidal cell spines, and parvalbumin (PV) and calretinin (CR) interneurons. My key findings are summarized below and are schematically represented in Figure 6-1.

1) The D_1 receptor is located in approximately 21% of PFC pyramidal cell spines, and the D_5 receptor is located in approximately 14% of spines. D_5 is always located with D_1 in those 14% of spines, and an additional 7% of spines contain only D_1.

2) Unlike PP1α and PP1γ1, I-1 and DARPP-32 are infrequently identified in PFC pyramidal cell spines.
3) PV interneurons predominately express the D_1 receptor, while CR interneurons predominately express D_5.
4) PV interneurons predominately express I-1 and PP1α, while CR interneurons express I-1, PP1α and PP1γ1. DARPP-32 is not enriched in either interneuron population.

D1R Signaling and Delay Cell Activity

Recording from awake, behaving monkeys have identified cells which selectively respond during the delay period of a WM task in a stimulus-specific manner. Moreover, these neurons also respond to D1R stimulation in an inverted-U manner. Because of these properties, these cells are proposed to be the cellular correlate of WM, and have been termed "delay cells" (reviewed in P. S. Goldman-Rakic, 1995). Peak delay cell firing rates are seen with low levels of D1R stimulation (S. Vijayraghavan et al., 2007). As D1R stimulation increases (G. V. Williams and P. S. Goldman-Rakic, 1995; S. Vijayraghavan et al., 2007), or is completely blocked by high ejection current application of D1R antagonists (G. V. Williams and P. S. Goldman-Rakic, 1995; T. Sawaguchi, 2001b), delay cell activity dramatically falls. Intriguingly, Vijayraghavan and colleagues (2007) have demonstrated that delay activity signal to noise is not associated with maximal delay cell activity, but rather at higher levels of D1R stimulation when overall firing rates are moderate (see their Figure 1B). These observed relationships between

D1R stimulation and cell activity and delay signal to noise levels are illustrated in Figure 6-2A.

The data presented in this dissertation on differential localization of D_1 and D_5 to PV and CR interneurons, respectively, along with the known connectivity of these cell types and differential receptor affinities for dopamine suggest a circuit mechanism by which D1R stimulation can control pyramidal cell output (Fig. 6-2B). Panel 1 reflects the output when there is no D1R stimulation, a condition which can only be induced experimentally with high doses of D1R antagonist or dopamine depletion, and in which there is no D1R mediated augmentation of glutamate currents. Panel 2 reflects the activity of these cells when there are low levels of dopamine. The D_5 receptors found on CR interneurons and pyramidal cell spines (J. R. Bordelon-Glausier et al., 2008) are preferentially activated due to their higher affinity for dopamine. Activation of G_s coupled D_5 would be expected to augment glutamatergic inputs to these pyramidal cell spines, as well as to CR interneurons. This increased activation of CR interneurons would increase inhibition of their postsynaptic targets, including PV interneurons, resulting in disinhibition and peak activity levels of their pyramidal cell targets. As dopamine levels rise, the activation of D_5 receptors would plateau, while D_1 receptors on PV interneurons and pyramidal cell spines would be activated. Glutamatergic neurotransmission in these circuitry components will be increasingly augmented, eventually allowing PV interneurons to escape from the inhibitory control of CR cell. As PV interneuron activity increases, pyramidal cell output would decrease accordingly (Panels 3 and 4).

The model proposed here provides a circuit basis for understanding the relationship between dopamine stimulation of D1R; however, additional work will be required to resolve several issues. First, this model does not account for data indicating the PV interneurons receive more direct dopaminergic input than CR interneurons (S. R. Sesack et al., 1995b; L. S. Krimer et al., 1997; S. R. Sesack et al., 1998). While this may impact the access these interneurons have to dopamine, D1R are not seen at symmetric synapses (J. F. Smiley et al., 1994; E. C. Muly et al., 1998; J. R. Bordelon-Glausier et al., In Press), the morphology of dopaminergic synapses (P. S. Goldman-Rakic et al., 1989; S. R. Sesack et al., 1995a). Thus extrasynaptic dopamine may be the primary means of D1R activation in the PFC. Second, this model cannot explain existing *in vivo* studies show that D1R stimulation produces a preferential decrease in activity for the non-preferred direction in spatially tuned delay cells (T. Sawaguchi, 2001b; S. Vijayraghavan et al., 2007). The mechanism by which this is achieved is unclear, though it may relate to the wider tangential spread of the axons and dendrites of PV compared to CR interneurons (reviewed in J. DeFelipe, 1997).

One important assumption of this model is that the D1R on spines and PV and CR interneurons are signaling via the cAMP/PKA/I-1, DARPP-32/PP1 pathway. My results, suggest that D1R can signal through a traditional I-1/PP1 pathway in PV and CR interneurons, but that they do not utilize I-1 or DARPP-32 to inhibit PP1 in all of the PFC pyramidal cell spines to which they are located. This is especially interesting in light of the fact that D_1 and D_5 are co-localized on pyramidal cell spines. Why would two $G_{\alpha s}$-coupled receptors be located on the same spine? As discussed earlier (Chapter 2), there is evidence that the two D1R subtypes can couple to different G- proteins (K. Kimura et al.,

1995; A. Sidhu et al., 1998; Q. Wang et al., 2001), can differentially signal via protein kinase C and phospholipase C (P. Y. Yu et al., 1996; M. Paolillo et al., 1998; A. Jackson et al., 2005; X. Zhen et al., 2005) and are physically linked to different effector proteins (F. Liu et al., 2000; F. J. Lee et al., 2002). My results now add to this growing data on non- $G_{\alpha s}$ signaling by showing that D1R cannot be signaling via I-1/DARPP-32 in all PFC spines. Furthermore, there is growing evidence that G-protein coupled receptors can signal via heterodimers or oligomers (M. Bouvier, 2001; S. C. Prinster et al., 2005), including a D_1-D_2 heterodimer (M. Dziedzicka-Wasylewska et al., 2006). Perhaps on these PFC pyramidal cells spines that contain both D1R, they are interacting and utilizing a completely different signal transduction cascade. Indeed, the group I metabotropic glutamate receptors 1 and 5 are frequently co-localized, even though they both classically signal via the same second messenger cascade. Using subtype-specific pharmacological tools, it is now known that activation of each receptor leads to discrete neuronal responses when the two are co-localized (reviewed in O. Valenti et al., 2002; O. V. Poisik et al., 2003). Future biochemical studies examining the possibility of a D_1-D_5 heterodimer and studies examining electrophysiological differences in activating cells which contain either or both D1R will prove helpful in understand D1R signaling.

Implications for Schizophrenia

Understanding the precise localization of D1R and their signal transduction proteins allows us to make better predictions about how D1R agents might affect PFC functioning in normal and disease groups. In order to understand how my results could

contribute to directing drug development for WM improvement in the schizophrenia patient population, we must first understand the basal state of their PFC.

Though it is currently technically very difficult to directly measure dopamine levels in the PFC of humans, several indirect measures strongly suggest that dopamine levels are low in the PFC of schizophrenia patients (D. G. Daniel et al., 1991; M. Laruelle et al., 1996; M. Akil et al., 1999; A. Abi-Dargham et al., 2002), including an increased availability of D1R in the dlPFC of non-mediated schizophrenia patients which strongly correlates with poor WM performance (A. Abi-Dargham et al., 2002). Moreover, chronic treatment with neuroleptics down regulates D_1 and D_5 receptors specifically in the PFC (M. S. Lidow et al., 1997) and impairs WM performance (S. A. Castner et al., 2000). So patients treated with neuroleptics likely already have low PFC dopamine levels, and any compensatory increase in D1R would be blocked by their pharmacological treatment. However, traditional neuroleptic treatment is important for outcome as well, so we must think of ways to improve WM performance concomitant with neuroleptic treatment.

An elegant study was performed by Stacy Castner and colleagues (2000) where monkeys were trained on a WM task and then chronically given haloperidol. The chronic haloperidol treatment significantly impaired their WM performance. To determine if the down regulation of PFC D1R contributed to the WM impairments, the monkeys were treated with D1R agonist. All monkeys showed significant WM performance improvement for over a year after their final agonist treatment (S. A. Castner et al., 2000). I propose that the WM performance and delay cell output in these monkeys became left-shifted when they were chronically treated with haloperidol (Fig. 6-2A, part 2). Thus D1R stimulation would have been low, WM was poor, and delay cell activity

was high. Their performance would have been shifted back to the right after D1R agonist treatment, and my dissertation work suggests that this behavioral response occurred in part to increasing D_1 stimulation on PV interneurons to decrease and focus the output of the pyramidal cell. If patients diagnosed with schizophrenia are in a similar biochemical predicament as these haloperidol-treated monkeys, I predict that treatment with moderate amounts of a D1R agonist would improve their WM ability. There is an encouraging study done with the compound stepholidine, which acts as a D2R antagonist and a D1R agonist. When this drug is applied in the medial PFC of rodents, it acts via D1R to inhibit pyramidal cell output (Z. T. Zhu et al., 2000). If, as I propose, there is too much PFC pyramidal cell output in patients diagnosed with schizophrenia, this compound may decrease that activity by activating D_1 receptors on PV interneurons, ultimately resulting in improvements to WM performance. My hypothesis that if un-focused, increased pyramidal cell output contributes to poor WM performance, then increasing the inhibition to pyramidal cells by augmenting PV interneuron activity will improve WM performance is best tested in the following way. Much like the Castner and colleagues study (2000), I would use the same behavioral and pharmacological protocol, such that monkeys are trained on a WM task, chronically given haloperidol to impair WM performance, then given D1R agonists to improve WM performance. However, at each of these steps, pyramidal cells should be recorded in the dlPFC. I would predict that with chronic haloperidol, WM will be poor and dlPFC activity will be high. With concomitant D1R agonist treatment, WM will improve and pyramidal cell activity will decrease. Furthermore, it would be very interesting to also record from PV interneurons during each testing step to identify if their activity inversely correlates with pyramidal cell

activity. These types of studies, in conjunction with neuroanatomical work, will shed a great deal of light on how the PFC works and how changes in neuronal activity and timing relate to behavioral outcomes.

Figure 6-1

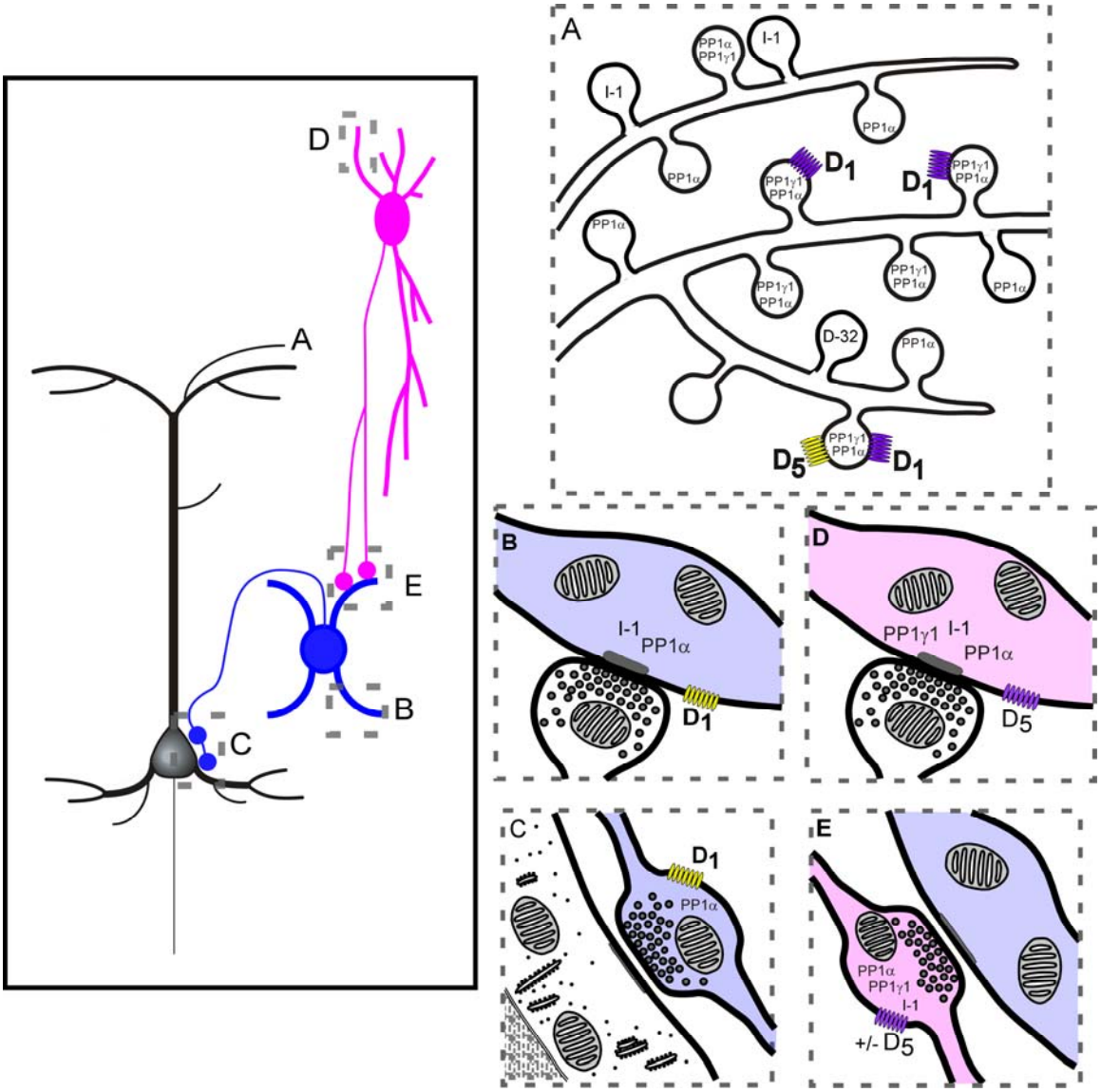

Figure 6-1. Schematic representation of key findings in the current dissertation. In PFC pyramidal cell spines, the D1R likely do not have access to I-1 and DARPP-32.

However, in PV dendrites, D_1 receptors likely have access to both I-1 and PP1α. In CR interneurons, the D_5 receptor has access to I-1, PP1α and PP1γ1. These results indicate that signaling environments can differ across specific components of the neuropil.

Figure 6-2

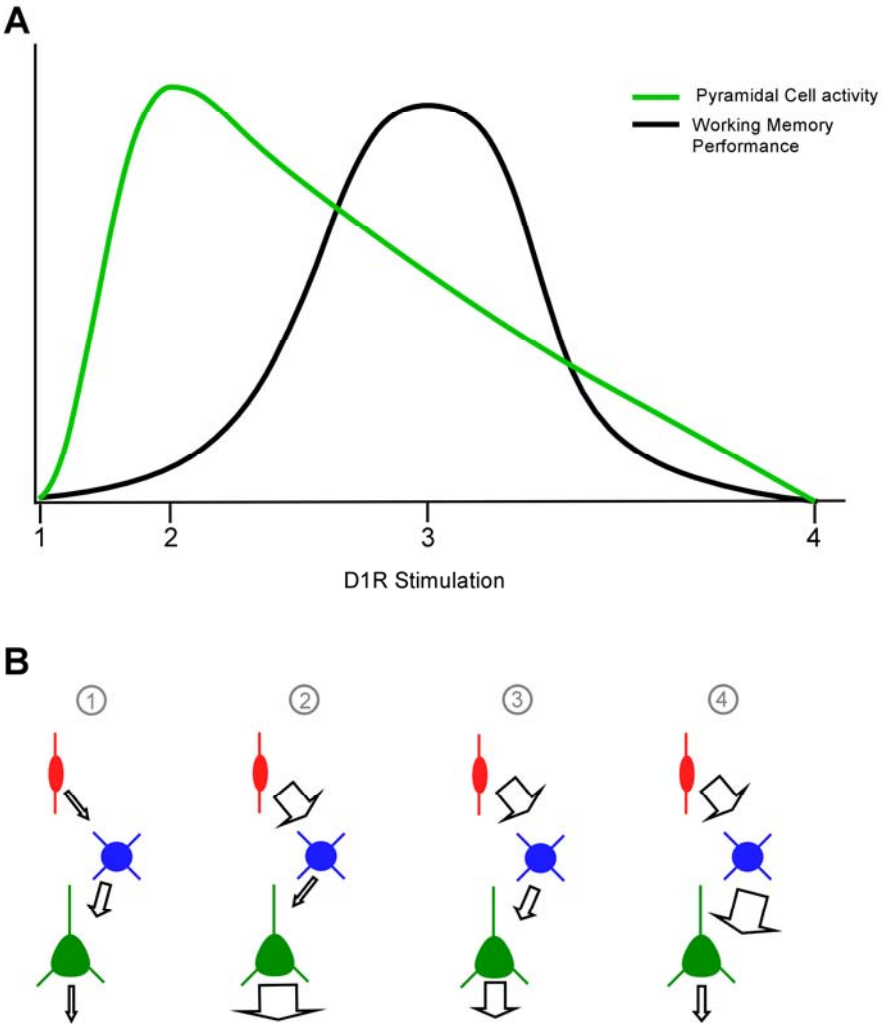

Figure 6-2. *A:* Graphical representation of the relationship between D1R stimulation and pyramidal cell activity (green), or WM performance (black). Different levels of D1R stimulation are indicated by numbers on the X axis. Point 1 represents no D1R stimulation, resulting in very little pyramidal cell output and poor WM performance. Point 2 represents low levels of D1R stimulation, with strong pyramidal cell activity but with suboptimal WM performance. Point 3 represents moderate levels of D1R stimulation. At this point, pyramidal cell activity is lower, but WM performance is

optimal. Finally, point 4 represents high levels of D1R stimulation, and both pyramidal cell activity and WM performance are diminished. Note that while both pyramidal cell activity and WM performance have inverted-U relationships with D1R activation, the cell activity peak is left- shifted compared to working memory performance. *B:* Simplified circuit model of the relationship between CR interneurons (red), PV interneurons (blue) and pyramidal cells (green). Panel 1 represents activity levels with there is no D1R stimulation. Panel 2 represents cellular activity levels at low D1R stimulation. D_5 receptors on CR interneurons would be preferentially activated, enhancing their output, resulting in decreased PV interneuron activity and disinhibiting the pyramidal cell. Panel 3 represents cellular activity levels at moderate D1R stimulation. While D_5 receptors on CR interneurons are still being activated, D_1 receptors on PV interneurons are also now stimulated, allowing the PV interneurons to overcome some of the inhibition by CR interneurons which in turn results in decreased pyramidal cell activity. Finally, panel 4 represents cellular activity levels at high D1R stimulation. D_1 receptors on the PV interneurons are now maximally stimulated, overriding most of the inhibition from CR interneurons. PV interneuron activity will be greatly enhanced, resulting in a dramatic reduction in pyramidal cell output.

Literature Cited

Abi-Dargham A, Mawlawi O, Lombardo I, Gil R, Martinez D, Huang Y, Hwang DR, Keilp J, Kochan L, Van Heertum R, Gorman JM, Laruelle M (2002) Prefrontal dopamine D1 receptors and working memory in schizophrenia. J Neurosci 22:3708-3719.

Aggen JB, Nairn AC, Chamberlin R (2000) Regulation of protein phosphatase-1. Chem Biol 7:R13-23.

Aitken A, Bilham T, Cohen P (1982) Complete primary structure of protein phosphatase inhibitor-1 from rabbit skeletal muscle. Eur J Biochem 126:235-246.

Akil M, Pierri JN, Whitehead RE, Edgar CL, Mohila C, Sampson AR, Lewis DA (1999) Lamina-specific alterations in the dopamine innervation of the prefrontal cortex in schizophrenic subjects. Am J Psychiatry 156:1580-1589.

Allen PB, Ouimet CC, Greengard P (1997) Spinophilin, a novel protein phosphatase 1 binding protein localized to dendritic spines. Proc Natl Acad Sci U S A 94:9956-9961.

Allen PB, Zachariou V, Svenningsson P, Lepore AC, Centonze D, Costa C, Rossi S, Bender G, Chen G, Feng J, Snyder GL, Bernardi G, Nestler EJ, Yan Z, Calabresi P, Greengard P (2006) Distinct roles for spinophilin and neurabin in dopamine-mediated plasticity. Neuroscience 140:897-911.

Alloway TP, Archibald L (2008) Working memory and learning in children with developmental coordination disorder and specific language impairment. J Learn Disabil 41:251-262.

Amador FC, Henriques AG, da Cruz ESOA, da Cruz ESEF (2004) Monitoring protein phosphatase 1 isoform levels as a marker for cellular stress. Neurotoxicol Teratol 26:387-395.

Arnsten AF, Goldman-Rakic PS (1998) Noise stress impairs prefrontal cortical cognitive function in monkeys: evidence for a hyperdopaminergic mechanism. Arch Gen Psychiatry 55:362-368.

Arnsten AF, Cai JX, Murphy BL, Goldman-Rakic PS (1994) Dopamine D1 receptor mechanisms in the cognitive performance of young adult and aged monkeys. Psychopharmacology (Berl) 116:143-151.

Association AP, ed (1994) Diagnostic and Statistical Manual of Mental Disorders (DSM-IV), Fourth Edition. Washington, D.C.: American Psychiatric Association.

Bacci A, Rudolph U, Huguenard JR, Prince DA (2003) Major differences in inhibitory synaptic transmission onto two neocortical interneuron subclasses. J Neurosci 23:9664-9674.

Baddeley A (1986) Working Memory. London: Oxford University Press.

Barch DM, Carter CS, Hachten PC, Usher M, Cohen JD (1999) The "benefits" of distractibility: mechanisms underlying increased Stroop effects in schizophrenia. Schizophr Bull 25:749-762.

Behr J, Gloveli T, Schmitz D, Heinemann U (2000) Dopamine depresses excitatory synaptic transmission onto rat subicular neurons via presynaptic D1-like dopamine receptors. J Neurophysiol 84:112-119.

Berger B, Febvret A, Greengard P, Goldman-Rakic PS (1990) DARPP-32, a phosphoprotein enriched in dopaminoceptive neurons bearing dopamine D1

receptors: distribution in the cerebral cortex of the newborn and adult rhesus monkey. J Comp Neurol 299:327-348.

Bergson C, Mrzljak L, Lidow MS, Goldman-Rakic P, Levenson R (1995a) Characterization of subtype-specific antibodies to the human D5 dopamine receptor: studies in primate brain and transfected mammalian cells. Proc Natl Acad Sci U S A 92:3468-3472.

Bergson C, Mrzljak L, Smiley JF, Pappy M, Levenson R, Goldman-Rakic PS (1995b) Regional, cellular, and subcellular variations in the distribution of D1 and D5 dopamine receptors in primate brain. J Neurosci 15:7821-7836.

Bibb JA, Snyder GL, Nishi A, Yan Z, Meijer L, Fienberg AA, Tsai LH, Kwon YT, Girault JA, Czernik AJ, Huganir RL, Hemmings HC, Jr., Nairn AC, Greengard P (1999) Phosphorylation of DARPP-32 by Cdk5 modulates dopamine signalling in neurons. Nature 402:669-671.

Bleuler E (1950) Dementia Praecox or the Group of Schizophrenias, 1 Edition. New York, NY: International Universities Press.

Bordelon-Glausier JR, Khan ZU, Muly EC (2008) Quantification of D1 and D5 dopamine receptor localization in layers I, III, and V of Macaca mulatta prefrontal cortical area 9: coexpression in dendritic spines and axon terminals. J Comp Neurol 508:893-905.

Bordelon-Glausier JR, Muly EC, Khan ZU (In Press) Quantification of D1 and D5 dopamine receptor localization in layers I, III and V of Macaca mulatta prefrontal cortical area 9: co-expression in dendritic spines and axon terminals. J Comp Neurol.

Bordelon JR, Smith Y, Nairn AC, Colbran RJ, Greengard P, Muly EC (2005) Differential Localization of Protein Phosphatase-1{alpha}, {beta} and {gamma}1 Isoforms in Primate Prefrontal Cortex. Cereb Cortex.

Bouvier M (2001) Oligomerization of G-protein-coupled transmitter receptors. Nat Rev Neurosci 2:274-286.

Brewer WJ, Francey SM, Wood SJ, Jackson HJ, Pantelis C, Phillips LJ, Yung AR, Anderson VA, McGorry PD (2005) Memory impairments identified in people at ultra-high risk for psychosis who later develop first-episode psychosis. Am J Psychiatry 162:71-78.

Brito V, Beyer C, Kuppers E (2004) BDNF-dependent stimulation of dopamine D5 receptor expression in developing striatal astrocytes involves PI3-kinase signaling. Glia 46:284-295.

Brown AM, Baucum AJ, Bass MA, Colbran RJ (2008) Association of protein phosphatase 1gamma 1 with spinophilin suppresses phosphatase activity in a Parkinson's disease model. J Biol Chem.

Brozoski TJ, Brown RM, Rosvold HE, Goldman PS (1979) Cognitive deficit caused by regional depletion of dopamine in prefrontal cortex of rhesus monkey. Science 205:929-932.

Brush MH, Weiser DC, Shenolikar S (2003) Growth arrest and DNA damage-inducible protein GADD34 targets protein phosphatase 1 alpha to the endoplasmic reticulum and promotes dephosphorylation of the alpha subunit of eukaryotic translation initiation factor 2. Mol Cell Biol 23:1292-1303.

Bucci S, Startup M, Wynn P, Heathcote A, Baker A, Lewin TJ (2008) Referential delusions of communication and reality discrimination deficits in psychosis. Br J Clin Psychol.

Buckley PF, Stahl SM (2007) Pharmacological treatment of negative symptoms of schizophrenia: therapeutic opportunity or cul-de-sac? Acta Psychiatr Scand 115:93-100.

Byrne M, Hodges A, Grant E, Owens DC, Johnstone EC (1999) Neuropsychological assessment of young people at high genetic risk for developing schizophrenia compared with controls: preliminary findings of the Edinburgh High Risk Study (EHRS). Psychol Med 29:1161-1173.

Callicott JH, Mattay VS, Verchinski BA, Marenco S, Egan MF, Weinberger DR (2003a) Complexity of prefrontal cortical dysfunction in schizophrenia: more than up or down. Am J Psychiatry 160:2209-2215.

Callicott JH, Egan MF, Mattay VS, Bertolino A, Bone AD, Verchinksi B, Weinberger DR (2003b) Abnormal fMRI response of the dorsolateral prefrontal cortex in cognitively intact siblings of patients with schizophrenia. Am J Psychiatry 160:709-719.

Cannon M, Caspi A, Moffitt TE, Harrington H, Taylor A, Murray RM, Poulton R (2002) Evidence for early-childhood, pan-developmental impairment specific to schizophreniform disorder: results from a longitudinal birth cohort. Arch Gen Psychiatry 59:449-456.

Carmody LC, Bauman PA, Bass MA, Mavila N, DePaoli-Roach AA, Colbran RJ (2004) A protein phosphatase-1gamma1 isoform selectivity determinant in dendritic spine-associated neurabin. J Biol Chem 279:21714-21723.

Carter CS, Perlstein W, Ganguli R, Brar J, Mintun M, Cohen JD (1998) Functional hypofrontality and working memory dysfunction in schizophrenia. Am J Psychiatry 155:1285-1287.

Castner SA, Williams GV, Goldman-Rakic PS (2000) Reversal of antipsychotic-induced working memory deficits by short-term dopamine D1 receptor stimulation. Science 287:2020-2022.

Centonze D, Grande C, Saulle E, Martin AB, Gubellini P, Pavon N, Pisani A, Bernardi G, Moratalla R, Calabresi P (2003) Distinct roles of D1 and D5 dopamine receptors in motor activity and striatal synaptic plasticity. J Neurosci 23:8506-8512.

Ceulemans H, Bollen M (2004) Functional diversity of protein phosphatase-1, a cellular economizer and reset button. Physiol Rev 84:1-39.

Chen G, Greengard P, Yan Z (2004) Potentiation of NMDA receptor currents by dopamine D1 receptors in prefrontal cortex. Proc Natl Acad Sci U S A 101:2596-2600.

Ciliax BJ, Nash N, Heilman C, Sunahara R, Hartney A, Tiberi M, Rye DB, Caron MG, Niznik HB, Levey AI (2000) Dopamine D(5) receptor immunolocalization in rat and monkey brain. Synapse 37:125-145.

Clark D, Dedova I, Cordwell S, Matsumoto I (2006) A proteome analysis of the anterior cingulate cortex gray matter in schizophrenia. Mol Psychiatry 11:459-470, 423.

Clinton SM, Ibrahim HM, Frey KA, Davis KL, Haroutunian V, Meador-Woodruff JH (2005) Dopaminergic abnormalities in select thalamic nuclei in schizophrenia: involvement of the intracellular signal integrating proteins calcyon and spinophilin. Am J Psychiatry 162:1859-1871.

Cohen JD, Barch DM, Carter C, Servan-Schreiber D (1999) Context-processing deficits in schizophrenia: converging evidence from three theoretically motivated cognitive tasks. J Abnorm Psychol 108:120-133.

Cohen PT (1988) Two isoforms of protein phosphatase 1 may be produced from the same gene. FEBS Lett 232:17-23.

Cohen PT (2002) Protein phosphatase 1--targeted in many directions. J Cell Sci 115:241-256.

Colbran RJ (2004) Protein phosphatases and calcium/calmodulin-dependent protein kinase II-dependent synaptic plasticity. J Neurosci 24:8404-8409.

Conde F, Lund JS, Jacobowitz DM, Baimbridge KG, Lewis DA (1994) Local circuit neurons immunoreactive for calretinin, calbindin D-28k or parvalbumin in monkey prefrontal cortex: distribution and morphology. J Comp Neurol 341:95-116.

Cornblatt BA, Keilp JG (1994) Impaired attention, genetics, and the pathophysiology of schizophrenia. Schizophr Bull 20:31-46.

da Cruz e Silva EF, Fox CA, Ouimet CC, Gustafson E, Watson SJ, Greengard P (1995) Differential expression of protein phosphatase 1 isoforms in mammalian brain. J Neurosci 15:3375-3389.

Daniel DG, Weinberger DR, Jones DW, Zigun JR, Coppola R, Handel S, Bigelow LB, Goldberg TE, Berman KF, Kleinman JE (1991) The effect of amphetamine on regional cerebral blood flow during cognitive activation in schizophrenia. J Neurosci 11:1907-1917.

DeFelipe J (1997) Types of neurons, synaptic connections and chemical characteristics of cells immunoreactive for calbindin-D28K, parvalbumin and calretinin in the neocortex. J Chem Neuroanat 14:1-19.

DeFelipe J, Hendry SH, Jones EG (1989) Visualization of chandelier cell axons by parvalbumin immunoreactivity in monkey cerebral cortex. Proc Natl Acad Sci U S A 86:2093-2097.

DeFelipe J, Hendry SH, Jones EG, Schmechel D (1985) Variability in the terminations of GABAergic chandelier cell axons on initial segments of pyramidal cell axons in the monkey sensory-motor cortex. J Comp Neurol 231:364-384.

Delawalla Z, Csernansky JG, Barch DM (2008) Prefrontal cortex function in nonpsychotic siblings of individuals with schizophrenia. Biol Psychiatry 63:490-497.

Deng YP, Xie JP, Wang HB, Lei WL, Chen Q, Reiner A (2007) Differential localization of the GluR1 and GluR2 subunits of the AMPA-type glutamate receptor among striatal neuron types in rats. J Chem Neuroanat 33:167-192.

Desdouits F, Siciliano JC, Greengard P, Girault JA (1995) Dopamine- and cAMP-regulated phosphoprotein DARPP-32: phosphorylation of Ser-137 by casein kinase I inhibits dephosphorylation of Thr-34 by calcineurin. Proc Natl Acad Sci U S A 92:2682-2685.

Dombradi V, Axton JM, Brewis ND, da Cruz e Silva EF, Alphey L, Cohen PT (1990) Drosophila contains three genes that encode distinct isoforms of protein phosphatase 1. Eur J Biochem 194:739-745.

Dombrowski SM, Hilgetag CC, Barbas H (2001) Quantitative architecture distinguishes prefrontal cortical systems in the rhesus monkey. Cereb Cortex 11:975-988.

Dumartin B, Jaber M, Gonon F, Caron MG, Giros B, Bloch B (2000) Dopamine tone regulates D1 receptor trafficking and delivery in striatal neurons in dopamine transporter-deficient mice. Proc Natl Acad Sci U S A 97:1879-1884.

Dziedzicka-Wasylewska M, Faron-Gorecka A, Andrecka J, Polit A, Kusmider M, Wasylewski Z (2006) Fluorescence studies reveal heterodimerization of dopamine D1 and D2 receptors in the plasma membrane. Biochemistry 45:8751-8759.

Dziewczapolski G, Menalled LB, Garcia MC, Mora MA, Gershanik OS, Rubinstein M (1998) Opposite roles of D1 and D5 dopamine receptors in locomotion revealed by selective antisense oligonucleotides. Neuroreport 9:1-5.

Elvevag B, Goldberg TE (2000) Cognitive impairment in schizophrenia is the core of the disorder. Crit Rev Neurobiol 14:1-21.

Erlenmeyer-Kimling L, Rock D, Roberts SA, Janal M, Kestenbaum C, Cornblatt B, Adamo UH, Gottesman, II (2000) Attention, memory, and motor skills as childhood predictors of schizophrenia-related psychoses: the New York High-Risk Project. Am J Psychiatry 157:1416-1422.

Fienberg AA, Greengard P (2000) The DARPP-32 knockout mouse. Brain Res Brain Res Rev 31:313-319.

Filip M, Thomas ML, Cunningham KA (2000) Dopamine D5 receptors in nucleus accumbens contribute to the detection of cocaine in rats. J Neurosci 20:RC98.

Flores-Hernandez J, Hernandez S, Snyder GL, Yan Z, Fienberg AA, Moss SJ, Greengard P, Surmeier DJ (2000) D(1) dopamine receptor activation reduces GABA(A) receptor currents in neostriatal neurons through a PKA/DARPP-32/PP1 signaling cascade. J Neurophysiol 83:2996-3004.

Flores-Hernandez J, Cepeda C, Hernandez-Echeagaray E, Calvert CR, Jokel ES, Fienberg AA, Greengard P, Levine MS (2002) Dopamine enhancement of NMDA currents in dissociated medium-sized striatal neurons: role of D1 receptors and DARPP-32. J Neurophysiol 88:3010-3020.

Floresco SB, Phillips AG (2001) Delay-dependent modulation of memory retrieval by infusion of a dopamine D1 agonist into the rat medial prefrontal cortex. Behav Neurosci 115:934-939.

Funahashi S, Bruce CJ, Goldman-Rakic PS (1989) Mnemonic coding of visual space in the monkey's dorsolateral prefrontal cortex. J Neurophysiol 61:331-349.

Gabbott PL, Bacon SJ (1996) Local circuit neurons in the medial prefrontal cortex (areas 24a,b,c, 25 and 32) in the monkey: I. Cell morphology and morphometrics. J Comp Neurol 364:567-608.

Galvan A, Kuwajima M, Smith Y (2006) Glutamate and GABA receptors and transporters in the basal ganglia: what does their subsynaptic localization reveal about their function? Neuroscience 143:351-375.

Gao WJ, Krimer LS, Goldman-Rakic PS (2001) Presynaptic regulation of recurrent excitation by D1 receptors in prefrontal circuits. Proc Natl Acad Sci U S A 98:295-300.

Geiger JR, Melcher T, Koh DS, Sakmann B, Seeburg PH, Jonas P, Monyer H (1995) Relative abundance of subunit mRNAs determines gating and Ca2+ permeability of AMPA receptors in principal neurons and interneurons in rat CNS. Neuron 15:193-204.

Genoux D, Haditsch U, Knobloch M, Michalon A, Storm D, Mansuy IM (2002) Protein phosphatase 1 is a molecular constraint on learning and memory. Nature 418:970-975.

Giguere M, Goldman-Rakic PS (1988) Mediodorsal nucleus: areal, laminar, and tangential distribution of afferents and efferents in the frontal lobe of rhesus monkeys. J Comp Neurol 277:195-213.

Gilbert CD (1983) Microcircuitry of the visual cortex. Annu Rev Neurosci 6:217-247.

Glantz LA, Lewis DA (2000) Decreased dendritic spine density on prefrontal cortical pyramidal neurons in schizophrenia. Arch Gen Psychiatry 57:65-73.

Goldberg JH, Yuste R, Tamas G (2003) Ca2+ imaging of mouse neocortical interneurone dendrites: contribution of Ca2+-permeable AMPA and NMDA receptors to subthreshold Ca2+dynamics. J Physiol 551:67-78.

Goldman-Rakic PS (1994) Working memory dysfunction in schizophrenia. J Neuropsychiatry Clin Neurosci 6:348-357.

Goldman-Rakic PS (1995) Cellular basis of working memory. Neuron 14:477-485.

Goldman-Rakic PS, Muly EC, 3rd, Williams GV (2000) D(1) receptors in prefrontal cells and circuits. Brain Res Brain Res Rev 31:295-301.

Goldman-Rakic PS, Leranth C, Williams SM, Mons N, Geffard M (1989) Dopamine synaptic complex with pyramidal neurons in primate cerebral cortex. Proc Natl Acad Sci U S A 86:9015-9019.

Gonchar Y, Burkhalter A (1997) Three distinct families of GABAergic neurons in rat visual cortex. Cereb Cortex 7:347-358.

Gonzalez-Burgos G, Krimer LS, Povysheva NV, Barrionuevo G, Lewis DA (2005a) Functional properties of fast spiking interneurons and their synaptic connections with pyramidal cells in primate dorsolateral prefrontal cortex. J Neurophysiol 93:942-953.

Gonzalez-Burgos G, Kroener S, Seamans JK, Lewis DA, Barrionuevo G (2005b) Dopaminergic modulation of short-term synaptic plasticity in fast-spiking interneurons of primate dorsolateral prefrontal cortex. J Neurophysiol 94:4168-4177.

Granado N, Ortiz O, Suarez LM, Martin ED, Cena V, Solis JM, Moratalla R (2008) D1 but not D5 dopamine receptors are critical for LTP, spatial learning, and LTP-Induced arc and zif268 expression in the hippocampus. Cereb Cortex 18:1-12.

Grandy DK, Zhang YA, Bouvier C, Zhou QY, Johnson RA, Allen L, Buck K, Bunzow JR, Salon J, Civelli O (1991) Multiple human D5 dopamine receptor genes: a functional receptor and two pseudogenes. Proc Natl Acad Sci U S A 88:9175-9179.

Gray EG (1959) Axo-somatic and axo-dendritic synapses of the cerebral cortex: an electron microscope study. J Anat 93:420-433.

Green MF (1996) What are the functional consequences of neurocognitive deficits in schizophrenia? Am J Psychiatry 153:321-330.

Green MF, Kern RS, Heaton RK (2004) Longitudinal studies of cognition and functional outcome in schizophrenia: implications for MATRICS. Schizophr Res 72:41-51.

Greengard P, Allen PB, Nairn AC (1999) Beyond the dopamine receptor: the DARPP-32/protein phosphatase-1 cascade. Neuron 23:435-447.

Gulyas AI, Hajos N, Freund TF (1996) Interneurons containing calretinin are specialized to control other interneurons in the rat hippocampus. J Neurosci 16:3397-3411.

Gustafson EL, Girault JA, Hemmings HC, Jr., Nairn AC, Greengard P (1991) Immunocytochemical localization of phosphatase inhibitor-1 in rat brain. J Comp Neurol 310:170-188.

Hara Y, Pickel VM (2007) Dendritic distributions of dopamine D1 receptors in the rat nucleus accumbens are synergistically affected by startle-evoking auditory stimulation and apomorphine. Neuroscience.

Harris KM, Kater SB (1994) Dendritic spines: cellular specializations imparting both stability and flexibility to synaptic function. Annu Rev Neurosci 17:341-371.

Hemmings HC, Jr., Greengard P (1986) DARPP-32, a dopamine- and adenosine 3':5'-monophosphate-regulated phosphoprotein: regional, tissue, and phylogenetic distribution. J Neurosci 6:1469-1481.

Hemmings HC, Jr., Greengard P, Tung HY, Cohen P (1984) DARPP-32, a dopamine-regulated neuronal phosphoprotein, is a potent inhibitor of protein phosphatase-1. Nature 310:503-505.

Hemmings HC, Jr., Girault JA, Nairn AC, Bertuzzi G, Greengard P (1992) Distribution of protein phosphatase inhibitor-1 in brain and peripheral tissues of various species: comparison with DARPP-32. J Neurochem 59:1053-1061.

Henze DA, Gonzalez-Burgos GR, Urban NN, Lewis DA, Barrionuevo G (2000) Dopamine increases excitability of pyramidal neurons in primate prefrontal cortex. J Neurophysiol 84:2799-2809.

Hersch SM, Ciliax BJ, Gutekunst CA, Rees HD, Heilman CJ, Yung KK, Bolam JP, Ince E, Yi H, Levey AI (1995) Electron microscopic analysis of D1 and D2 dopamine receptor proteins in the dorsal striatum and their synaptic relationships with motor corticostriatal afferents. J Neurosci 15:5222-5237.

Hersi AI, Kitaichi K, Srivastava LK, Gaudreau P, Quirion R (2000) Dopamine D-5 receptor modulates hippocampal acetylcholine release. Brain Res Mol Brain Res 76:336-340.

Huang FL, Glinsmann WH (1976) Separation and characterization of two phosphorylase phosphatase inhibitors from rabbit skeletal muscle. Eur J Biochem 70:419-426.

Jablensky A (1995) Schizophrenia: recent epidemiologic issues. Epidemiol Rev 17:10-20.

Jackson A, Sedaghat K, Minerds K, James C, Tiberi M (2005) Opposing effects of phorbol-12-myristate-13-acetate, an activator of protein kinase C, on the signaling

of structurally related human dopamine D1 and D5 receptors. J Neurochem 95:1387-1400.

Jakab RL, Goldman-Rakic PS (2000) Segregation of serotonin 5-HT2A and 5-HT3 receptors in inhibitory circuits of the primate cerebral cortex. J Comp Neurol 417:337-348.

Jones EG (1975) Lamination and differential distribution of thalamic afferents within the sensory-motor cortex of the squirrel monkey. J Comp Neurol 160:167-203.

Kawaguchi Y (1995) Physiological subgroups of nonpyramidal cells with specific morphological characteristics in layer II/III of rat frontal cortex. J Neurosci 15:2638-2655.

Kawaguchi Y, Kubota Y (1997) GABAergic cell subtypes and their synaptic connections in rat frontal cortex. Cereb Cortex 7:476-486.

Kawaguchi Y, Kondo S (2002) Parvalbumin, somatostatin and cholecystokinin as chemical markers for specific GABAergic interneuron types in the rat frontal cortex. J Neurocytol 31:277-287.

Kebabian JW, Calne DB (1979) Multiple receptors for dopamine. Nature 277:93-96.

Keefe RS (2007) Cognitive deficits in patients with schizophrenia: effects and treatment. J Clin Psychiatry 68 Suppl 14:8-13.

Keefe RS, Roitman SE, Harvey PD, Blum CS, DuPre RL, Prieto DM, Davidson M, Davis KL (1995) A pen-and-paper human analogue of a monkey prefrontal cortex activation task: spatial working memory in patients with schizophrenia. Schizophr Res 17:25-33.

Keefe RS, Bilder RM, Davis SM, Harvey PD, Palmer BW, Gold JM, Meltzer HY, Green MF, Capuano G, Stroup TS, McEvoy JP, Swartz MS, Rosenheck RA, Perkins DO, Davis CE, Hsiao JK, Lieberman JA (2007) Neurocognitive effects of antipsychotic medications in patients with chronic schizophrenia in the CATIE Trial. Arch Gen Psychiatry 64:633-647.

Khan ZU, Gutierrez A, Martin R, Penafiel A, Rivera A, de la Calle A (2000) Dopamine D5 receptors of rat and human brain. Neuroscience 100:689-699.

Kimura K, Sela S, Bouvier C, Grandy DK, Sidhu A (1995) Differential coupling of D1 and D5 dopamine receptors to guanine nucleotide binding proteins in transfected GH4C1 rat somatomammotrophic cells. J Neurochem 64:2118-2124.

Kraepelin E (1896) Lehrbuch der Psychiatrie, 5 Edition. Barth, Leipzig.

Krimer LS, Jakab RL, Goldman-Rakic PS (1997) Quantitative three-dimensional analysis of the catecholaminergic innervation of identified neurons in the macaque prefrontal cortex. J Neurosci 17:7450-7461.

Kritzer MF, Goldman-Rakic PS (1995) Intrinsic circuit organization of the major layers and sublayers of the dorsolateral prefrontal cortex in the rhesus monkey. J Comp Neurol 359:131-143.

Kudwa AE, Dominguez-Salazar E, Cabrera DM, Sibley DR, Rissman EF (2005) Dopamine D5 receptor modulates male and female sexual behavior in mice. Psychopharmacology (Berl) 180:206-214.

Kumar U, Patel SC (2007) Immunohistochemical localization of dopamine receptor subtypes (D1R-D5R) in Alzheimer's disease brain. Brain Res 1131:187-196.

Laplante F, Sibley DR, Quirion R (2004) Reduction in acetylcholine release in the hippocampus of dopamine D5 receptor-deficient mice. Neuropsychopharmacology 29:1620-1627.

Laruelle M, Abi-Dargham A, van Dyck CH, Gil R, D'Souza CD, Erdos J, McCance E, Rosenblatt W, Fingado C, Zoghbi SS, Baldwin RM, Seibyl JP, Krystal JH, Charney DS, Innis RB (1996) Single photon emission computerized tomography imaging of amphetamine-induced dopamine release in drug-free schizophrenic subjects. Proc Natl Acad Sci U S A 93:9235-9240.

Lee FJ, Xue S, Pei L, Vukusic B, Chery N, Wang Y, Wang YT, Niznik HB, Yu XM, Liu F (2002) Dual regulation of NMDA receptor functions by direct protein-protein interactions with the dopamine D1 receptor. Cell 111:219-230.

Lei W, Jiao Y, Del Mar N, Reiner A (2004) Evidence for differential cortical input to direct pathway versus indirect pathway striatal projection neurons in rats. J Neurosci 24:8289-8299.

Lewis DA (1992) The catecholaminergic innervation of primate prefrontal cortex. J Neural Transm Suppl 36:179-200.

Lewis DA, Lund JS (1990) Heterogeneity of chandelier neurons in monkey neocortex: corticotropin-releasing factor- and parvalbumin-immunoreactive populations. J Comp Neurol 293:599-615.

Lewis DA, Foote SL, Goldstein M, Morrison JH (1988) The dopaminergic innervation of monkey prefrontal cortex: a tyrosine hydroxylase immunohistochemical study. Brain Res 449:225-243.

Lewis DA, Glantz LA, Pierri JN, Sweet RA (2003) Altered cortical glutamate neurotransmission in schizophrenia: evidence from morphological studies of pyramidal neurons. Ann N Y Acad Sci 1003:102-112.

Lhuillier L, Mombereau C, Cryan JF, Kaupmann K (2007) GABA(B) receptor-positive modulation decreases selective molecular and behavioral effects of cocaine. Neuropsychopharmacology 32:388-398.

Li A, Guo H, Luo X, Sheng J, Yang S, Yin Y, Zhou J, Zhou J (2006) Apomorphine-induced activation of dopamine receptors modulates FGF-2 expression in astrocytic cultures and promotes survival of dopaminergic neurons. Faseb J 20:1263-1265.

Lidow MS, Elsworth JD, Goldman-Rakic PS (1997) Down-regulation of the D1 and D5 dopamine receptors in the primate prefrontal cortex by chronic treatment with antipsychotic drugs. J Pharmacol Exp Ther 281:597-603.

Lidow MS, Wang F, Cao Y, Goldman-Rakic PS (1998) Layer V neurons bear the majority of mRNAs encoding the five distinct dopamine receptor subtypes in the primate prefrontal cortex. Synapse 28:10-20.

Lin JW, Wyszynski M, Madhavan R, Sealock R, Kim JU, Sheng M (1998) Yotiao, a novel protein of neuromuscular junction and brain that interacts with specific splice variants of NMDA receptor subunit NR1. J Neurosci 18:2017-2027.

Liu F, Wan Q, Pristupa ZB, Yu XM, Wang YT, Niznik HB (2000) Direct protein-protein coupling enables cross-talk between dopamine D5 and gamma-aminobutyric acid A receptors. Nature 403:274-280.

Lowenstein PR, Shering AF, MacDougall LK, Cohen P (1995) Immunolocalisation of protein phosphatase inhibitor-1 in the cerebral cortex of the rat, cat and ferret. Brain Res 676:80-92.

Lund JS, Lewis DA (1993) Local circuit neurons of developing and mature macaque prefrontal cortex: Golgi and immunocytochemical characteristics. J Comp Neurol 328:282-312.

Lysaker PH, Bell MD, Bioty S, Zito WS (1996) Performance on the Wisconsin Card Sorting Test as a predictor of rehospitalization in schizophrenia. J Nerv Ment Dis 184:319-321.

MacDonald AW, 3rd, Pogue-Geile MF, Johnson MK, Carter CS (2003) A specific deficit in context processing in the unaffected siblings of patients with schizophrenia. Arch Gen Psychiatry 60:57-65.

MacMillan LB, Bass MA, Cheng N, Howard EF, Tamura M, Strack S, Wadzinski BE, Colbran RJ (1999) Brain actin-associated protein phosphatase 1 holoenzymes containing spinophilin, neurabin, and selected catalytic subunit isoforms. J Biol Chem 274:35845-35854.

Mair RG, Burk JA, Porter MC (1998) Lesions of the frontal cortex, hippocampus, and intralaminar thalamic nuclei have distinct effects on remembering in rats. Behav Neurosci 112:772-792.

Malchiodi-Albedi F, Petrucci TC, Picconi B, Iosi F, Falchi M (1997) Protein phosphatase inhibitors induce modification of synapse structure and tau hyperphosphorylation in cultured rat hippocampal neurons. J Neurosci Res 48:425-438.

Mandyam CD, Wee S, Eisch AJ, Richardson HN, Koob GF (2007) Methamphetamine self-administration and voluntary exercise have opposing effects on medial prefrontal cortex gliogenesis. J Neurosci 27:11442-11450.

Mani SK, Fienberg AA, O'Callaghan JP, Snyder GL, Allen PB, Dash PK, Moore AN, Mitchell AJ, Bibb J, Greengard P, O'Malley BW (2000) Requirement for DARPP-32 in progesterone-facilitated sexual receptivity in female rats and mice. Science 287:1053-1056.

Maragakis NJ, Rothstein JD (2006) Mechanisms of Disease: astrocytes in neurodegenerative disease. Nat Clin Pract Neurol 2:679-689.

Markram H, Toledo-Rodriguez M, Wang Y, Gupta A, Silberberg G, Wu C (2004) Interneurons of the neocortical inhibitory system. Nat Rev Neurosci 5:793-807.

Maunsell JH, van Essen DC (1983) The connections of the middle temporal visual area (MT) and their relationship to a cortical hierarchy in the macaque monkey. J Neurosci 3:2563-2586.

McGurk SR, Meltzer HY (2000) The role of cognition in vocational functioning in schizophrenia. Schizophr Res 45:175-184.

McGurk SR, Carter C, Goldman R, Green MF, Marder SR, Xie H, Schooler NR, Kane JM (2005) The effects of clozapine and risperidone on spatial working memory in schizophrenia. Am J Psychiatry 162:1013-1016.

Meador-Woodruff JH, Damask SP, Wang J, Haroutunian V, Davis KL, Watson SJ (1996) Dopamine receptor mRNA expression in human striatum and neocortex. Neuropsychopharmacology 15:17-29.

Melchitzky DS, Lewis DA (2003) Pyramidal neuron local axon terminals in monkey prefrontal cortex: differential targeting of subclasses of GABA neurons. Cereb Cortex 13:452-460.

Melchitzky DS, Sesack SR, Lewis DA (1999) Parvalbumin-immunoreactive axon terminals in macaque monkey and human prefrontal cortex: laminar, regional, and target specificity of type I and type II synapses. J Comp Neurol 408:11-22.

Melchitzky DS, Eggan SM, Lewis DA (2005) Synaptic targets of calretinin-containing axon terminals in macaque monkey prefrontal cortex. Neuroscience 130:185-195.

Meskenaite V (1997) Calretinin-immunoreactive local circuit neurons in area 17 of the cynomolgus monkey, Macaca fascicularis. J Comp Neurol 379:113-132.

Missale C, Nash SR, Robinson SW, Jaber M, Caron MG (1998) Dopamine receptors: from structure to function. Physiol Rev 78:189-225.

Mitrano DA, Smith Y (2007) Comparative analysis of the subcellular and subsynaptic localization of mGluR1a and mGluR5 metabotropic glutamate receptors in the shell and core of the nucleus accumbens in rat and monkey. J Comp Neurol 500:788-806.

Miyazaki I, Asanuma M, Diaz-Corrales FJ, Miyoshi K, Ogawa N (2004) Direct evidence for expression of dopamine receptors in astrocytes from basal ganglia. Brain Res 1029:120-123.

Momiyama T, Sim JA (1996) Modulation of inhibitory transmission by dopamine in rat basal forebrain nuclei: activation of presynaptic D1-like dopaminergic receptors. J Neurosci 16:7505-7512.

Moorhead G, Johnson D, Morrice N, Cohen P (1998) The major myosin phosphatase in skeletal muscle is a complex between the beta-isoform of protein phosphatase 1 and the MYPT2 gene product. FEBS Lett 438:141-144.

Morishita W, Connor JH, Xia H, Quinlan EM, Shenolikar S, Malenka RC (2001) Regulation of synaptic strength by protein phosphatase 1. Neuron 32:1133-1148.

Mulkey RM, Endo S, Shenolikar S, Malenka RC (1994) Involvement of a calcineurin/inhibitor-1 phosphatase cascade in hippocampal long-term depression. Nature 369:486-488.

Muly EC, Szigeti K, Goldman-Rakic PS (1998) D1 receptor in interneurons of macaque prefrontal cortex: distribution and subcellular localization. J Neurosci 18:10553-10565.

Muly EC, Greengard P, Goldman-Rakic PS (2001) Distribution of protein phosphatases-1 alpha and -1 gamma 1 and the D(1) dopamine receptor in primate prefrontal cortex: Evidence for discrete populations of spines. J Comp Neurol 440:261-270.

Muly EC, Smith Y, Allen P, Greengard P (2004a) Subcellular distribution of spinophilin immunolabeling in primate prefrontal cortex: Localization to and within dendritic spines. J Comp Neurol 469:185-197.

Muly EC, Allen P, Mazloom M, Aranbayeva Z, Greenfield AT, Greengard P (2004b) Subcellular distribution of neurabin immunolabeling in primate prefrontal cortex: comparison with spinophilin. Cereb Cortex 14:1398-1407.

Muly EC, Allen P, Mazloom M, Aranbayeva Z, Greenfield AT, Greengard P (2004c) Subcellular Distribution of Neurabin Immunolabeling in Primate Prefrontal Cortex: Comparison with Spinophilin. Cereb Cortex.

Murphy BL, Arnsten AF, Goldman-Rakic PS, Roth RH (1996) Increased dopamine turnover in the prefrontal cortex impairs spatial working memory performance in rats and monkeys. Proc Natl Acad Sci U S A 93:1325-1329.

Nagai T, Takuma K, Kamei H, Ito Y, Nakamichi N, Ibi D, Nakanishi Y, Murai M, Mizoguchi H, Nabeshima T, Yamada K (2007) Dopamine D1 receptors regulate protein synthesis-dependent long-term recognition memory via extracellular signal-regulated kinase 1/2 in the prefrontal cortex. Learn Mem 14:117-125.

Nairn AC, Hemmings HC, Jr., Walaas SI, Greengard P (1988) DARPP-32 and phosphatase inhibitor-1, two structurally related inhibitors of protein phosphatase-1, are both present in striatonigral neurons. J Neurochem 50:257-262.

Nakanishi H, Obaishi H, Satoh A, Wada M, Mandai K, Satoh K, Nishioka H, Matsuura Y, Mizoguchi A, Takai Y (1997) Neurabin: a novel neural tissue-specific actin filament-binding protein involved in neurite formation. J Cell Biol 139:951-961.

Nguyen C, Hosokawa T, Kuroiwa M, Ip NY, Nishi A, Hisanaga S, Bibb JA (2007a) Differential regulation of the Cdk5-dependent phosphorylation sites of inhibitor-1 and DARPP-32 by depolarization. J Neurochem 103:1582-1593.

Nguyen C, Nishi A, Kansy JW, Fernandez J, Hayashi K, Gillardon F, Hemmings HC, Jr., Nairn AC, Bibb JA (2007b) Regulation of protein phosphatase inhibitor-1 by cyclin-dependent kinase 5. J Biol Chem 282:16511-16520.

NIMH (2006) Schizophrenia. In. Bethesda, MD: National Institute of Mental Health.

Nimmo GA, Cohen P (1978) The regulation of glycogen metabolism. Purification and characterisation of protein phosphatase inhibitor-1 from rabbit skeletal muscle. Eur J Biochem 87:341-351.

Nyiri G, Stephenson FA, Freund TF, Somogyi P (2003) Large variability in synaptic N-methyl-D-aspartate receptor density on interneurons and a comparison with pyramidal-cell spines in the rat hippocampus. Neuroscience 119:347-363.

Oliver CJ, Terry-Lorenzo RT, Elliott E, Bloomer WA, Li S, Brautigan DL, Colbran RJ, Shenolikar S (2002) Targeting protein phosphatase 1 (PP1) to the actin cytoskeleton: the neurabin I/PP1 complex regulates cell morphology. Mol Cell Biol 22:4690-4701.

Ouimet CC, da Cruz e Silva EF, Greengard P (1995) The alpha and gamma 1 isoforms of protein phosphatase 1 are highly and specifically concentrated in dendritic spines. Proc Natl Acad Sci U S A 92:3396-3400.

Ouimet CC, Miller PE, Hemmings HC, Jr., Walaas SI, Greengard P (1984) DARPP-32, a dopamine- and adenosine 3':5'-monophosphate-regulated phosphoprotein enriched in dopamine-innervated brain regions. III. Immunocytochemical localization. J Neurosci 4:111-124.

Ouimet CC, LaMantia AS, Goldman-Rakic P, Rakic P, Greengard P (1992) Immunocytochemical localization of DARPP-32, a dopamine and cyclic-AMP-regulated phosphoprotein, in the primate brain. J Comp Neurol 323:209-218.

Paolillo M, Montecucco A, Zanassi P, Schinelli S (1998) Potentiation of dopamine-induced cAMP formation by group I metabotropic glutamate receptors via protein kinase C in cultured striatal neurons. Eur J Neurosci 10:1937-1945.

Park S, Holzman PS (1992) Schizophrenics show spatial working memory deficits. Arch Gen Psychiatry 49:975-982.

Park S, Puschel J, Sauter BH, Rentsch M, Hell D (1999) Spatial working memory deficits and clinical symptoms in schizophrenia: a 4-month follow-up study. Biol Psychiatry 46:392-400.

Paspalas CD, Goldman-Rakic PS (2004) Microdomains for dopamine volume neurotransmission in primate prefrontal cortex. J Neurosci 24:5292-5300.

Paspalas CD, Goldman-Rakic PS (2005) Presynaptic D1 dopamine receptors in primate prefrontal cortex: target-specific expression in the glutamatergic synapse. J Neurosci 25:1260-1267.

Peters A (1987) Synaptic specificity in the cerebral cortex. In: Syanptic Function (Edelman GM, Gall WE, Cowan WM, eds), pp 373-397. New York: John Wiley and Sons.

Peters A, Palay SL, Webster HD (1991) The fine structure of the nervous system: neurons and their supporting cells, 3 Edition. New York: Oxford University Press.

Pickel VM, Colago EE, Mania I, Molosh AI, Rainnie DG (2006) Dopamine D1 receptors co-distribute with N-methyl-D-aspartic acid type-1 subunits and modulate synaptically-evoked N-methyl-D-aspartic acid currents in rat basolateral amygdala. Neuroscience 142:671-690.

Poisik OV, Mannaioni G, Traynelis S, Smith Y, Conn PJ (2003) Distinct functional roles of the metabotropic glutamate receptors 1 and 5 in the rat globus pallidus. J Neurosci 23:122-130.

Povysheva NV, Gonzalez-Burgos G, Zaitsev AV, Kroner S, Barrionuevo G, Lewis DA, Krimer LS (2006) Properties of excitatory synaptic responses in fast-spiking

interneurons and pyramidal cells from monkey and rat prefrontal cortex. Cereb Cortex 16:541-552.

Price NE, Mumby MC (1999) Brain protein serine/threonine phosphatases. Curr Opin Neurobiol 9:336-342.

Prinster SC, Hague C, Hall RA (2005) Heterodimerization of g protein-coupled receptors: specificity and functional significance. Pharmacol Rev 57:289-298.

Rao SG, Williams GV, Goldman-Rakic PS (1999) Isodirectional tuning of adjacent interneurons and pyramidal cells during working memory: evidence for microcolumnar organization in PFC. J Neurophysiol 81:1903-1916.

Rao SG, Williams GV, Goldman-Rakic PS (2000) Destruction and creation of spatial tuning by disinhibition: GABA(A) blockade of prefrontal cortical neurons engaged by working memory. J Neurosci 20:485-494.

Rausell E, Avendano C (1985) Thalamocortical neurons projecting to superficial and to deep layers in parietal, frontal and prefrontal regions in the cat. Brain Res 347:159-165.

Reuss B, Unsicker K (2001) Atypical neuroleptic drugs downregulate dopamine sensitivity in rat cortical and striatal astrocytes. Mol Cell Neurosci 18:197-209.

Reuss B, Lorenzen A, Unsicker K (2001) Dopamine and epinephrine, but not serotonin, downregulate dopamine sensitivity in cultured cortical and striatal astroglial cells. Receptors Channels 7:441-451.

Rockland KS, Pandya DN (1979) Laminar origins and terminations of cortical connections of the occipital lobe in the rhesus monkey. Brain Res 179:3-20.

Runyan JD, Dash PK (2004) Intra-medial prefrontal administration of SCH-23390 attenuates ERK phosphorylation and long-term memory for trace fear conditioning in rats. Neurobiol Learn Mem 82:65-70.

Sahin B, Shu H, Fernandez J, El-Armouche A, Molkentin JD, Nairn AC, Bibb JA (2006) Phosphorylation of protein phosphatase inhibitor-1 by protein kinase C. J Biol Chem 281:24322-24335.

Sasaki K, Shima H, Kitagawa Y, Irino S, Sugimura T, Nagao M (1990) Identification of members of the protein phosphatase 1 gene family in the rat and enhanced expression of protein phosphatase 1 alpha gene in rat hepatocellular carcinomas. Jpn J Cancer Res 81:1272-1280.

Sawaguchi T (2001a) The role of D1-dopamine receptors in working memory-guided movements mediated by frontal cortical areas. Parkinsonism and Related Disorders 7:9-19.

Sawaguchi T (2001b) The effects of dopamine and its antagonists on directional delay-period activity of prefrontal neurons in monkeys during an oculomotor delayed-response task. Neurosci Res 41:115-128.

Sawaguchi T, Goldman-Rakic PS (1991) D1 dopamine receptors in prefrontal cortex: involvement in working memory. Science 251:947-950.

Sawaguchi T, Goldman-Rakic PS (1994) The role of D1-dopamine receptor in working memory: local injections of dopamine antagonists into the prefrontal cortex of rhesus monkeys performing an oculomotor delayed-response task. J Neurophysiol 71:515-528.

Sawaguchi T, Iba M (2001) Prefrontal cortical representation of visuospatial working memory in monkeys examined by local inactivation with muscimol. J Neurophysiol 86:2041-2053.

Sawaguchi T, Matsumura M, Kubota K (1988) Delayed response deficit in monkeys by locally disturbed prefrontal neuronal activity by bicuculline. Behav Brain Res 31:193-198.

Sawaguchi T, Matsumura M, Kubota K (1989) Delayed response deficits produced by local injection of bicuculline into the dorsolateral prefrontal cortex in Japanese macaque monkeys. Exp Brain Res 75:457-469.

Seamans JK, Yang CR (2004) The principal features and mechanisms of dopamine modulation in the prefrontal cortex. Prog Neurobiol 74:1-58.

Seamans JK, Floresco SB, Phillips AG (1998) D1 receptor modulation of hippocampal-prefrontal cortical circuits integrating spatial memory with executive functions in the rat. J Neurosci 18:1613-1621.

Sesack SR, Snyder CL, Lewis DA (1995a) Axon terminals immunolabeled for dopamine or tyrosine hydroxylase synapse on GABA-immunoreactive dendrites in rat and monkey cortex. J Comp Neurol 363:264-280.

Sesack SR, Bressler CN, Lewis DA (1995b) Ultrastructural associations between dopamine terminals and local circuit neurons in the monkey prefrontal cortex: a study of calretinin-immunoreactive cells. Neurosci Lett 200:9-12.

Sesack SR, Hawrylak VA, Melchitzky DS, Lewis DA (1998) Dopamine innervation of a subclass of local circuit neurons in monkey prefrontal cortex: ultrastructural

analysis of tyrosine hydroxylase and parvalbumin immunoreactive structures. Cereb Cortex 8:614-622.

Shakiryanova D, Tully A, Levitan ES (2006) Activity-dependent synaptic capture of transiting peptidergic vesicles. Nat Neurosci 9:896-900.

Shima H, Haneji T, Hatano Y, Kasugai I, Sugimura T, Nagao M (1993) Protein phosphatase 1 gamma 2 is associated with nuclei of meiotic cells in rat testis. Biochem Biophys Res Commun 194:930-937.

Sidhu A, Kimura K, Uh M, White BH, Patel S (1998) Multiple coupling of human D5 dopamine receptors to guanine nucleotide binding proteins Gs and Gz. J Neurochem 70:2459-2467.

Silver H (2003) Selective serotonin reuptake inhibitor augmentation in the treatment of negative symptoms of schizophrenia. Int Clin Psychopharmacol 18:305-313.

Silver H, Feldman P, Bilker W, Gur RC (2003) Working memory deficit as a core neuropsychological dysfunction in schizophrenia. Am J Psychiatry 160:1809-1816.

Smiley JF, Goldman-Rakic PS (1993) Silver-enhanced diaminobenzidine-sulfide (SEDS): a technique for high-resolution immunoelectron microscopy demonstrated with monoamine immunoreactivity in monkey cerebral cortex and caudate. J Histochem Cytochem 41:1393-1404.

Smiley JF, Levey AI, Ciliax BJ, Goldman-Rakic PS (1994) D1 dopamine receptor immunoreactivity in human and monkey cerebral cortex: predominant and extrasynaptic localization in dendritic spines. Proc Natl Acad Sci U S A 91:5720-5724.

Snyder GL, Fienberg AA, Huganir RL, Greengard P (1998) A dopamine/D1 receptor/protein kinase A/dopamine- and cAMP-regulated phosphoprotein (Mr 32 kDa)/protein phosphatase-1 pathway regulates dephosphorylation of the NMDA receptor. J Neurosci 18:10297-10303.

Snyder GL, Allen PB, Fienberg AA, Valle CG, Huganir RL, Nairn AC, Greengard P (2000) Regulation of phosphorylation of the GluR1 AMPA receptor in the neostriatum by dopamine and psychostimulants in vivo. J Neurosci 20:4480-4488.

Somogyi P, Dalezios Y, Lujan R, Roberts JD, Watanabe M, Shigemoto R (2003) High level of mGluR7 in the presynaptic active zones of select populations of GABAergic terminals innervating interneurons in the rat hippocampus. Eur J Neurosci 17:2503-2520.

Strack S, Kini S, Ebner FF, Wadzinski BE, Colbran RJ (1999) Differential cellular and subcellular localization of protein phosphatase 1 isoforms in brain. J Comp Neurol 413:373-384.

Sunahara RK, Guan HC, O'Dowd BF, Seeman P, Laurier LG, Ng G, George SR, Torchia J, Van Tol HH, Niznik HB (1991) Cloning of the gene for a human dopamine D5 receptor with higher affinity for dopamine than D1. Nature 350:614-619.

Surmeier DJ, Bargas J, Hemmings HC, Jr., Nairn AC, Greengard P (1995) Modulation of calcium currents by a D1 dopaminergic protein kinase/phosphatase cascade in rat neostriatal neurons. Neuron 14:385-397.

Svenningsson P, Lindskog M, Rognoni F, Fredholm BB, Greengard P, Fisone G (1998) Activation of adenosine A2A and dopamine D1 receptors stimulates cyclic AMP-

dependent phosphorylation of DARPP-32 in distinct populations of striatal projection neurons. Neuroscience 84:223-228.

Svenningsson P, Tzavara ET, Liu F, Fienberg AA, Nomikos GG, Greengard P (2002a) DARPP-32 mediates serotonergic neurotransmission in the forebrain. Proc Natl Acad Sci U S A 99:3188-3193.

Svenningsson P, Tzavara ET, Witkin JM, Fienberg AA, Nomikos GG, Greengard P (2002b) Involvement of striatal and extrastriatal DARPP-32 in biochemical and behavioral effects of fluoxetine (Prozac). Proc Natl Acad Sci U S A 99:3182-3187.

Swadlow HA (1983) Efferent systems of primary visual cortex: a review of structure and function. Brain Res 287:1-24.

Takizawa N, Mizuno Y, Komatsu M, Matsuzawa S, Kawamura T, Inagaki N, Inagaki M, Kikuchi K (1997) Alterations in type-1 serine/threonine protein phosphatase PP1alpha in response to B-cell receptor stimulation. J Biochem (Tokyo) 122:730-737.

Tamas G, Buhl EH, Somogyi P (1997) Fast IPSPs elicited via multiple synaptic release sites by different types of GABAergic neurone in the cat visual cortex. J Physiol 500 (Pt 3):715-738.

Tang TS, Bezprozvanny I (2004) Dopamine receptor-mediated Ca(2+) signaling in striatal medium spiny neurons. J Biol Chem 279:42082-42094.

Tang TS, Tu H, Wang Z, Bezprozvanny I (2003) Modulation of type 1 inositol (1,4,5)-trisphosphate receptor function by protein kinase a and protein phosphatase 1alpha. J Neurosci 23:403-415.

Teclemariam-Mesbah R, Wortel J, Romijn HJ, Buijs RM (1997) A simple silver-gold intensification procedure for double DAB labeling studies in electron microscopy. J Histochem Cytochem 45:619-621.

Terry-Lorenzo RT, Carmody LC, Voltz JW, Connor JH, Li S, Smith FD, Milgram SL, Colbran RJ, Shenolikar S (2002) The neuronal actin-binding proteins, neurabin I and neurabin II, recruit specific isoforms of protein phosphatase-1 catalytic subunits. J Biol Chem 277:27716-27724.

Terunuma M, Jang IS, Ha SH, Kittler JT, Kanematsu T, Jovanovic JN, Nakayama KI, Akaike N, Ryu SH, Moss SJ, Hirata M (2004) GABAA receptor phospho-dependent modulation is regulated by phospholipase C-related inactive protein type 1, a novel protein phosphatase 1 anchoring protein. J Neurosci 24:7074-7084.

Thomson AM, West DC, Hahn J, Deuchars J (1996) Single axon IPSPs elicited in pyramidal cells by three classes of interneurones in slices of rat neocortex. J Physiol 496 (Pt 1):81-102.

Tiberi M, Caron MG (1994) High agonist-independent activity is a distinguishing feature of the dopamine D1B receptor subtype. J Biol Chem 269:27925-27931.

Tiberi M, Jarvie KR, Silvia C, Falardeau P, Gingrich JA, Godinot N, Bertrand L, Yang-Feng TL, Fremeau RT, Jr., Caron MG (1991) Cloning, molecular characterization, and chromosomal assignment of a gene encoding a second D1 dopamine receptor subtype: differential expression pattern in rat brain compared with the D1A receptor. Proc Natl Acad Sci U S A 88:7491-7495.

Towers SK, Hestrin S (2008) D1-like dopamine receptor activation modulates GABAergic inhibition but not electrical coupling between neocortical fast-spiking interneurons. J Neurosci 28:2633-2641.

Trantham-Davidson H, Kroner S, Seamans JK (2008) Dopamine modulation of prefrontal cortex interneurons occurs independently of DARPP-32. Cereb Cortex 18:951-958.

Tu H, Tang TS, Wang Z, Bezprozvanny I (2004) Association of type 1 inositol 1,4,5-trisphosphate receptor with AKAP9 (Yotiao) and protein kinase A. J Biol Chem 279:19375-19382.

Urban NN, Gonzalez-Burgos G, Henze DA, Lewis DA, Barrionuevo G (2002) Selective reduction by dopamine of excitatory synaptic inputs to pyramidal neurons in primate prefrontal cortex. J Physiol 539:707-712.

Valenti O, Conn PJ, Marino MJ (2002) Distinct physiological roles of the Gq-coupled metabotropic glutamate receptors Co-expressed in the same neuronal populations. J Cell Physiol 191:125-137.

Valjent E, Pascoli V, Svenningsson P, Paul S, Enslen H, Corvol JC, Stipanovich A, Caboche J, Lombroso PJ, Nairn AC, Greengard P, Herve D, Girault JA (2005) Regulation of a protein phosphatase cascade allows convergent dopamine and glutamate signals to activate ERK in the striatum. Proc Natl Acad Sci U S A 102:491-496.

Venugopalan VV, Ghali Z, Senecal J, Reader TA, Descarries L (2006) Catecholaminergic activation of G-protein coupling in rat spinal cord: further

evidence for the existence of dopamine and noradrenaline receptors in spinal grey and white matter. Brain Res 1070:90-100.

Vermeulen RJ, Jongenelen CA, Langeveld CH, Wolters EC, Stoof JC, Drukarch B (1994) Dopamine D1 receptor agonists display a different intrinsic activity in rat, monkey and human astrocytes. Eur J Pharmacol 269:121-125.

Vijayraghavan S, Wang M, Birnbaum SG, Williams GV, Arnsten AF (2007) Inverted-U dopamine D1 receptor actions on prefrontal neurons engaged in working memory. Nat Neurosci 10:376-384.

Vissavajjhala P, Janssen WG, Hu Y, Gazzaley AH, Moran T, Hof PR, Morrison JH (1996) Synaptic distribution of the AMPA-GluR2 subunit and its colocalization with calcium-binding proteins in rat cerebral cortex: an immunohistochemical study using a GluR2-specific monoclonal antibody. Exp Neurol 142:296-312.

Walaas SI, Greengard P (1984) DARPP-32, a dopamine- and adenosine 3':5'-monophosphate-regulated phosphoprotein enriched in dopamine-innervated brain regions. I. Regional and cellular distribution in the rat brain. J Neurosci 4:84-98.

Walaas SI, Nairn AC, Greengard P (1983) Regional distribution of calcium- and cyclic adenosine 3':5'-monophosphate-regulated protein phosphorylation systems in mammalian brain. II. Soluble systems. J Neurosci 3:302-311.

Walker A (1940) A cytoarchitectural study of the prefrontal area of the macaque monkey. J Comp Neurol 73:59-86.

Wang LY, Orser BA, Brautigan DL, MacDonald JF (1994) Regulation of NMDA receptors in cultured hippocampal neurons by protein phosphatases 1 and 2A. Nature 369:230-232.

Wang Q, Jolly JP, Surmeier JD, Mullah BM, Lidow MS, Bergson CM, Robishaw JD (2001) Differential dependence of the D1 and D5 dopamine receptors on the G protein gamma 7 subunit for activation of adenylylcyclase. J Biol Chem 276:39386-39393.

Wang XJ, Tegner J, Constantinidis C, Goldman-Rakic PS (2004) Division of labor among distinct subtypes of inhibitory neurons in a cortical microcircuit of working memory. Proc Natl Acad Sci U S A 101:1368-1373.

Weinshank RL, Adham N, Macchi M, Olsen MA, Branchek TA, Hartig PR (1991) Molecular cloning and characterization of a high affinity dopamine receptor (D1 beta) and its pseudogene. J Biol Chem 266:22427-22435.

Westphal RS, Tavalin SJ, Lin JW, Alto NM, Fraser ID, Langeberg LK, Sheng M, Scott JD (1999) Regulation of NMDA receptors by an associated phosphatase-kinase signaling complex. Science 285:93-96.

Williams GV, Goldman-Rakic PS (1995) Modulation of memory fields by dopamine D1 receptors in prefrontal cortex. Nature 376:572-575.

Williams GV, Castner SA (2006) Under the curve: critical issues for elucidating D1 receptor function in working memory. Neuroscience 139:263-276.

Williams KR, Hemmings HC, Jr., LoPresti MB, Konigsberg WH, Greengard P (1986) DARPP-32, a dopamine- and cyclic AMP-regulated neuronal phosphoprotein. Primary structure and homology with protein phosphatase inhibitor-1. J Biol Chem 261:1890-1903.

Williams SM, Goldman-Rakic PS, Leranth C (1992) The synaptology of parvalbumin-immunoreactive neurons in the primate prefrontal cortex. J Comp Neurol 320:353-369.

Wilson FA, O'Scalaidhe SP, Goldman-Rakic PS (1994) Functional synergism between putative gamma-aminobutyrate-containing neurons and pyramidal neurons in prefrontal cortex. Proc Natl Acad Sci U S A 91:4009-4013.

Wilson KM, Swanson HL (2001) Are mathematics disabilities due to a domain-general or a domain-specific working memory deficit? J Learn Disabil 34:237-248.

Woodruff AR, Sah P (2007) Inhibition and Synchronization of Basal Amygdala Principal Neuron Spiking by Parvalbumin-Positive Interneurons. J Neurophysiol 98:2956-2961.

Wouterlood FG, Pattiselanno A, Jorritsm-Byham B, Arts MPM, Meredith GE (1993) Connectional, immunocytochemical and ultrastructual characterization of neurons injected intracellularly in fixed brain tissue. In: Morphological investigations of single neurons in vitro (Meredith GE, Arbuthnott GW, eds), pp 47-169. New York: Wiley.

Wu EQ, Birnbaum HG, Shi L, Ball DE, Kessler RC, Moulis M, Aggarwal J (2005) The economic burden of schizophrenia in the United States in 2002. J Clin Psychiatry 66:1122-1129.

Wykes T (1994) Predicting symptomatic and behavioural outcomes of community care. Br J Psychiatry 165:486-492.

Xiang Z, Huguenard JR, Prince DA (2002) Synaptic inhibition of pyramidal cells evoked by different interneuronal subtypes in layer v of rat visual cortex. J Neurophysiol 88:740-750.

Yan Z, Surmeier DJ (1997) D5 dopamine receptors enhance Zn2+-sensitive GABA(A) currents in striatal cholinergic interneurons through a PKA/PP1 cascade. Neuron 19:1115-1126.

Yan Z, Hsieh-Wilson L, Feng J, Tomizawa K, Allen PB, Fienberg AA, Nairn AC, Greengard P (1999) Protein phosphatase 1 modulation of neostriatal AMPA channels: regulation by DARPP-32 and spinophilin. Nat Neurosci 2:13-17.

Yang CR, Seamans JK (1996) Dopamine D1 receptor actions in layers V-VI rat prefrontal cortex neurons in vitro: modulation of dendritic-somatic signal integration. J Neurosci 16:1922-1935.

Yang CR, Seamans JK, Gorelova N (1999) Developing a neuronal model for the pathophysiology of schizophrenia based on the nature of electrophysiological actions of dopamine in the prefrontal cortex. Neuropsychopharmacology 21:161-194.

Yi KD, Chung J, Pang P, Simpkins JW (2005) Role of protein phosphatases in estrogen-mediated neuroprotection. J Neurosci 25:7191-7198.

Young CE, Yang CR (2005) Dopamine D1-like receptor modulates layer- and frequency-specific short-term synaptic plasticity in rat prefrontal cortical neurons. Eur J Neurosci 21:3310-3320.

Yu PY, Eisner GM, Yamaguchi I, Mouradian MM, Felder RA, Jose PA (1996) Dopamine D1A receptor regulation of phospholipase C isoform. J Biol Chem 271:19503-19508.

Zachariou V, Benoit-Marand M, Allen PB, Ingrassia P, Fienberg AA, Gonon F, Greengard P, Picciotto MR (2002) Reduction of cocaine place preference in mice lacking the protein phosphatase 1 inhibitors DARPP 32 or Inhibitor 1. Biol Psychiatry 51:612-620.

Zahrt J, Taylor JR, Mathew RG, Arnsten AF (1997) Supranormal stimulation of D1 dopamine receptors in the rodent prefrontal cortex impairs spatial working memory performance. J Neurosci 17:8528-8535.

Zaitsev AV, Gonzalez-Burgos G, Povysheva NV, Kroner S, Lewis DA, Krimer LS (2004) Localization of Calcium-binding Proteins in Physiologically and Morphologically Characterized Interneurons of Monkey Dorsolateral Prefrontal Cortex. Cereb Cortex.

Zaitsev AV, Gonzalez-Burgos G, Povysheva NV, Kroner S, Lewis DA, Krimer LS (2005) Localization of calcium-binding proteins in physiologically and morphologically characterized interneurons of monkey dorsolateral prefrontal cortex. Cereb Cortex 15:1178-1186.

Zanassi P, Paolillo M, Montecucco A, Avvedimento EV, Schinelli S (1999) Pharmacological and molecular evidence for dopamine D(1) receptor expression by striatal astrocytes in culture. J Neurosci Res 58:544-552.

Zhen X, Goswami S, Friedman E (2005) The role of the phosphatidyinositol-linked D1 dopamine receptor in the pharmacology of SKF83959. Pharmacol Biochem Behav 80:597-601.

Zhen X, Torres C, Wang HY, Friedman E (2001) Prenatal exposure to cocaine disrupts D1A dopamine receptor function via selective inhibition of protein phosphatase 1 pathway in rabbit frontal cortex. J Neurosci 21:9160-9167.

Zhu ZT, Fu Y, Hu GY, Jin GZ (2000) Modulation of medical prefrontal cortical D1 receptors on the excitatory firing activity of nucleus accumbens neurons elicited by (-)-Stepholidine. Life Sci 67:1265-1274.